

Development of micro-beads that contain functional excipients for effective oral delivery of macromolecular drugs

A Laux



[orcid.org/ 0000-0002-9792-6373](https://orcid.org/0000-0002-9792-6373)

Dissertation submitted in partial fulfilment of the requirements
for the degree Master of Science in Pharmaceutics at the
North-West University

Supervisor: Prof JH Hamman

Co-supervisor: Prof JH Steenekamp

Graduation May 2018

Student number: 23479612



ACKNOWLEDGEMENTS

First and foremost, I need to thank God for granting me this opportunity and empowering me with the knowledge and ability to have undertaken this task. Without His gracious love, guidance and protection none of this would have been possible.

To Prof Sias Hamman my study leader, thank you for taking me on as a post graduate student and guiding me with so much compassion and dedication. I have the utmost respect and admiration for your outstanding academic ability as a leader in pharmaceutical research. Thank you for sharing your expertise and for teaching me never to give up, but always to persevere in order to find answers and solutions. It has been an honour and privilege to have worked under your guidance.

Prof Jan Steenekamp, thank you for your dedication and input over these past two years. Thank you for advising me and taking the time to help me find solutions. Your effort is greatly appreciated.

To my parents Wilma and Francois Laux. Thank you for your love and continuous motivation over the years. I feel blessed and honoured to have you as parents. Without you none of this would have been possible.

To my brother Jean-Pierre Laux. Thank you for always being there when I needed support and assistance.

Kaylee Havenga. Thank you for your advice, invaluable contribution and constant motivation. You were my pillar of strength. Thank you for all the lunches and snacks when I was burning the midnight oil. Thank you for the love and support I received from you and your family. You were always there for me when I needed you. You believed in me and kept me going.

To the Free State Department of Education, that made the funds available for my pre- and post-graduate studies, a special word of thanks to you. I am eternally grateful for the financial support and academic empowerment. I wish to thank Dr. Vishu Abhilak (now retired), Mr Lesiu and the honorable Premier in person, for believing in me and granting me this opportunity to conduct a post graduate study. Thank you to every staff member of the Free State Education Bursary Department that made sure that my academic portfolio was well managed.

To my fellow students, especially Corneli Jacobz and Anja Haasbroek, thank you that you were always prepared to lend a helping hand, share advice and contributed to a positive working environment.

To the North-West University and all of the staff, thank you for making this research study possible. I am privileged and honoured to have been part of such an outstanding, efficient and well managed institution.

ABSTRACT

Biotechnology advancements have made it possible to produce proteins and peptides for therapeutic applications on a large scale. These peptides are mostly administered parenterally, which hampers patient compliance due to the intrusive nature of the injections. The oral route of drug administration remains the most popular and convenient delivery route. Whilst effective after administration as injections, these protein and peptide drugs are not sufficiently absorbed after oral administration due to pre-systemic enzymatic degradation as well as poor intestinal membrane permeability. With the aid of safe and effective absorption enhancers, these problems can be overcome. Previous studies have proven that *Aloe vera* leaf materials as well as other absorption enhancing agents (chitosan, *N*-trimethyl chitosan chloride (TMC) and bile salts) can increase intestinal membrane permeability of drugs across *in vitro* and *ex vivo* models when applied as solutions. These absorption enhancers have also proven effective when formulated into macro-beads.

The purpose of this study was to develop and evaluate micro-beads containing selected drug absorption enhancers as functional excipients in order to effectively deliver macromolecular drugs across the intestinal epithelium using an *ex vivo* transport model. Spherical micro-beads were prepared by means of extrusion spheronisation, with each formulation containing fluorescein isothiocyanate (FITC)-dextran (FD-4) as model compound and a different absorption enhancer (i.e. *Aloe vera* gel, *Aloe vera* whole leaf extract, chitosan, TMC and sodium glycocholate hydrate). One micro-bead formulation containing only FD-4 was used as the control group. The micro-bead formulations were characterised in terms of FD-4 content, morphology, size and drug release profiles. The delivery of FD-4 across excised porcine jejunum by the different micro-bead formulations was evaluated using a Sweetana-Grass diffusion apparatus.

All of the micro-bead formulations prepared in this study showed relatively spherical shapes along with fairly narrow particle size distribution values. *Ex vivo* transport studies revealed that all five of the selected drug absorption enhancers formulated into micro-beads, could increase FD-4 transport across the intestinal epithelium compared to the control group, albeit to varying extents. The micro-beads containing *A. vera* gel showed the highest increase in FD-4 transport of all the micro-bead formulations followed by *A. vera* whole leaf extract > TMC > chitosan > sodium glycocholate hydrate. This study has shown that absorption enhancers formulated into micro-beads can effectively deliver macromolecular compounds across the intestinal epithelium. Although very promising results have been obtained from these *ex vivo* studies, it is important to mention that *in vivo* studies are needed to confirm if these absorption enhancing effects are sufficient to deliver macromolecular drugs at therapeutic levels.

Key words: Absorption enhancer, macromolecule, *Aloe vera* gel/whole leaf extract, chitosan, sodium glycocholate hydrate, *N*-trimethyl chitosan chloride (TMC), *ex vivo*, Micro-bead

UITTREKSEL

Biotegnologiese vordering het die produksie van proteïene en peptiedgeneesmiddels op grootskaal in die afgelope jare moontlik gemaak. Die toediening van hierdie peptiede geskied meestal deur die parenterale roete en verlaag pasiënt meewerkendheid as gevolg van die ongemak en pyn wat met hierdie toedieningsroete gepaardgaan. Die orale toedieningsroete word steeds as die mees gerieflike en gewildste toedieningsroete ervaar. Alhoewel dié proteïene en peptiedgeneesmiddels effektief is na parenterale toediening, word die bogenoemde geneesmiddels nie effektief geabsorbeer na orale toediening nie as gevolg van pre-sistemiese ensimitiese afbraak, sowel as swak penetrasie van die intestinale mukosa. Die laasgenoemde probleme kan wel oorkom word deur die insluiting van veilige en effektiewe absorpsiebevordersaars in doseervorme. Vorige studies het wel bewys dat die insluiting van *Aloe vera* blaarmateriaal en ander absorpsiebevordersaars (kitosaan, *N*-trimetiel kitosaan chloried (TMC) en gal sout) in oplossing wel die geneesmiddel se beweging oor *in vitro* en *ex vivo* intestinale epiteelmodelle kon bevorder. Dit is ook bewys dat hierdie absorpsiebevordersaars effektief is wanneer dit ingesluit word in makro-kraal formules.

Die doel van hierdie studie was om mikro-krale te formuleer en te evalueer, wat spesifieke absorpsiebevordersaars bevat om makromolekulegeneesmiddels effektief te kon aflewer deur gebruik te maak van 'n *ex vivo* afleweringmodel. Sferiese mikro-krale is berei deur gebruik te maak van die uitpers-sferonisasie metode. Elke formule het fluoresien isotiosinaat (FITC)-dekstraan (FD-4) bevat as 'n makromolekule model tesam met 'n spesifieke absorpsiebevordersaar (d.w.s. *Aloe vera* jel, *Aloe vera* heelblaar ekstrak, kitosaan, TMC en natrium glikocholaat hidraat). Een van die formules het slegs FD-4 bevat en het gedien as die kontrolegroep. Die mikro-kraal formules is gekarakteriseer ten opsigte van FD-4 konsentrasie, morfologie, kraalgrootte en geneesmiddelvystellingsprofiel. Die aflewering van FD-4 deur die mikro-kraalformules is geëvalueer oor uitgesnyde vark intestinale weefsel in 'n Sweetana-Grass diffusieapparaat.

Al die mikro-kraal formules wat berei is vir die studie het relatiewe sferiese vorms gehad en ook redelike nou deeltjiegrootteverspreidingswaardes getoon. *Ex vivo* transport studies het gewys dat al vyf van die gekose absorpsiebevordersaars, in hul mikro-kraal formulerings, wel 'n toename getoon het in FD-4 aflewering oor die uitgesnyde vark intestinale weefsel. Die mikro-kraalformule wat *A. vera* jel bevat het, het die grootste toename in FD-4 transport opgelewer. Dit was gevolg deur *A. vera* heelblaar ekstrak > TMC > kitosaan > natrium glikokolaat hidraat. Die studie het dus bewys dat absorpsiebevordersaars wat in mikro-kraal formules ingesluit word, die effektiewe aflewering van makromolekules oor intestinale weefsel kan bewerkstellig. Alhoewel die resultate van hierdie *ex vivo* studie baie belowend lyk, moet die absorpsiebevordersaars se effektiwiteit deur

in vivo studies ook getoets word om te verseker dat die absorpsiebevorderende effekte voldoende is om geneesmiddels by 'n terapeutiese vlak te kan aflewer.

Sleutelwoorde: Absorpsiebevorderaar, parenterale toediening, orale roete, kitosaan, *N*-trimetiel kitosaan chloried (TMC), natrium glikocholaat hidraat, mikro-krale, *ex vivo*

TABLE OF CONTENTS

ACKNOWLEDGEMENTS.....	I
ABSTRACT.....	III
UITTREKSEL.....	V
LIST OF TABLES.....	XIV
LIST OF FIGURES.....	XV
CHAPTER 1 INTRODUCTION.....	1
1.1 BACKGROUND AND JUSTIFICATION.....	1
1.1 Drug absorption enhancement of protein and peptide drugs.....	1
1.2 Preparation of spherical beads by means of extrusion-spheronisation.....	2
1.3 Models that can be used to study drug membrane permeation.....	2
1.2 RESEARCH PROBLEM.....	3
1.3 AIM AND OBJECTIVES.....	4
1.3.1 General aims.....	4
1.3.2 Objectives of the study.....	4
1.4 ETHICS REGARDING RESEARCH.....	4
1.5 EXPERIMENTAL SETUP.....	5
1.6 LAYOUT OF DISSERTATION.....	6
CHAPTER 2 LITERATURE REVIEW ON THE DEVELOPMENT OF MICRO-BEADS FOR EFFECTIVE ORAL DELIVERY OF MACROMOLECULAR DRUGS.....	7
2.1 INTRODUCTION.....	7
2.2 DRUG ABSORPTION FROM THE GASTROINTESTINAL TRACT.....	8
2.2.1 Drug absorption mechanisms.....	9
2.2.1.1 Transcellular passive diffusion.....	9

2.2.1.2 Carrier-mediated transport.....	9
2.2.1.2.1 Active transport.....	10
2.2.1.2.2 Facilitated diffusion or transport.....	11
2.2.1.3 Endocytosis.....	11
2.2.1.3.1 Pinocytosis.....	11
2.2.1.3.2 Phagocytosis.....	11
2.2.1.3.3 Receptor-mediated endocytosis.....	12
2.2.1.3.4 Transcytosis.....	12
2.3 CHALLENGES ASSOCIATED WITH ORAL PEPTIDE DRUG DELIVERY.....	12
2.3.1 Physical barriers against peptide drug absorption.....	13
2.3.1.1 Intestinal epithelial cell membranes.....	13
2.3.1.2 Unstirred water layer.....	13
2.3.1.3 Tight junctions.....	14
2.3.2 Biochemical barriers against peptide drug absorption.....	14
2.4 APPROACHES TO IMPROVE ORAL PEPTIDE DRUG.....	15
2.4.1 Chemical approaches.....	15
2.4.1.1 Analogue formation.....	15
2.4.1.2 Polyethylene glycolation (PEGylation).....	15
2.4.1.3 Reverse aqueous lipidisation and cell-penetrating peptides.....	16
2.4.1.4 Pro-drugs.....	16
2.4.1.5 Synthesis of substrates (peptidomimetics) for peptide transporters.....	17
2.4.2 Pharmaceutical approaches.....	17
2.4.2.1 Enzyme inhibitors.....	17

2.4.2.2 Mucoadhesive systems.....	18
2.4.2.3 Carrier type drug delivery systems.....	18
2.4.2.4 Site specific delivery.....	18
2.4.2.5 Drug absorption enhancers.....	20
2.4.2.5.1 <i>Aloe vera</i>	22
2.4.2.5.2 Chitosan and chitosan derivatives.....	22
2.5 SUMMARY.....	23
CHAPTER 3 METHODS AND MATERIALS.....	25
3.1 INTRODUCTION.....	25
3.2 MATERIALS.....	25
3.2.1 Materials used for micro-bead formulations.....	25
3.2.2 Materials used for dissolution studies.....	26
3.2.3 Materials used for particle size analysis.....	26
3.2.4 Materials used for proton nuclear magnetic resonance.....	26
3.2.5 Materials used for transport studies.....	26
3.3 VALIDATION OF ANALYTICAL PROCEDURES.....	26
3.3.1 Linearity.....	27
3.3.2 Limit of detection.....	28
3.3.3 Limit of quantification	28
3.3.4 Precision.....	29
3.3.4.1 Intra-day precision.....	29
3.3.4.2 Inter-day precision.....	29
3.3.5 Specificity.....	29

3.3.6 Accuracy.....	30
3.4 MICRO-BEAD FORMULATIONS.....	30
3.4.1 Micro-bead preparation.....	31
3.5 EVALUATION OF MICRO-BEADS.....	32
3.5.1 Assay.....	32
3.5.2 Dissolution studies.....	32
3.5.3 Particle size analysis.....	33
3.5.4 Micro-bead structure and morphology.....	33
3.6 CHEMICAL CHARACTERIZATION OF N-TRIMETHYL CHITOSAN CHLORIDE WITH PROTON NUCLEAR MAGNETIC RESONANCE.....	34
3.7 EX VIVO TRANSPORT STUDIES ACROSS EXCISED PIG INTESTINAL.....	34
3.7.1 Preparation of buffer.....	34
3.7.2 Collection and preparation of porcine intestinal tissue.....	34
3.7.3 Transport studies across the mounted intestinal tissues.....	38
3.7.4 Membrane integrity using Lucifer yellow.....	39
3.7.5 Statistical analysis.....	39
CHAPTER 4 RESULTS AND DISCUSSION.....	40
4.1 INTRODUCTION.....	40
4.2 FLUORESCENCE SPECTROMETRY METHOD VALIDATION.....	41
4.2.1 Linearity.....	41
4.2.1.1 Linearity of FD-4.....	41
4.2.1.2 Linearity of LY.....	42
4.2.2 Precision.....	44
4.2.2.1.1 FD-4 intra-day precision.....	44

4.2.2.1.2 LY intra-day precision.....	45
4.2.2.2.1 FD-4 inter-day precision.....	45
4.2.2.2.2 LY inter-day precision.....	46
4.2.3 Limit of detection and limit of quantification.....	47
4.2.4 Specificity.....	49
4.2.4.1 Calibration curve for FD-4 in the presence of <i>Aloe vera</i> gel.....	49
4.2.4.2 Calibration curve for FD-4 in the presence of <i>Aloe vera</i> whole leaf extract.....	49
4.2.4.3 Calibration curve for FD-4 in the presence of chitosan.....	50
4.2.4.4 Calibration curve for FD-4 in the presence of <i>N</i> -trimethyl chitosan chloride (TMC).....	51
4.2.4.5 Calibration curve for FD-4 in the presence of sodium glycocholate hydrate.....	51
4.2.4.6 Calibration curve for FD-4 in the presence of Pharmacel®.....	52
4.2.5 Accuracy.....	53
4.2.6 Validation results summary.....	54
4.3 CHEMICAL CHARACTERIZATION OF <i>N</i>-TRIMETHYL CHITOSAN CHLORIDE.....	55
4.4 MICRO-BEAD EVALUATION.....	56
4.4.1 Assay.....	56
4.4.2 Particle size analysis.....	56
4.4.2.1 Micro-bead formulation consisting of Pharmacel® (Control).....	56
4.4.2.2 Micro-bead formulation containing <i>Aloe vera</i> gel.....	57
4.4.2.3 Micro-bead formulation containing <i>Aloe vera</i> whole leaf extract.....	58
4.4.2.4 Micro-bead formulation containing chitosan.....	58
4.4.2.5 Micro-bead formulation containing <i>N</i> -trimethyl chitosan chloride (TMC).....	59
4.4.2.6 Micro-bead formulation containing sodium glycocholate hydrate.....	60

4.4.3 Micro-bead structure and morphology.....	60
4.4.3.1 Micro-bead formulation consisting of Pharmacel®	60
4.4.3.2 Micro-bead formulation containing <i>Aloe vera</i> gel.....	62
4.4.3.3 Micro-bead formulation containing <i>Aloe vera</i> whole leaf extract.....	63
4.4.3.4 Micro-bead formulation containing chitosan.....	65
4.4.3.5 Micro-bead formulation containing <i>N</i> -trimethyl chitosan chloride (TMC).....	66
4.4.3.6 Micro-bead formulation containing sodium glycocholate hydrate.....	68
4.4.5 Dissolution.....	69
4.5 EX VIVO TRANSPORT STUDIES.....	65
4.5.1 Transport of FD-4 across excised intestinal tissues after application of micro-beads consisting of Pharmacel® and FD-4 (control group).....	71
4.5.2 Transport of FD-4 across excised intestinal tissues after application of micro-beads containing <i>Aloe vera</i> gel.....	72
4.5.3 Transport of FD-4 across excised intestinal tissues after application of micro-beads containing <i>Aloe vera</i> whole leaf extract.....	73
4.5.4 Transport of FD-4 across excised intestinal tissues after application of micro-beads containing chitosan.....	74
4.5.5 Transport of FD-4 across excised intestinal tissues after application of micro-beads containing <i>N</i> -trimethyl chitosan chloride (TMC).....	75
4.5.6 Transport of FD-4 across excised intestinal tissues after application of micro-beads containing sodium glycocholate hydrate.....	76
4.5.7 Transport of Lucifer Yellow.....	76
4.5.8 Comparison of the FD-4 delivery across excised pig intestinal tissues from all the micro-bead formulations.....	78
4.6 CONCLUSION.....	79
CHAPTER 5 FINAL CONCLUSIONS AND FUTURE RECOMMENDATIONS.....	80

5.1 FINAL CONCLUSIONS.....	80
5.2 FUTURE RECOMMENDATIONS.....	81
REFERENCES	82
ADDENDUM A.....	89
ADDENDUM B.....	99
ADDENDUM C.....	100
ADDENDUM D.....	102
ADDENDUM E.....	105

LIST OF TABLES

Table 1.1: Composition of the micro-beads used in <i>ex vivo</i> transport studies in order to determine their intestinal macromolecular drug delivery capabilities.....	5
Table 2.1: A list of chemical drug permeation enhancers and their mechanisms of action by which membrane permeability can be enhanced (Hamman <i>et al.</i> , 2005; Kesarwani & Gupta, 2013; Beneke <i>et al.</i> , 2012).....	20
Table 3.1: Concentrations of the FD-4 solutions used to construct a standard/calibration curve for evaluation of linearity.....	28
Table 3.2: Composition of the micro-bead formulations prepared in this study.....	31
Table 4.1: Mean fluorescent values of FD-4 over a specified concentration range.....	42
Table 4.2: Mean fluorescent values of LY over a specified concentration range.....	43
Table 4.3: Fluorescence values obtained during intra-day precision measurements of FD-4 as well as standard deviation and percentage relative standard deviation (%RSD) values.....	44
Table 4.4: Fluorescence values obtained during intra-day precision measurements of LY as well as standard deviation and percentage relative standard deviation (%RSD) values.....	45
Table 4.5: Fluorescence values obtained during inter-day precision measurements of FD-4 as well as standard deviation and percentage relative standard deviation (%RSD) values.....	46
Table 4.6: Fluorescence values obtained during inter-day precision measurements of LY as well as standard deviation and percentage relative standard deviation (%RSD) values.....	47
Table 4.7: Fluorescence values of the blanks (KRB buffer) for FD-4.....	48
Table 4.8: Fluorescence values of the blanks (KRB buffer) for LY.....	48
Table 4.9: Percentage recovery of FD-4 as an indication of accuracy of the fluorometric analytical method.....	53
Table 4.10: Percentage recovery of LY as an indication of accuracy of the fluorometric analytical method.....	54
Table 4.11: Quantity of FD-4 in each of the micro-bead formulations.....	56

LIST OF FIGURES

Figure 2.1: Schematic illustration representing the pathways and mechanisms of the movement of molecules across the intestinal epithelium: a) Transcellular pathway (through epithelial cells), b) Paracellular pathway (between adjacent cells), c) Receptor-mediated endocytosis and transcytosis, d) Absorption into the lymphatic circulation via M-cells of Peyer's patches (Goldberg & Gomez-Orellana, 2003).....	8
Figure 2.2: Diagrammatic illustration of drug absorption from the gastrointestinal tract via the mechanism of passive diffusion (Liu <i>et al.</i> , 2009).....	9
Figure 2.3: Diagrammatic illustration of drug carrier-mediated transport across the intestinal epithelial cell membrane (Liu <i>et al.</i> , 2009).....	10
Figure 2.4: Presentation of diverse PEGylation strategies (Pfister & Morbidelli, 2014:137).....	16
Figure 2.5: Graph illustrating ideal release profile of a time controlled double phase peptide drug delivery system (Dorkoosh <i>et al.</i> , 2001).....	19
Figure 3.1: Photographs illustrating A) excised jejunum being pulled over glass tube, B) alignment of mesenteric border, C) wetting of tissue using KRB buffer, D) removal of serosa, E) cutting jejunum along the mesenteric border and F) jejunum tissue after removal from the glass tube flattened out onto filter paper.....	35
Figure 3.2: Photographs illustrating A) cutting of flattened jejunum tissue into even sized pieces, B) jejunum pieces ready to be mounted on Sweetana Grass diffusion chamber and C) mounted tissues on the half-cells with the spikes visible and filter paper on the basolateral side facing up.....	37
Figure 3.3: Photographs illustrating A) assembled half-cells, B) adding of sir-clips to hold half-cells together.....	37
Figure 3.4: Photograph illustrating assembled half-cells placed in diffusion apparatus with KRB buffer in the chambers and connected O ₂ /CO ₂ supply.....	38
Figure 4.1: Linear regression curve of FD-4 with the straight line equation and correlation coefficient (R ²).....	41
Figure 4.2: Linear regression curve of LY with the straight line equation and correlation coefficient (R ²).....	43

Figure 4.3: Graph illustrating calibration curve for FD-4 in the presence of <i>A. vera</i> gel and Pharmacel®	49
Figure 4.4: Graph illustrating calibration curve for FD-4 in the presence of <i>A vera</i> whole leaf and Pharmacel®	50
Figure 4.5: Graph illustrating calibration curve for FD-4 in the presence of chitosan and Pharmacel®	50
Figure 4.6: Graph illustrating calibration curve for FD-4 in the presence of TMC and Pharmacel®	51
Figure 4.7: Graph illustrating calibration curve for FD-4 in the presence of sodium glycocholate hydrate and Pharmacel®	52
Figure 4.8: Graph illustrating calibration curve for FD-4 in the presence of Pharmacel®	52
Figure 4.9: ¹ H-NMR spectrum of <i>N</i> -trimethyl chitosan chloride (TMC).....	55
Figure 4.10: : Pharmacel® and FD-4 micro-bead formulation particle size distribution plot	57
Figure 4.11: <i>Aloe vera</i> gel micro-bead formulation particle size distribution plot	57
Figure 4.12: <i>Aloe vera</i> whole leaf extract micro-bead formulation particle size distribution plot	58
Figure 4.13: Chitosan micro-bead formulation particle size distribution plot.....	59
Figure 4.14: TMC micro-bead formulation particle size distribution plot.....	59
Figure 4.15: Sodium glycocholate hydrate micro-bead formulation particle size distribution plot.....	60
Figure 4.16: Micrograph illustrating the surface of a micro-bead containing Pharmacel®	61
Figure 4.17: Micrograph illustrating the internal structure of a micro-bead containing Pharmacel®	61
Figure 4.18: Micrograph illustrating the surface of a micro-bead containing <i>Aloe vera</i> gel.....	62

Figure 4.19: Micrograph illustrating the internal structure of a micro-bead containing <i>Aloe vera</i> gel.....	63
Figure 4.20: Micrograph illustrating the surface of a micro-bead containing <i>Aloe vera</i> whole leaf extract.....	64
Figure 4.21 Micrograph illustrating the internal structure of a micro-bead containing <i>Aloe vera</i> whole leaf extract.....	64
Figure 4.22: Micrograph illustrating the surface of micro-beads containing chitosan.....	65
Figure 4.23: Micrograph illustrating the internal structure of a micro-bead containing chitosan.....	66
Figure 4.24: Micrograph illustrating the surface of a micro-bead containing <i>N</i> -trimethyl chitosan chloride (TMC).....	67
Figure 4.25: Micrograph illustrating the internal structure of a micro-bead containing <i>N</i> -trimethyl chitosan chloride (TMC).....	67
Figure 4.26 Micrograph illustrating the surface of a micro-bead containing sodium glycocholate hydrate.....	68
Figure 4.27: Micrograph illustrating the internal structure of a micro-bead containing sodium glycocholate hydrate.....	69
Figure 4.28: Percentage dissolution of FD-4 from micro-bead formulations containing <i>Aloe vera</i> gel (AVG), <i>Aloe vera</i> whole leaf extract (AVWL), chistosan, <i>N</i> -trimethyl chitosan chloride (TMC), sodium glycocholate hydrate (SG) and FD-4 and Pharmacel [®] (FDPH).....	70
Figure 4.29: Graph illustrating the percentage FD-4 transported across excised pig intestinal tissue during exposure to micro-beads consisting of Pharmacel [®] and FD-4 (control group without any absorption enhancing agents).....	71
Figure 4.30: Graph illustrating the percentage FD-4 transported across excised pig intestinal tissue during exposure to micro-beads containing FITC-dextran and Pharmacel [®] (control), as well as <i>Aloe vera</i> gel (AVG) as absorption enhancer.....	72
Figure 4.31: Graph illustrating the percentage FD-4 transport across excised pig intestinal tissue for micro-beads containing <i>Aloe vera</i> whole leaf extract compared to the control group (Control FDPH).....	73

Figure 4.32: Graph illustrating the percentage FD-4 transport across excised pig intestinal tissue for micro-beads containing chitosan compared to the control group (Control FDPH).....	74
Figure 4.33: Graph illustrating the percentage FD-4 transport across excised pig intestinal tissue for micro-beads containing <i>N</i> -trimethyl chitosan chloride (TMC) compared to the control group (Control FDPH).....	75
Figure 4.34: Graph illustrating the percentage FD-4 transport across excised pig intestinal tissue for micro-beads containing sodium glycocholate hydrate (SG) compared to the control group (Control FDPH).....	76
Figure 4.35: Graph illustrating the average percentage Lucifer Yellow transport.....	77
Figure 4.36: Graph illustrating the apparent permeability coefficient (P_{app}) of Lucifer Yellow solution applied to intestine after transport study.....	77
Figure 4.37: Graph illustrating the apparent permeability coefficient (P_{app}) for FD-4 after application of micro-beads containing <i>Aloe vera</i> gel (AVG), <i>Aloe vera</i> whole leaf extract (AVWL), chitosan, <i>N</i> -trimethyl chitosan chloride (TMC), sodium glycocholate (SodGly) and the control group (FDPH). * denotes a statistically significant difference from the control group based on an ANOVA analysis.....	78

CHAPTER 1

INTRODUCTION

1.1 BACKGROUND AND JUSTIFICATION

1.1.1 Drug absorption enhancement of protein and peptide drugs

Biotechnology has made it possible to produce protein and peptide drugs cost-effectively on a large scale. These drugs are pharmacologically effective after parenteral administration in the form of injections, but they are not sufficiently absorbed after oral administration to produce a pharmacological effect due to enzymatic instability and poor membrane permeability. An example of such a drug that needs to be administered on a chronic basis is insulin. Less than 1% of the insulin dose will reach the systemic circulation after oral administration. Protein and peptide drugs have relatively large molecular structures, which prevents them from being passively absorbed across the intestinal epithelial cell membranes. One solution to this problem is the co-administration of drug absorption enhancers, which are chemical substances that can increase the uptake of drugs across the intestinal epithelium without causing cell damaging or toxic effects (Renukuntla *et al.*, 2013; Aguirre *et al.*, 2016).

Absorption enhancers can increase membrane permeability of poorly absorbable drugs by means of different mechanisms such as opening of tight junctions between epithelial cells, changing the fluidity of the membrane, lowering the viscosity of the mucous layer or targeting transporter proteins (Moroz *et al.*, 2016). Tight junctions are dynamic structures found between intestinal epithelial cells that can be modulated to allow the paracellular transport of hydrophilic macromolecules through the intercellular spaces. This paracellular pathway has the advantage of avoiding enzymatic degradation of molecules that are susceptible to enzymatic degradation during the absorption process, especially inside the epithelial cells (Beneke *et al.*, 2012). Examples of chemical absorption enhancers that have shown potential to increase drug absorption after oral administration include surfactants, steroidal detergents (bile salts), fatty acids, medium chain glycerides, acyl carnitine and alkanoylcholines, *N*-acetylated α -amino acids and *N*-acetylated non- α -amino acids, chitosans and other mucoadhesive polymers (Aungst, 2000).

Co-administration of *Aloe vera* gel as well as *Aloe vera* whole leaf liquid preparations have increased the bioavailability of both vitamin C and E in humans (Vinson *et al.*, 2005). Transepithelial electrical resistance (TEER) and *in vitro* transport studies have shown that aloe gel materials have the ability to reversibly open tight junctions between intestinal epithelial cells with the potential to improve paracellular drug permeation across the intestinal epithelium (Chen *et al.*, 2009; Lebitsa *et al.*, 2012). Previous *in vitro* studies conducted, have demonstrated that

chitosan opens epithelial tight junctions in a concentration and pH-dependent manner. At an acidic pH, 0.1% chitosan increased Caco-2 cells' permeability to mannitol. However, at pH 7, at a 1% concentration, chitosan had no effect on the Caco-2 cells' TEER, and a 1.5% concentration didn't have any effect on the permeation of mannitol. It was established that a vehicle containing 1.5% chitosan at pH 6.7 increased the bioavailability of buserelin in rats from 0.1 to 5.1%. TMC has shown in previous studies to increase the permeation and/or absorption of neutral and cationic peptide analogs across intestinal epithelia. The mechanism by which TMC enhances intestinal permeability is similar to that of protonated chitosan (Aungst, 2000). Sodium glycocholate was found to be more efficient in improving the physiological availability of insulin in the large intestine (Lee & Amidon, 2002).

1.1.2 Preparation of spherical beads by means of extrusion-spheronisation

Pharmaceutical beads are spherical granules that consist of agglomerated fine powders (consisting of a mixture of active ingredients and pharmaceutical excipients) that are usually formed by addition of a binder solution or by means of a mechanical process (Gandhi *et al.*, 1999). There are many techniques that can be used to produce beads namely cross-linking, spray drying, cryopelletisation, hot-melt extrusion and extrusion-spheronisation. During the process of extrusion-spheronisation, a wetted powder mixture is forced through a screen with apertures of pre-determined size in order to produce extruded spaghetti-type cylinders. The extruded cylinders are then spheronised by rotating them on a friction plate at a specific rotation speed. The spheronisation of the extrudate occurs as a result of frictional forces generated during particle-particle and particle-equipment collisions. Once the desired sphericity of the beads/pellets are acquired, they are dried (Osarde *et al.*, 2012).

Although pharmaceutical beads are typically in the range of 0.5 – 2.0 mm for pharmaceutical applications, they may even be produced in sizes up to 3 mm in diameter (Gandhi *et al.*, 1999; Rahman *et al.*, 2009). For the purpose of this study, micro-beads with a diameter within the micrometre range (i.e. < 1 mm) (Quang *et al.*, 2011) were prepared by means of extrusion-spheronisation.

1.1.3 Models that can be used to study drug membrane permeation

The experimental models available for testing drug absorption/membrane permeation as well as to test the efficacy of drug absorption enhancers can be divided into the following classes:

- *In vivo* models (e.g. experiments in live animals such as rats);
- *In vitro* models (e.g. culturing cells in monolayers on membranes such as the Caco-2 cell line);
- *Ex vivo* models (e.g. excised animal intestinal tissues mounted in diffusion chambers);

- *In silico models* (e.g. simulations on computers).

Ex vivo drug permeation experiments can be conducted across excised animal intestinal tissues after the excised tissues are being mounted in a diffusion apparatus. The excised tissues are usually obtained from animals slaughtered at an abattoir and taken to the laboratory. The tissues are then mounted between acrylic half-cells of the diffusion chambers and a physiological buffer is circulated parallel to the tissue with the help of a gas lift, whilst a constant temperature is maintained by means of a heating block. Pig intestinal tissues are often used for drug permeation studies due to the anatomical as well as physiological similarities of this animal's gastrointestinal tract with that of the human gastrointestinal tract (Sjogren *et al.*, 2014:99-151; Hatton *et al.*, 2015).

1.2 RESEARCH PROBLEM

The discovery of insulin as an effective treatment for type 1 diabetes mellitus patients brought hope to a large population of people diagnosed with this metabolic disease. Unfortunately, insulin therapy requires multiple daily subcutaneous injections over the entire life span of these patients. Due to the obvious drawbacks of injections, there has always been a need to deliver insulin at therapeutic levels via the oral route of administration (Wallis *et al.*, 2014). Although research on chemical drug absorption enhancing agents commenced about five decades ago, their development into oral dosage forms has been hampered by the lack of reproducibility as well as toxicity concerns (Maher & Brayden, 2012). Drug delivery research indicated that simpler solubilising technologies were more successful in the oral delivery of macromolecular drugs than other complicated approaches. This renewed interest in drug absorption enhancement by formulation of solid oral dosage forms that contain multi-functional excipients capable of enhancing the bioavailability of protein and peptide drugs (Brayden & Maher, 2010). Furthermore, reversible opening of tight junctions between epithelial cells remains one of the most promising strategies to deliver protein drugs systemically by means of the oral route of drug administration (Rosenthal *et al.*, 2012). An effective and safe drug absorption enhancing agent has yet to be found that can consistently deliver macromolecular drugs across the intestinal epithelium into the systemic circulation in therapeutic doses at an affordable price.

1.3 AIM AND OBJECTIVES

1.3.1 General aims

The aim of this study was to develop and evaluate different dosage forms for macromolecular drug delivery across the intestinal epithelium by incorporating selected absorption enhancers into micro-beads prepared by means of extrusion-spheronisation.

1.3.2 Objectives of the study

- To prepare different micro-bead dosage forms ($\leq 500 \mu\text{m}$ in diameter) by means of *extrusion-spheronisation*, each containing a different selected absorption enhancer (i.e. *A. vera* gel, *A. vera* whole leaf material, chitosan, *N*-trimethyl chitosan chloride (TMC), sodium glycocholate) and a model compound (i.e. fluorescein isothiocyanate (FITC)-dextran) representing macromolecular drugs.
- To characterise the micro-bead formulations in terms of composition, size, and drug release profiles.
- To validate a fluorometric analytical method for measurement of FITC-dextran in the transport samples by means of linearity, specificity, accuracy, precision, limit of detection and limit of quantification.
- To evaluate the effectiveness of the micro-bead preparations to deliver the model macromolecular compound across excised pig intestinal tissues in a Sweetana-Grass diffusion apparatus by means of permeation studies in the apical-to-basolateral direction.

1.4 ETHICS REGARDING RESEARCH

An ethics application was approved under application number NWU-00025-15-A5 for experimental procedures on excised pig intestinal tissues. The tissues were collected at an abattoir from animals slaughtered routinely for meat production purposes. The animals were euthanised at this abattoir by means of electric stunning followed by exsanguination, which is an internationally acceptable method of euthanasia of animals slaughtered at an abattoir for culinary meat production. The study therefore complied with the three R's principle (reduce, refine and replace), since no animals were specifically bred or euthanised for research purposes. The excised tissue samples were disposed by means of an approved standard operating procedure (Addendum A) for biological waste at NWU (Pharmacien SOP001 v02 Biological waste management).

1.5 EXPERIMENTAL SETUP

During this study, the effect of selected drug absorption enhancing agents formulated into micro-beads on the permeation of a macromolecule (i.e. FITC-dextran) was tested across excised pig intestinal tissues. The micro-bead formulations (Table 1.1) were prepared by means of extrusion-spheronisation and evaluated in terms of physical and chemical properties as well as drug delivery characteristics using an *ex vivo* diffusion model.

Table 1.1: Composition of the micro-beads used in *ex vivo* transport studies in order to determine their intestinal macromolecular drug delivery capabilities

Micro bead formulation	Composition
Formulation 1	Micro-beads containing <i>Aloe vera</i> whole leaf extract 10% w/w, Pharmacel [®] 89.7% and FITC-dextran 0.3% w/w
Formulation 2	Micro-beads containing <i>Aloe vera</i> gel 10% w/w, Pharmacel [®] 89.7% and FITC-dextran 0.3% w/w
Formulation 3	Micro-beads containing chitosan 10% w/w, Pharmacel [®] 89.7% and FITC-dextran 0.3% w/w
Formulation 4	Micro-beads containing TMC 10% w/w, Pharmacel [®] 89.7% and FITC-dextran 0.3% w/w
Formulation 5	Micro-beads containing sodium glycocholate 10% w/w Pharmacel [®] 89.7% and FITC-dextran 0.3% w/w
Formulation 6	Micro-beads containing only Pharmacel [®] 99.7% and FITC-dextran 0.3% w/w (Control group containing no absorption enhancers)

FITC-dextran = Fluorescein isothiocyanate dextran. TMC = *N*-trimethyl chitosan chloride

1.6 LAYOUT OF DISSERTATION

A brief introduction, the aims and objectives as well as the motivation as to why this study was undertaken is provided in Chapter 1. Chapter 2 contains relevant background literature regarding macromolecular drug absorption enhancers and transport models. The scientific methods that were followed as well as the materials used in this study are described in Chapter 3. Results obtained from the study are presented and discussed in Chapter 4. A final conclusion is reached in Chapter 5 along with future recommendations for further studies.

CHAPTER 2

LITERATURE REVIEW ON THE DEVELOPMENT OF MICRO-BEADS FOR EFFECTIVE ORAL DELIVERY OF MACROMOLECULAR DRUGS

2.1 INTRODUCTION

The introduction of recombinant DNA technology paved the way for large-scale peptide and protein production. Therapeutic peptides and proteins tend to have low membrane permeability due to their relatively large molecular structures and because they are susceptible to enzymatic degradation. Since the oral bioavailability of peptide and protein drugs is encumbered by the aforementioned properties, these type of drugs are commonly administered by means of injections. Insulin is a particularly good candidate for oral delivery because when injected, insulin does not follow normal physiological release patterns. Whilst effective, injections have a number of drawbacks such as causing pain and infections, which reduce patient compliance (Wallis *et al.*, 2014).

In general, very few peptide and protein drugs have been formulated in oral dosage forms. When insulin is administered orally for example, less than 1% of the dose reaches the systemic circulation. If insulin could be effectively delivered into the systemic circulation by means of the oral route of drug administration, it would increase patient compliance as well as mimic the normal physiological process of insulin secretion more realistically (Aguirre *et al.*, 2016).

One promising way of overcoming the problem of low bioavailability is to include a membrane permeation enhancer in the oral dosage form. In fact, inclusion of chemical permeation enhancers in oral drug delivery systems have shown potential to deliver macromolecular drugs across intestinal epithelial membranes in sufficient quantities to reach the systemic circulation at therapeutic levels in order to exert a pharmacological response (Renukuntla *et al.*, 2013). Many compounds from natural origin, for example *Aloe vera* gel and whole leaf materials, have exhibited the capacity to increase the transport of insulin across human intestinal epithelial cell culture monolayers (Caco-2) (Chen *et al.*, 2009).

Drug delivery research indicated that simpler solubilising technologies were more commercially successful than other complicated formulation approaches, which renewed interest in oral drug absorption enhancement. Functional excipients that are generally regarded as safe or that are components of foodstuff are particularly of interest as effective drug absorption enhancers (Brayden and Maher, 2010). Furthermore, selective and reversible opening of tight junctions between epithelial cells remains one of the most promising strategies to deliver macromolecular drugs systemically by means of the oral route of drug administration (Rosenthal *et al.*, 2012).

2.2 DRUG ABSORPTION FROM THE GASTROINTESTINAL TRACT

Absorption of a drug from the gastrointestinal tract after oral administration can be defined as the movement of the drug molecules across the intestinal epithelial membranes and appearance of the unchanged drug in the blood draining the gastrointestinal tract (Mayersohn, 2002). Two pathways and various drug absorption mechanisms across the intestinal epithelium have been identified. A compound can either be absorbed by the paracellular pathway (transport through the intercellular spaces between cells) or by the transcellular pathway (transport through the epithelial cells) as schematically illustrated in Figure 2.1. More than 99.9% of the total surface area (microvilli with absorptive cells) is occupied by the transcellular pathway and therefore most compounds are therefore absorbed by this pathway (Versantvoort *et al.*, 2000). Absorption mechanisms include carrier mediated transport (active or facilitated), simple diffusion or pinocytosis. The basolateral membrane and other plasma membranes have similar permeability properties (Liu *et al.*, 2009).

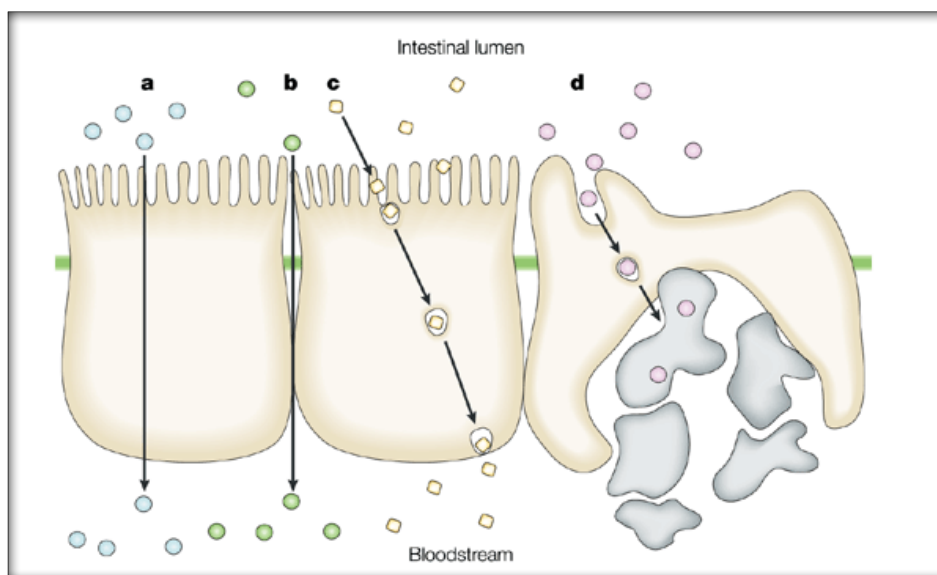


Figure 2.1: Schematic illustration representing the pathways and mechanisms of the movement of molecules across the intestinal epithelium: **a)** Transcellular pathway (through epithelial cells), **b)** Paracellular pathway (between adjacent cells), **c)** Receptor-mediated endocytosis and transcytosis, **d)** Absorption into the lymphatic circulation via M-cells of Peyer's patches (Goldberg & Gomez-Orellana, 2003)

The paracellular pathway represents the aqueous extracellular space that separates adjacent cells. Paracellular drug uptake requires the transfer of molecules through a region of densely packed, hydrophobic intercellular proteins referred to as the “tight junctions” that reduces paracellular movement of solutes (Artursson *et al.*, 2012:282).

2.2.1 Drug absorption mechanisms

2.2.1.1 Transcellular passive diffusion

Transcellular passive diffusion can be described as the process where drug molecules move from a high concentration in the gastrointestinal tract lumen fluids via the cellular lipid bilayer membrane to a low concentration in the blood. Drug molecules have to pass across the apical membrane of epithelial cells and then move across the cytoplasm before exiting the cells via the basolateral membrane (Liu *et al.*, 2009; Kerns & Di, 2008). No external energy is used and there are three factors that determine the rate of transport, which include the membrane character, drug concentration gradient across the membrane and the physico-chemical properties of the drug molecules (Shargel *et al.*, 2005).

Absorption via passive diffusion can only occur once the drug is dissolved. After drug dissolution has occurred in the aqueous fluids present in the lumen of the gastrointestinal tract, the drug molecules partition into the lipoidal-like epithelial membrane (apical membrane) and then partition out of the membrane into the cytoplasm. The drug molecules then diffuse through the epithelial cell's cytoplasm to the basolateral membrane. Due to a constant blood flow and distribution of the drug molecules into the tissues, a lower drug concentration is sustained in the blood compared to that found at the site of absorption (Ashford, 2007). The steps involved in drug absorption via passive diffusion are schematically represented in the Figure 2.2.

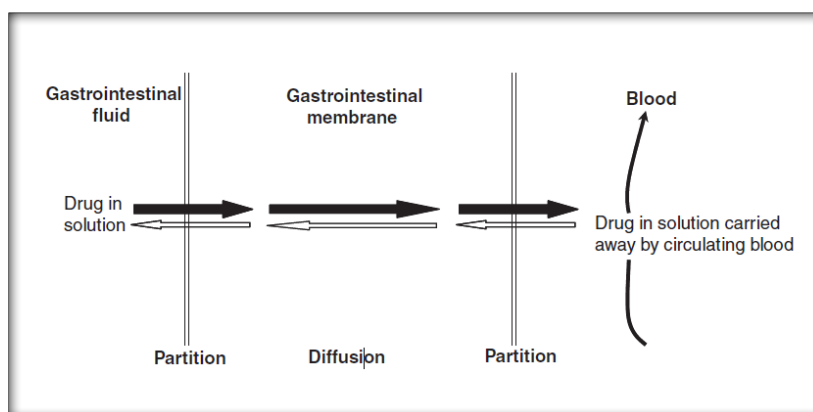


Figure 2.2: Diagrammatic illustration of drug absorption from the gastrointestinal tract via the mechanism of passive diffusion (Liu *et al.*, 2009)

2.2.1.2 Carrier-mediated transport

There are numerous carrier-mediated transport systems present in the gastrointestinal tract for the absorption of nutrients and ions that are required by the body. The carrier-mediated transport mechanism involves specific interactions between the drug molecules and the transporter proteins as illustrated in Figure 2.2 (Liu *et al.*, 2009). Transporter proteins can be divided

functionally into channels, carriers and pumps based on the mechanism by which each facilitate the transport of non-electrolytes and ions. Two types of carrier-mediated transport systems are found in the human body namely active transport and facilitated diffusion (Grass, 2012; Dobson & Kell, 2008).

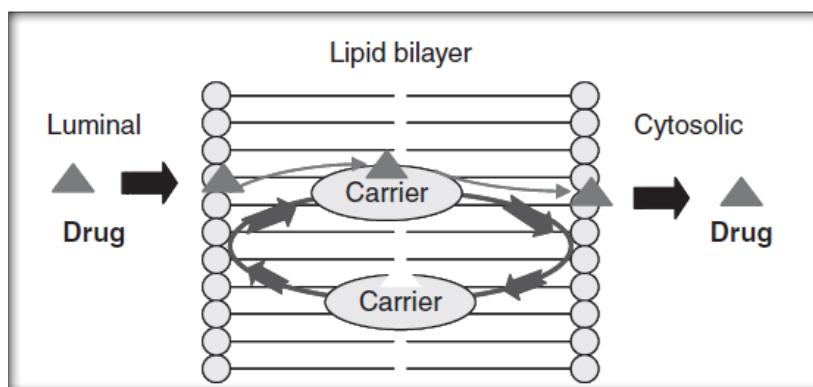


Figure 2.3: Diagrammatic illustration of drug carrier-mediated transport across the intestinal epithelial cell membrane (Liu *et al.*, 2009)

2.2.1.2.1 Active transport

Unlike passive diffusion, active transport of drug molecules involves the participation of transporter proteins in the apical cell membrane of the columnar absorptive epithelial cells in the absorption process. A transporter protein is accountable for binding to a drug molecule and thereafter transporting it through the membrane. There are substances that can be simultaneously absorbed by means of carrier-mediated transport and passive diffusion. Normally when both transport mechanisms are present, the carrier-mediated process's contribution to the general absorption rate decreases with an increase in concentration and is negligible at an adequately high concentration (Liu *et al.*, 2009).

A carrier-drug complex is established when a transporter protein or carrier binds to the drug molecule and the complex is then transported across the membrane. On the other side of the epithelial membrane, the drug molecule is liberated. The carrier returns to the cell membrane surface after drug delivery and awaits the arrival of another drug molecule (Asford, 2007b). Not all drugs will be transported by carriers because they are selective and only bind to substrates. Furthermore, transporter proteins are susceptible to saturation because only a limited number of carrier molecules are present in the gastrointestinal tract (Shargel *et al.*, 2005).

Active transport occurs against a concentration gradient (i.e. transport occurring from a low to high concentration). This transport process is energy-consuming and acquires it either from

hydrolysis of ATP or from a trans-membranous sodium gradient or electrical potential. Certain peptides or peptide-like drugs make use of peptide transporters for their effective absorption (Grassl, 2012).

2.2.1.2.2 Facilitated diffusion or transport

Facilitated diffusion differs from active transport with respect to the fact that it can't transport a substance against a concentration gradient. As a result, this transport mechanism does not need energy, but requires a concentration gradient to act as its driving force. However, drug molecules are transported by facilitated transport at a faster rate than anticipated for passive diffusion down the concentration gradient. This transport system is also saturable and encounters competitive inhibition by molecules of a similar chemical structure. Facilitated diffusion appears to have a minor contribution in drug absorption, except in the absorption of nucleoside analogues (Liu *et al.*, 2009).

2.2.1.3 Endocytosis

Endocytosis can be described as the transport process where membrane vesicles encircle a volume of material/fluid and invagination occurs. The invaginated material is transported to lysosomes or enzyme containing vesicles. Exocytosis occurs when some of the vesicles' contents manage to escape the enzymatic degradation and get released from the basolateral membrane. Endocytosis can be sub-divided into pinocytosis, phagocytosis, receptor-mediated endocytosis and transcytosis (Silverstein *et al.*, 1977).

2.2.1.3.1 Pinocytosis

Pinocytosis is described as the process of vesicular uptake of tiny particles (i.e. colloids, lipoproteins and immune complexes), soluble macromolecules (i.e. hormones, antibodies and enzymes), low molecular-weight solutes and fluids. Small droplets that consist of these mentioned materials and extracellular fluids are interiorised in membrane vesicles that are transported by means of endocytosis as described above (Silverstein *et al.*, 1977).

2.2.1.3.2 Phagocytosis

Phagocytosis is the uptake of relatively large particles (> 500 nm) and possibly including viruses. This uptake mechanism occurs by the apposition of a part of plasma membrane to the surface of the particles, which excludes most of the adjacent fluid if not all. Vaccines such as the polio vaccine consist of particles that are absorbed from the gastrointestinal tract by the process of phagocytosis (Asford, 2007b; Silverstein *et al.*, 1977).

2.2.1.3.3 Receptor-mediated endocytosis

Receptor-mediated endocytosis occurs when a specific receptor on the cell surface forms a tight bond with the extracellular macromolecule (the ligand). The plasma-membrane region that contains this receptor-ligand complex undergoes endocytosis, forming a transport vesicle (Ashford, 2007a). The receptor undergoes a conformational change due to the binding process that occurs between the cell surface receptor and the ligand. This conformational change causes complexes to cluster on the surface of the cell which then invaginate and separate from the membrane and layered vesicles are developed. The coating of these layered vesicles is lost once they have entered the cell cytoplasm. This sequentially results in uncoated vesicles and their contents are delivered to endosomes. The receptors that were internalised returns to the surface of the cell and further binding takes place. The internalised ligand is organised and thereafter transported to the lysosomes where degradation occurs (Sato *et al.*, 1996).

2.2.1.3.4 Transcytosis

Transcytosis can be described as a form of transcellular transport that involves transportation of various materials (i.e. macromolecules, vitamins and ions) in vesicles without enzymes across the interior of a cell and thereafter get ejected on the basolateral side of the cell. The process is possibly discriminatively receptor-mediated but at times can also be non-discriminative in the vesicles fluid stage (Di Paquale & Chiorini, 2006).

2.3 CHALLENGES ASSOCIATED WITH ORAL PEPTIDE DRUG DELIVERY

The effective delivery of peptide and protein therapeutics into the systemic circulation by means of the oral route of administration is extremely challenging. This is due to stability issues regarding enzymatic degradation and limited permeability of the gastrointestinal mucosa, leading to extremely low and erratic drug absorption (Moroz *et al.*, 2016). As a result, peptides and proteins require the parenteral route of administration to reach therapeutic levels in the systemic circulation. Unfortunately, most patients have an unpleasant experience with injections and find self-administration by means of injection generally difficult. Oral administration is a more acceptable drug delivery route of administration and is associated with a higher degree of patient compliance (Hamman *et al.*, 2005).

Physical and biochemical barriers obstruct the intestinal absorption of peptide and protein drug molecules (Hamman *et al.*, 2005). Pre-systemic degradation is an example of a biochemical barrier, while the plasma membrane of epithelial cells is an example of a physical barrier (Hochman & Artursson, 1994; Hamman *et al.*, 2005).

2.3.1 Physical barriers against peptide drug absorption

The gastrointestinal tract is mainly designed for the uptake and digestion of electrolytes, nutrients, and fluids, but also simultaneously protects humans against the systemic invasion of harmful toxins, pathogens and antigens. These protective mechanisms are present in the gastrointestinal tract to prevent the uptake of unwanted xenobiotics, which unfortunately can also counteract the absorption of drugs after oral administration. The physical barrier of the gastrointestinal tract can predominately be attributed to the epithelial cell lining, which includes the cell membranes and tight junctions found between adjacent epithelial cells. Active efflux transporter systems and the mucus layer can also act against drug absorption (Hamman *et al.*, 2005).

2.3.1.1 Intestinal epithelial cell membranes

The epithelium of the gastrointestinal tract consists of a single layer of mainly columnar cells, but this layer of cells also contains enterocytes, endocrine cells, goblet cells and Paneth cells (Hochman & Artursson, 1994). Drug compounds have to pass through this layer of epithelial cells in order to be absorbed into the blood draining the gastrointestinal tract. The phospholipid structure of the plasma membranes renders them semi-permeable. Lipid-soluble molecules can pass through the plasma membranes by passive diffusion, while the passage of large and highly charged molecules is prevented (Hamman *et al.*, 2005). Drug molecules therefore require the appropriate physico-chemical properties in terms of charge, size, lipophilicity (octanol/water partitioning), solution conformation and hydrogen-bonding potential in order to move through the lipophilic barriers of the apical and basolateral membranes (Pauletti *et al.*, 1996). Peptides and proteins are relative large and have hydrophilic characteristics, which prevent their partitioning into cell membranes (Hamman *et al.*, 2005). Tight junctions are physical structures that prevent the movement of large sized molecules through the intercellular spaces (Shen, 2003).

2.3.1.2 Unstirred water layer

A stagnant aqueous boundary layer covers the epithelial cells of the intestine, which consists of mucus, water and the glycocalyx adjacent to the intestinal wall (Lennernäs, 1998). The unstirred water layer has demonstrated *in vivo* to be of limited importance as a barrier to drug absorption for both passive and active mechanisms. The mucus layer may, however, restrict the access of large molecules (e.g. peptides and proteins) to the epithelial surface (Hamman *et al.*, 2005). Glycoproteins (mucins) form the main components of the mucus gel layer and may act as a drug absorption barrier by stabilising the unstirred water layer or through interactions found between the mucus layer components and diffusing molecules (Sinko *et al.*, 1987).

2.3.1.3 Tight junctions

The absence of proteolytic activity in the aqueous extracellular spaces between epithelial cells (paracellular pathway) makes it an attractive pathway for the delivery of peptides (Hamman *et al.*, 2005). The intercellular junctional complexes found between adjacent intestinal epithelial cells consist of three types. The different complexes include the tight junctions (zonula occludens), underlying adherence junctions (zonula adherens) as well as the basally located spot desmosomes (macula adherens). The tight junctions are the only occluding junction of these types of junctional complexes (Hamman *et al.*, 2005). It consists of a group of cytosolic and transmembrane proteins that interacts with the cytoskeleton and the membrane as well as with each other (Ward *et al.*, 2000). The tight junctions have pores or fenestrae with estimated dimensions of 3 to 10 Å. The tight junction has as a 'gate' and 'fence' function and is selectively permeable to specific small hydrophilic molecules such as certain drugs and nutrients. The gate function controls the diffusion of molecules via the paracellular pathway, and the fence function supports polar distributions of plasma membrane proteins in both apical and basolateral regions. The functional asymmetry required in the membrane is maintained by the separation present between the apical and basolateral surfaces (Hamman *et al.*, 2005). It is commonly accepted that the tight junctions are dynamic structures that can be modulated by substances to open up and thereby increase the paracellular permeability (Ward *et al.*, 2000).

2.3.2 Biochemical barriers against peptide drug absorption

The acidic environment in the stomach, digestive enzymes and luminal micro-organisms cause the degradation of peptides in the gastrointestinal tract. One of the most challenging obstacles for the effective delivery of intact peptide molecules is the enzymatic barrier due to its specific characteristics and features. An example is that of proteolytic enzymes that are omnipresent and degradation of peptides is therefore most likely to occur at more than one site. All proteases capable of peptide degradation have the possibility to occur in a given anatomical site and a peptide molecule is normally susceptible to degradation at a few linkages within the backbone of the peptide molecule (Lee *et al.*, 1991).

The pH of fluids varies significantly in the different parts of the gastrointestinal tract, influencing pH-dependent hydrolysis of drugs. Bacteria that are primarily situated within the colon secrete enzymes that are capable of reactions such as decarboxylation, deglucuronidation, amide hydrolysis, reduction of double bonds and esters, and dehydroxylation reactions. These enzymes have been employed in the designing of dosage forms for colon targeted delivery (Ashford, 2002).

Enzymes present in the gastrointestinal tract are responsible for the breakdown of dietary proteins into a mixture of sufficiently small sub-units that can be absorbed (i.e. di-peptides, tri-peptides,

and amino acids). Digestive processes are catalysed by these enzymes through hydrolytic cleavage of peptide bonds (proteases) or protein chemical modification such as phosphorylation (kinases) and oxidation (xanthine oxidases) (Lee *et al.*, 1991). Proteolysis begins in the stomach with pepsin and continues throughout the intestine. Peptide luminal degradation occurs because of its exposure to enzymes that are released from the pancreas into the intestine. Elastase, α -chymotrypsin, serine endopeptidases trypsin, and exopeptidases carboxypeptidase A and B are the most significant pancreatic proteases. Pre-systemic degradation of peptides also takes place when contact is made with enzymes associated with enterocytes, such as those found in the cytoplasm, brush border membrane, and lysosomes. Although proteins and dietary peptides are exposed to metabolism in the intestine and thereafter absorbed as amino acids, it is vital that protein and peptide drugs are transported intact into the systemic circulation and eventually to the site of action for their pharmacological actions to be exerted (Hamman *et al.*, 2005).

2.4 APPROACHES TO IMPROVE ORAL PEPTIDE DRUG

2.4.1 Chemical approaches

Chemical modification of peptides drugs can help to improve the bioavailability of these drugs by enhancing enzymatic stability, increasing intestinal permeability as well as decreasing immunogenicity (Moeller & Jorgensen *et al.*, 2008).

2.4.1.1 Analogue formation

Analogue formation is a process in which a specific amino acid in the structure of a peptide molecule can be substituted with another amino acid. These modifications can be done by substituting an L-amino acid with a D-amino acid or with a completely different amino acid. Desmopressin (DDAVP) acetate is currently on the market as treatment for diabetes insipidus. DDAVP is a cyclic analogue derived from 8-arginine vasopressin, available as an injection, nasal solution and oral dosage form (Brown, 2005).

2.4.1.2 Polyethylene glycolation (PEGylation)

The structure of peptide drugs can be modified by means of conjugation with polyethylene glycol (PEG) as seen in Figure 2.4. In the past, insulin has been successfully conjugated with PEG using an amide bond. When injected, this conjugate stayed in the systemic circulation for a longer period of time compared to the unmodified insulin and had no immunogenic, allergenic or antigenic properties. Hexal-insulin-monoconjugate-2 (HIM2) might be an apt candidate for oral delivery of insulin as clinical trials have reported bioavailability of more or less 5% after oral administration (Hinds & Kim, 2002).

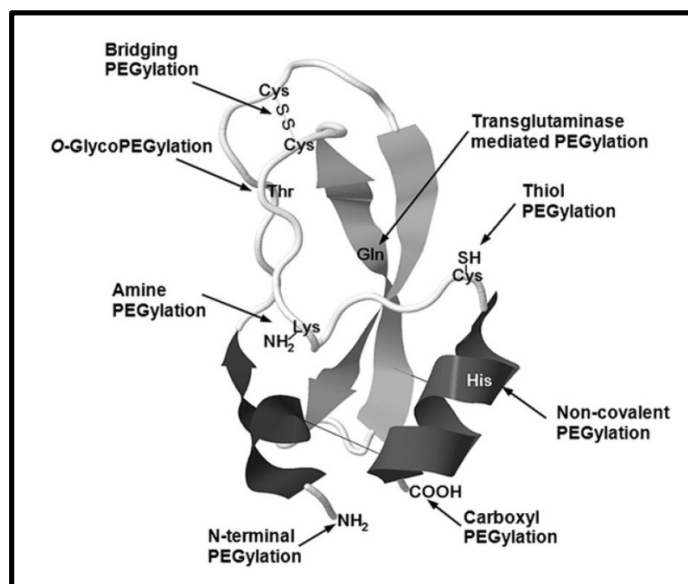


Figure 2.4: Presentation of diverse PEGylation strategies (Pfister & Morbidelli, 2014:137)

2.4.1.3 Reverse aqueous lipidisation and cell-penetrating peptides

Reverse aqueous lipidisation is a method in which fatty acids are conjugated to a protein or peptide drug. A peptide drug can then be made more lipophilic and thus increase its membrane permeation properties as well as bioavailability. Cell-penetrating peptides (CPPs) are short peptides that assist with the cellular uptake of several molecular compounds such as nano size particles, tiny chemical molecules and large fragments of DNA. CPPs can be used to cross cell membranes with minimal toxicity. These CPPs can be used as a carrier for protein and peptide molecules, but the exact mechanism of action is still unclear (Renukuntla *et al.*, 2013).

2.4.1.4 Pro-drugs

Pro-drug formation is another example of chemical modification used to increase bioavailability of drugs. Pro-drugs are pharmacologically inactive substances that need to be transformed within the body in order to become active. Once active, these drugs tend to overcome the shortcomings of the parent drugs they are based upon, such as poor solubility or membrane permeability. Whilst pro-drug strategies have been successfully used in organic based drugs, it might be challenging to apply it to peptide drugs. Due to the structural complexities of the peptide drugs, there are very few methods available to produce new pro-drugs (Anderle, 2009; Gangwar *et al.*, 1997).

2.4.1.5 Synthesis of substrates (peptidomimetics) for peptide transporters

Mammals express two proton coupled energy dependant peptide transporters known as PepT1 and PepT2, which facilitates active transport of certain peptides by use of an electrochemical proton driving force. These transporters are present in the epithelial cells of the small intestine and have a wide range of capabilities, such as being able to transport dipeptides, tripeptides and hydrophilic peptidomimetic drugs. Angiotensin converting enzyme (ACE) inhibitors, captopril and enalapril, are substrates of PepT1 which might explain their good oral bioavailability (Rubio-Aliaga & Daniel 2002).

2.4.2 Pharmaceutical approaches

Since the oral route of drug administration is considered to be one of the least intrusive delivery methods, scientists have been trying to overcome problems such as low solubility and poor membrane permeability of macromolecular drugs in the gastrointestinal tract (GIT). There are various dosage form design approaches that showed potential to increase the bioavailability of macromolecular drugs after oral administration.

2.4.2.1 Enzyme inhibitors

Enzyme inhibitors can be included in the dosage form with the peptide drug and are used to circumvent enzymatic degradation of the active ingredient in the gastrointestinal tract after oral administration. In theory, decreased pre-systemic breakdown of macromolecules such as peptides should lead to increased bioavailability. Yamamoto *et al*, (1994) evaluated the effects of five different enzyme inhibitors on the intestinal absorption of insulin in rats. It was found that sodium glycocholate, bacitracin and camostat mesilate did in fact increase the insulin bioavailability after absorption from the large intestine.

An enzyme inhibitor was discovered in the form of ovomucoids derived from the egg whites of avian species. Duck and chicken ovomucoids were tested in order to evaluate their efficacy in preventing insulin degradation by trypsin and α -chymotrypsin. The results suggested that the inhibitory effects of insulin breakdown were credited to the inhibition of the enzyme α -chymotrypsin by the duck ovomucoid (Agarwal *et al.*, 2000).

Whilst effective, there are some drawbacks associated with enzyme inhibition that need to be taken into consideration. Using enzyme inhibitors on a daily basis and in high concentrations may lead to toxicity. The use of these inhibitors may also alter metabolic patterns in the gastrointestinal tract due to impaired digestion of foods and proteins (Hamman *et al.*, 2005).

2.4.2.2 Mucoadhesive systems

Mucoadhesive drug delivery systems can prolong the intestinal residence time of drugs by adsorbing to the mucosal surface of the gastrointestinal tract. Mucoadhesion intensifies contact with the surface ensuring localised delivery, whilst also increasing the drug concentration gradient by preventing drug degradation and/or reducing dilution by the luminal fluids. Mucoadhesive binding can occur due to hydrogen bonds or ionic interactions of polymers (e.g. polyacrylates, cellulose derivatives or chitosan derivatives) with biological surfaces. In some cases, mucoadhesive polymers have been reported to also act as enzyme inhibitors or absorption enhancers (Lehr, 2000).

Thiomers, which are mucoadhesive based polymers with thiol bearing side chains, are useful as they form disulfide bonds with the surrounding cysteine rich mucus. Due to these bond formations, administered dosage forms display strong cohesive properties, which result in increased stability, prolonged residence time and also more controlled release of the administered macromolecular drug (Bernkop-Schnürch *et al.*, 2004). As mentioned above, these mucoadhesive systems do seem to be effective, but long term effects and toxicity have not yet been established for some of the mucoadhesive polymers.

2.4.2.3 Carrier type drug delivery systems

The development of carrier systems for delivery of macromolecular drugs largely focuses on circumventing the barriers to oral drug delivery. These systems aim to protect the protein and peptide drugs from enzymatic degradation, aid in transfer of drugs across the intestinal epithelium, control the release rate and target specific intestinal areas for drug delivery (Ponchel *et al.*, 1997).

Pharmaceutical micro-beads are multiple-unit dosage forms that can provide site-specific delivery and controlled release of the included drug. Beads are able to disperse freely in the gastrointestinal tract, thereby maximising drug absorption whilst also minimizing potential side effects. When formulated as a controlled release dosage form, beads are less susceptible to dose dumping than single-unit formulations (Gandhi *et al.*, 1999).

2.4.2.4 Site specific delivery

Absorption from the gastrointestinal tract can vary in the different regions depending on a number of factors such as surface area, pH, thickness, as well as composition of mucus layer and enzyme activity. Ideally, peptide drugs need to be delivered to parts of the gastrointestinal tract with a maximum absorption area along with low enzyme activity. The colon offers a relatively good environment for drug absorption due to the reduced enzymatic activity, and prolonged residence time (Khafagy *et al.*, 2007).

Poly(methacrylic-g-ethylene glycol) hydrogels were used as a site-specific oral delivery system for insulin. These hydrogels were administered to healthy as well as diabetic Wistar rats. Within 2 hours after oral administration, hypoglycemic effects were observed that lasted for up to 8 hours. Whilst in the acidic environment of the stomach, these hydrogels remain intact and unswollen. Once the hydrogel reaches the basic environment of the small intestine, it readily dissociates with an increase in pore size in order to release the insulin at the target site (Lowman *et al.*, 1999).

Another example of a hydrogel delivery system, is the use of a super-porous hydrogel (SPH) and SPH composite (SPHC) in a double phase dosage form. Figure 2.4 illustrates an ideal release profile of such a double phase time controlled hydrogel system. This hydrogel system is capable of swelling rapidly to such an extent that it is mechanically attached to the intestinal walls after which a drug can be released from the core. In order to facilitate effective transport of a drug by this system, a lag time of 20 - 30 min in drug release is required. During this time, proteolytic enzymes can be inhibited and tight junctions opened. The attachment of the SPH system to the intestine wall and subsequent swelling will provide the above mentioned lag time after which the drug can be released from the core in a burst action, in order to provide optimum absorption (Dorkoosh *et al.*, 2001).

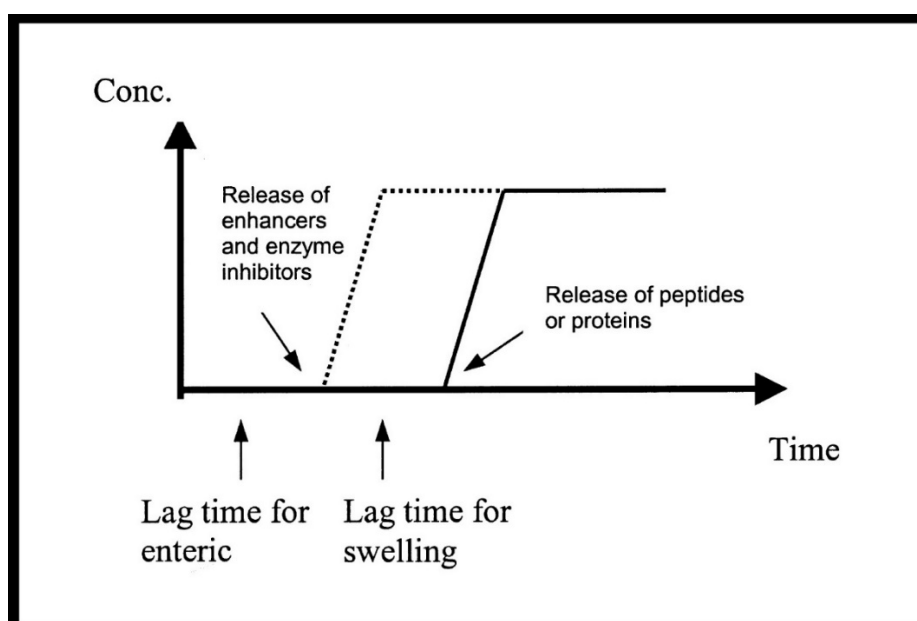


Figure 2.5: Graph illustrating the ideal release profile of a time controlled double phase peptide drug delivery system (Dorkoosh *et al.*, 2001)

2.4.2.5 Drug absorption enhancers

Drug absorption/permeation enhancers are functional excipients that are able to reversibly open, or temporarily disrupt intestinal barriers whilst causing minimal tissue damage. This will in turn allow the drugs to penetrate epithelial cells and be able to enter the blood and/or lymphatic circulation (Muranishi 1990:3). The mechanism of action by which these adjuvants are able to function as drug absorption enhancers include opening of tight junctions in order to increase paracellular transport, improving membrane fluidity and decreasing mucus viscosity (Choonara *et al.*, 2014). A wide range of compounds (listed in Table 2.1) with various chemical properties have exhibited potential to be able to enhance intestinal uptake of small hydrophilic molecules as well as protein and peptide drugs.

Table 2.1: A list of chemical drug permeation enhancers and their mechanisms of action by which membrane permeability can be enhanced (Hamman *et al.*, 2005; Kesarwani & Gupta, 2013; Beneke *et al.*, 2012)

Absorption enhancers	Examples	Mechanism of action
Anionic polymers	Poly(acrylic acid) derivatives	Combination action of calcium depletion and enzyme inhibition
Bile salts	Sodium glycocholate, sodium taurodeoxycholate, sodium taurodihydrofusidate	Membrane integrity disruption by means of phospholipid solubilisation. Reduction in mucus viscosity
Cationic polymers	Chitosan salts, <i>N</i> -trimethyl chitosan chloride	Opening of tight junctions by ionic interaction with cell membrane in combination with mucoadhesive properties
Complexation	Cyclodextrins	Increases drug solubility and dissolution rate
Chelating agents	Ethylene-diamine-tetraacetic acid (EDTA), ethylene-glycol-tetraacetic acid (EGTA)	Complexation of calcium and magnesium (tight junction opening)
Efflux pump inhibitors	First, second and third generation	Altering cell membrane integrity, blocking drug binding site on P-

		glycoprotein (Pgp) and interfering with adenosine triphosphate (ATP) hydrolysis
Fatty acids	Medium chain glycerides, long chain fatty acid esters (palmitoylcarnitine)	Paracellular (dilation of tight junctions) and transcellular (epithelial cell damage or disruption of cell membranes)
Salicylates	Sodium salicylate, salicylate ion	Increasing cell membrane fluidity, decreasing concentration of non-protein thiols
Surfactants	Sodium dodecyl sulfate, nonylphenoxy (polyoxyethylene), sodium dioctyl sulfosuccinate	Membrane damage by extracting membrane proteins or lipids, phospholipid acyl chain perturbation
Toxins and venom extracts	Zonula occludens toxin (ZOT), melittin (bee venom extract)	Interaction with the zonulin surface receptor induces tight junction opening, α -helix ion channel formation, bilayer micellisation and fusion
Plant materials	<p><i>Aloe vera</i> gel and whole leaf</p> <p>Piperine</p> <p>Naringin (flavonoid glycoside in grapefruit)</p>	<p>Significantly reduces transepithelial electrical resistance (TEER) and opens tight junctions to allow paracellular transport.</p> <p>Inhibits drug metabolising enzymes, stimulates gut amino acid transporters, inhibits drug efflux and inhibits intestinal production of glucuronic acid.</p> <p>Inhibits human cytochrome P450 metabolising enzymes and inhibits efflux transport by inhibiting P-glycoprotein.</p>

2.4.2.5.1 *Aloe vera*

Aloe vera (L.) Burm.f. (*Aloe barbadensis* Miller) is a perennial xerophyte plant belonging to the *Aloe* genus. The leaves contain water storage tissue in order to survive in harsh dry areas with minimal rain fall. Water is stored in the form of viscous mucilage that accounts for the majority of the leaf volume. The pulp of *Aloe vera* leaf refers to the intact fleshy part of the leaves that include the cell walls and organelles. The mucilage or 'gel' in turn refers to clear viscous liquid contained within the parenchyma cells. The gel consists primarily of water (> 98%), whilst the remaining materials are made up of a range of compounds such as polysaccharides, enzymes, minerals and organic acids (Ni & Tizard, 2004).

Polysaccharides are the main constituents of *Aloe vera* parenchyma. The polysaccharides present are mainly mannose, cellulose, pectins, acemannan and glucomannan. Acemannan consists of a chain of partly acetylated polymanose that has been said to be the primary functional phytocomponent in *Aloe vera* gel (Beneke *et al.*, 2012).

During a study conducted by Chen *et al.*, (2009) it was found that *A. vera* was able to significantly reduce the transepithelial electrical resistance (TEER) of Caco-2 cell monolayers. This reduction indicated the opening of tight junctions between the epithelial cells that could enable larger protein and peptide molecules to be absorbed through the intestines. *A. vera* gel was able to increase the transport of insulin 2.54-fold across the Caco-2 cell monolayers compared to the control group. TEER readings returned to their original values after the *A. vera* test solutions had been removed from the cell surface, indicating no loss of structural integrity and a reversibility of the tight junction opening effect.

Vinson *et al.*, (2005) compared the oral bioavailability of vitamin C and E in the presence of *Aloe vera* (gel and whole leaf) to that of a control group. When comparing the areas under the curves, *A. vera* gel showed a 3-fold increase in bioavailability compared to the control. With the concentration of vitamin C reaching 36 μM in the presence of *Aloe vera* gel in comparison to 15 μM for the control after 8 hours, whilst after 24 hours the *A. vera* gel vitamin C combination had an increase of 18 μM compared to the 5 μM increase of the control test. Co-administration of *A. vera* gel and vitamin E exhibited a 3.7-fold increase in bioavailability, whilst *A. vera* whole leaf showed a 2-fold increase in bioavailability compared to the control group.

2.4.2.5.2 Chitosan and chitosan derivatives

Chitosan is a linear polysaccharide composed of β -(1 \rightarrow 4) linked polymers of 2-amino-2-deoxy-b-D-glucan, which is obtained by the alkaline deacetylation of chitin. Chitin is a naturally abundant polysaccharide found mainly in the exoskeleton of crustaceans, insects and some fungi (Hejazi

& Amiji, 2003). Variations in chitosan's chemical structure exist with different degrees of *N*-deacetylation and molecular weight. These chemical characteristics determine the biological properties of chitosan (Thanou *et al.*, 2000).

Chitosan has mucoadhesive properties and is capable of opening tight junctions between epithelial cells in order to increase paracellular transport of macromolecular drugs. However, the above-mentioned absorption enhancing capabilities are only exerted in an acidic environment. At neutral and basic pH values, chitosan will precipitate from the solution which renders it ineffective as an absorption enhancer. This is problematic for drug delivery systems targeting specific sites of the small intestine, for instance the jejunum or ileum (Kotzé *et al.*, 1998).

In order to overcome the solubility problems of chitosan in neutral and basic environments, a partially quaternised derivative of chitosan, *N*-trimethyl chitosan chloride (TMC), was synthesised. TMC exhibited much higher aqueous solubility over a wider pH range compared to chitosan. The substitution of the hydrogen atoms with three methyl groups on the primary amine to form a quaternary amine group is one of the main reasons for the improved solubility of TMC (Kotzé *et al.*, 1998).

A study conducted, tested the intestinal absorption of octreotide when co-administered with TMC. Using Caco-2 cell monolayers, TMC showed an increase of octreotide absorption of 34- to 121-fold. The intra-jejunal administration of a TMC/octreotide solution to male Wistar rats showed a 5-fold increase in octreotide bioavailability compared to rats receiving octreotide alone (Thanou *et al.*, 2000).

Absorption enhancing capabilities of the different degrees of quaternisation of TMC were tested on [¹⁴C]-mannitol. It was found that the absorption of [¹⁴C]-mannitol increased with an increase in the degree of quaternisation of TMC. Only polymers with a degree of quaternisation higher than 36% were able to increase permeation at a pH of 7.40. An optimum degree of quaternisation at pH 7.40 was reached at 48%. There were no further significant increases in permeation even after the degree of quaternisation was increased to 59% (Hamman *et al.*, 2002).

2.5 SUMMARY

Peptide and protein drugs usually have low membrane permeability because they are moderately large molecular structures and are susceptible to enzymatic degradation. Peptide and protein drugs are commonly administered by injections as the oral bioavailability of these drugs is affected by the above-mentioned properties. Injections can result in pain and infections thereby reducing patient compliance. Only a few peptide and protein drugs have been formulated in oral dosage forms. Insulin is a good candidate for oral delivery because it does not follow normal physiological release patterns when injected. Patient compliance would increase and the normal

physiological process of insulin secretion would be mimicked more realistically if insulin was administered effectively by the oral route.

Membrane permeation enhancers can be included in the oral dosage form to overcome the problem of low drug bioavailability. This can increase membrane permeability of poorly absorbable drugs by means of various mechanisms such as opening of tight junctions between epithelial cells, changing the fluidity of the membrane, lowering the viscosity of the mucous layer or targeting transporter proteins. Examples of chemical permeation enhancers include surfactants, steroidal detergents (bile salts), fatty acids, medium chain glycerides, acyl carnitine and alkanoylcholines, *N*-acetylated α -amino acids and *N*-acetylated non- α -amino acids, chitosans and other mucoadhesive polymers. Many compounds from natural origin have also demonstrated to be effective as absorption enhancers. *Aloe vera* gel and whole leaf materials have exhibited the ability to increase the transport of insulin across human intestinal epithelial cell culture monolayers.

The selective and reversible opening of tight junctions between epithelial cells remains one of the most promising strategies to deliver macromolecular drugs systemically by means of the oral route of drug administration.

CHAPTER 3

METHODS AND MATERIALS

3.1 INTRODUCTION

Six micro-bead formulations were prepared, each containing a different drug absorption enhancer for macromolecular drug delivery. The idea was to design multiple-unit dosage forms consisting of small particles (i.e. micro-beads) with relatively large accumulative surface areas to optimise the interaction of the drug absorption enhancing agent with the epithelial cells. Since proof of the concept has been shown for many drug absorption enhancers when applied in solutions, it is important to formulate these absorption enhancers into oral dosage forms and to evaluate their effectiveness in terms of macromolecular drug delivery across the intestinal epithelium.

To evaluate the macromolecular drug delivery potential of the drug delivery systems, they were tested using an *ex vivo* technique where excised pig intestinal tissue was mounted between half-cells in a diffusion apparatus. All the micro-bead formulations were also evaluated in terms of their physical properties, particle size distribution, dissolution and active ingredient concentration (assay).

3.2 MATERIALS

3.2.1 Materials used for micro-bead formulations

- Fluorescein isothiocyanate-dextran with a molecular weight of 4000 Da (FITC-dextran or FD-4) was purchased from Sigma-Aldrich (Johannesburg, South Africa)
- Pharmacel[®] 101 (microcrystalline cellulose) was purchased from DB Fine chemicals (Johannesburg, South Africa)
- Sodium glycocholate hydrate was purchased from Sigma-Aldrich (Johannesburg, South Africa)
- Chitosan was purchased from Warren Chem Specialties (Johannesburg, South Africa)
- *N*-trimethyl chitosan was synthesised by Dr. Righard Lemmer at the North West University (Potchefstroom, South Africa)
- *Aloe vera* gel was donated by Improve USA (Texas, United States of America)
- *Aloe vera* whole leaf extract was donated by Improve USA (Texas, United States of America)
- Lucifer Yellow was purchased from Sigma-Aldrich (Johannesburg, South Africa)

3.2.2 Materials used for dissolution studies

- Potassium dihydrogen orthophosphate was purchased from Ace chemicals (Johannesburg, South Africa)
- Di-sodium hydrogen orthophosphate was purchased from Rochelle Chemicals (Johannesburg, South Africa)
- Hydrochloric acid was purchased from Ace chemicals (Johannesburg, South Africa)

3.2.3 Materials used for particle size analysis

- Ethanol (99.5% v/v) was purchased from Ace chemicals (Johannesburg, South Africa)

3.2.4 Materials used for proton nuclear magnetic resonance

- Deuterium oxide (D₂O) was purchased from Sigma-Aldrich (Johannesburg, South Africa)

3.2.5 Materials used for transport studies

- Sodium bicarbonate was purchased from Sigma-Aldrich (Johannesburg, South Africa)
- Krebs-Ringer bicarbonate (KRB) buffer mixture was purchased from Sigma-Aldrich (Johannesburg, South Africa)
- Porcine proximal jejunum tissue was collected from the local abattoir (Potchefstroom, South Africa)
- Corning® Costar® 96-well plates were purchased from The Scientific Group (Johannesburg, South Africa)
- Syringe filters (PVDF-L, 0.45 µm) were purchased from Kayla Africa suppliers & distributors (Germiston, South Africa)

3.3 VALIDATION OF ANALYTICAL PROCEDURES

To ensure that an analytical method produces reliable and accurate data during the quantification of an active ingredient, the procedure must comply with certain requirements. In this study, FITC-dextran with a molecular weight of 4000 Da (FD-4) was used as a model compound in the *ex vivo* transport studies. Lucifer Yellow (LY), a fluorescent marker, was used to evaluate membrane integrity. LY as well as FD-4 in the transport samples was quantified by means of a fluorometric analytical method using a SpectraMax Paradigm® plate reader.

3.3.1 Linearity

Linearity of an analytical method is the ability to obtain detection values that are directly proportional to the concentration of an analyte within a given range. A stock solution was prepared by dissolving 11 mg of FD-4 in 100 ml of Krebs-Ringer bicarbonate (KRB) buffer to produce a concentration of 110 µg/ml. A working concentration of 11 µg/ml was produced by diluting 10 ml of stock solution to 100 ml. Dilutions were prepared from the working concentration as shown in Table 3.1. Samples from these solutions were transferred to a Costar® 96-well plate in duplicate. Fluorescence values obtained from these samples were plotted as a function of FD-4 concentration and a linear regression analysis was done on this standard/calibration curve using Microsoft Excel®. In order for the analytical method to be acceptable, a correlation coefficient (R^2) value of ≥ 0.995 must be obtained. The straight line obtained from the standard curve can be described by equation 3.1:

$$y = mx + c$$

Equation 3.1

Where y is the fluorescence value of the of FD-4 solution, m is the slope, x is the concentration of the analyte (FD-4) and c is the y intercept.

Linearity for Lucifer Yellow (LY) was determined by dissolving 5 mg of LY in 100 ml of KRB buffer to produce a working concentration of 50 µg/ml. Dilutions were prepared from the working concentration as shown in Table 3.1. Samples from these solutions were transferred to a Costar® 96-well plate in duplicate. Fluorescence values obtained from these samples were plotted as a function of LY concentration and a linear regression analysis was done on this standard/calibration curve using Microsoft Excel®. In order for the analytical method to be acceptable, a correlation coefficient (R^2) value of ≥ 0.995 must be obtained. The straight line obtained from the standard curve can also be described by equation 3.1, where y is the fluorescence value of the of LY solution, m is the slope, x is the concentration of the analyte (LY) and c is the y intercept.

Table 3.1: Concentrations of the FD-4 and LY solutions used to construct standard/calibration curves for evaluation of linearity

Solution	Concentration FD-4 (µg/ml)	Concentration LY (µg/ml)
1	11.000	50
2	5.500	16.667
3	2.750	5.556
4	1.375	1.852
5	0.687	0.617
6	0.343	0.206
7	0.171	0.069
8	0.085	0.023
9	0.042	0.008
10	0.021	0.003
11	0.010	0.001
12	0.005	0.0003

3.3.2 Limit of detection

The limit of detection (LOD) is the lowest amount of analyte that can be detected in a sample, but not necessarily quantified, under the stated experimental conditions (Lee, 2004).

The following equation was used to determine the LOD for FD-4 and LY measured with the fluorometric analytical method:

$$\text{LOD} = 3.3 \times \frac{\text{SD}}{\text{S}} \quad \text{Equation 3.2}$$

Where SD is the standard deviation of the response of a blank (background noise) and S is the slope of the standard curve obtained for FD-4 and LY, respectively.

3.3.3 Limit of quantification

The limit of quantification (LOQ) is the lowest amount of analyte that can accurately be determined with acceptable precision under the experimental procedures (Lee, 2004).

The following equation was used to determine the LOQ for FD-4 and LY measured with the fluorometric analytical method:

$$\text{LOQ} = 10 \times \frac{\text{SD}}{S} \quad \text{Equation 3.3}$$

Where SD is the standard deviation of the response of a blank (background noise) and S is the slope of the standard curve obtained for FD-4 and LY, respectively.

3.3.4 Precision

Precision of an analytical procedure is the ability to produce consistent results when multiple samples of the same solution are subjected to repeated measurements. Precision can be split into two different categories namely inter-day precision and intra-day precision (Shabir, 2004:214).

3.3.4.1 Intra-day precision

Intra-day precision or repeatability is a measurement of precision carried out under the same conditions, over a relatively short time period. Intra-day precision for FD-4 and LY was carried out using fluorometric analysis of samples from three different concentrations in triplicate (ICH, 2005:4) taken from three different time points on the same day between 09:00 and 15:00. In order for intra-day precision to be acceptable, a relative standard deviation (RSD) of $\leq 2\%$ should have been obtained (Shabir, 2004:214).

3.3.4.2 Inter-day precision

Inter-day precision was determined by analyzing solutions with three different concentrations on three consecutive days. In order for inter-day precision to be acceptable, a RSD of $\leq 5\%$ should have been obtained (ICH, 2005:4).

3.3.5 Specificity

Specificity is the ability of an analytical method to clearly and accurately detect an analyte in the presence of components that may interfere with the detection process (Lee, 2004).

In order to eliminate potential interferences by the other substances used in the formulations, a standard/calibration curve was constructed with FD-4 in the presence of each of the drug absorption enhancers. These standard/calibration curves were used to calculate the FD-4 concentrations in samples where the drug absorption enhancers were also present.

3.3.6 Accuracy

Accuracy is the closeness of an obtained test result to that of the true value. During this study, accuracy was determined in terms of the percentage recovery, using nine samples over three different concentration ranges. A mean recovery of $100 \pm 2\%$ is required in order for an analytical method to be deemed acceptable in terms of accuracy (Shabir, 2004:214). Nine samples of three concentrations were prepared for FD-4 (3 x 55 µg/ml, 3 x 27.5 µg/ml and 3 x 13.75 µg/ml) and LY (3 x 50 µg/ml, 3 x 25 µg/ml and 3 x 12.5 µg/ml) along with a group of series dilutions from which a calibration curve could be obtained. Samples were then analysed using a SpectraMax Paradigm® plate reader. The concentrations of samples as determined with the fluorometer were used to calculate the percentage recovery in relation to the theoretical values.

3.4 MICRO-BEAD FORMULATIONS

Six micro-bead formulations were prepared using Pharmacel® 101 as the basic filler material by means of an extrusion spheronisation technique as described below. Five formulations each containing a different drug absorption enhancer and one formulation containing Pharmacel® 101 alone (control group) were prepared. The composition of the micro-bead formulations is shown in Table 3.2.

Table 3.2: Composition of the micro-bead formulations prepared in this study

Drug absorption enhancer	Filler material (qs)	Active ingredient (0.3% w/w)	Wetting agent (water, ml)
<i>Aloe vera</i> gel (AVG) (10% w/w)	Pharmacel [®] 101	Fluorescein isothiocyanate-dextran 4000 Da	69 ml
<i>Aloe vera</i> whole leaf extract (AVWL) (10% w/w)	Pharmacel [®] 101	Fluorescein isothiocyanate-dextran 4000 Da	62 ml
Chitosan (10% w/w)	Pharmacel [®] 101	Fluorescein isothiocyanate-dextran 4000 Da	69 ml
<i>N</i> -trimethyl chitosan chloride (TMC) (10% w/w)	Pharmacel [®] 101	Fluorescein isothiocyanate-dextran 4000 Da	68 ml
Sodium glycocholate hydrate (SGH) (10% w/w)	Pharmacel [®] 101	Fluorescein isothiocyanate-dextran 4000 Da	64 ml
Control group (Pharmacel [®] 101 alone)	Pharmacel [®] 101	Fluorescein isothiocyanate-dextran 4000 Da	73 ml

3.4.1 Micro-bead preparation

All powders were weighed off (i.e. the ingredients as mentioned in Table 3.2) in separate weighing boats and added to a mixing jar. The powders were mixed for 10 min using a Turbula[®] T2C (WA Bachofen Maschinenfabrik, Germany) mixer to provide a homogenous powder mixture. The powder mixtures were each transferred to the mixing bowl of a Kenwood Chef mixer (Maraisburg, South Africa). The wetting agent (i.e. distilled water) was slowly added to each powder mixture (volumes listed in Table 3.2) whilst mixing with the Kenwood mixer. The wetted powder mass was transferred to a Type 20 Caleva[®] extruder (Caleva[®] Process Solutions, Sturminster Newton, England) where it was pressed through a 0.5 mm extrusion screen (Addendum D) at a speed of 35 revolutions per minute (rpm) in order to form spaghetti-like extrudates.

The extrudates were transferred to the bowl of the Caleva[®] spheroniser (Caleva[®] Process Solutions, Sturminster Newton, England), which was operated for 10 min at a speed of 2000 rpm to form spherical micro-beads.

The micro-beads were frozen in a -80°C freezer, after which it was dried under vacuum in a Virtis[®] Sentry 2.0 (Virtis, Gardiner N.Y. USA) lyophilizer for up to 48 h.

3.5 EVALUATION OF MICRO-BEADS

3.5.1 Assay

Assays were carried out to determine the quantity of FD-4 present in each micro-bead formulation. A sample of 500 mg of each micro-bead formulation was crushed using a mortar and pestle. The resulting powder of each micro-bead formulation was transferred to a 50 ml volumetric flask and made up to volume using distilled water. The dispersion was placed on a magnetic stirrer and stirred for 1 h. A series of dilutions were prepared using FD-4, Pharmacel[®] 101 and the absorption enhancing agent in the specific micro-bead formulation being assayed. These solutions were used to construct standard/regression curves from which the concentration in each assay dispersion (based on the fluorescence value) could be calculated. Samples (180 µl) from the assay dispersions were filtered (0.45 µm syringe filter) and placed in 96 well plates after which the fluorescence values were obtained by using a SpectraMax[®] Paradigm[®] plate reader.

The experimental value obtained for the FD-4 quantity in each micro-bead formulation was compared to the theoretical value in order to express the FD-4 content as a percentage of the intended dose (i.e. % content) by using the following equation:

$$\% \text{ Content} = \frac{\text{experimental value FD-4}}{\text{theoretical value FD-4}} \times 100 \quad \text{Equation 3.4}$$

3.5.2 Dissolution studies

Dissolution medium (phosphate buffer, (BP, 2013)) was prepared by dissolving 28.8 g di-sodium hydrogen orthophosphate and 11.45 g of potassium di-hydrogen orthophosphate in 5 liters of distilled water. The pH of the above mentioned buffer was adjusted to 6.8 by adding sufficient hydrochloric acid (0.1 M HCl).

The dissolution profiles for the formulated micro-beads were determined by using a Distek six-vessel dissolution apparatus (Distek 2500 dissolution apparatus, North Brunswick, NJ, USA) by employing the paddle method. All dissolution experiments were done in triplicate by placing 500 mg of each micro-bead formulation in a vessel at a constant paddle stirring rate of 150 rpm in 900 ml of dissolution medium. The temperature was kept constant at 37°C ± 0.5°C.

Using the auto sampler, 2 ml samples were withdrawn through a 10 μm filter from each vessel at time intervals of 15, 30, 60, 90, 120, 180, 240 and 300 min. Filtration ensured that no suspended particles from the micro-beads would be present in the samples that were analysed for FD-4 content. The dissolution medium was replenished after each sample withdrawal. Once the last sample had been withdrawn, a step was added in which the paddle speed was set to 250 rpm for 15 min, after which another sample was taken. The latter was done to ensure that all the FD-4 was released from the micro-beads. The samples were analysed using a SpectraMax[®] Paradigm[®] plate reader to determine the concentration of FD-4 released from the micro-beads at each pre-determined time point.

3.5.3 Particle size analysis

Particle size analysis was done with a Malvern Mastersizer 2000 instrument fitted with a Hydro 2000 MU dispersion unit (Malvern Instruments, Malvern, UK). Absolute ethanol was used as dispersion medium at a stirring rate of 1500 rpm.

The Hydro 2000 MU dispersion unit was filled with 500 ml of absolute ethanol and a background measurement was taken to compensate for electrical interference as well as possible interference from the dispersion medium. Upon completion of the background measurement, a sample of the appropriate micro-bead formulation was added to the dispersion unit. A sufficient quantity of the sample was added to obtain an obscuration of between 5 and 10%. After a suitable obscuration was obtained, the particle size of the sample was measured consisting of 12000 sweeps. The particle size distribution of each formulation was measured in triplicate. The average particle size and size distribution parameters were calculated with Malvern Software (Malvern Instruments, Malvern, UK).

3.5.4 Micro-bead structure and morphology

To investigate the surface morphology as well as the internal structure of the micro-beads, scanning electron microscope images were captured with an FEI Quanta 200 environmental scanning electron microscope (ESEM) (FEI Company, Netherlands).

To visualize the internal structure, a cross section of a single micro-bead from each of the different formulations were exposed by applying pressure with a scalpel blade on the micro-bead until it split in two parts. Prior to capturing the images, all samples were mounted on aluminium mounts and coated under vacuum with carbon before being sputter-coated with gold-palladium to minimize surface charge.

3.6 CHEMICAL CHARACTERIZATION OF N-TRIMETHYL CHITOSAN CHLORIDE WITH PROTON NUCLEAR MAGNETIC RESONANCE

Chemical characterization of TMC was done by means of proton nuclear magnetic resonance (^1H -NMR) spectroscopy using an Avance III 600 Hz NMR spectrometer (Bruker BioSpin Corporation, Rheinstetten, Germany). A sample of the TMC (100 mg) was dissolved in 2 ml D_2O and analysed in the NMR spectrometer at 80°C with suppression of the water peak. The degree of quaternisation was calculated in the ^1H -NMR spectra (Equation 3.5), by using the integral of the H-1 peak at δ 5.2-6.2 ppm (Hamman & Kotzé, 2001):

$$\% \text{ N,N,N-Trimethylation} = \left[\frac{[\text{N}(\text{CH}_3)_3]}{[\text{H-1}]} \times \frac{1}{9} \times 100 \right] \quad \text{Equation 3.5}$$

Where $[\text{N}(\text{CH}_3)_3]$ is the integral of the *N,N,N*-trimethyl-amino (3.8 ppm) singlet peak. The integral of H-1 represents one proton. The degree of quaternisation is expressed as the percentage trimethylation (Rúnarsson *et al.*, 2007:2662; Hamman & Kotzé, 2001).

3.7 EX VIVO TRANSPORT STUDIES ACROSS EXCISED PIG INTESTINAL

A wide variety of techniques are available to evaluate drug permeability across the intestinal epithelium. In this study, a Sweetana Grass diffusion chamber was used to perform unidirectional transport studies on excised porcine intestinal tissue. This study was conducted to evaluate the transport of a macromolecular marker compound (FD-4) in the presence of absorption enhancing excipients formulated into micro-bead formulations as shown in Table 3.2.

3.7.1 Preparation of buffer

Krebs-ringer bicarbonate (KRB) buffer was used as transport medium. In order to prepare the buffer, a mass of 1.26 g of sodium bicarbonate and an entire container of KRB buffer mixture (Sigma-Aldrich, Johannesburg) was added to a 1 l volumetric flask and made up to volume with distilled water. The buffer was placed on a magnetic stirrer and stirred for 5 min, after which the buffer was stored in a refrigerator until the experiments commenced.

3.7.2 Collection and preparation of porcine intestinal tissue

Approval was granted from the Animal Ethics Committee at North-West University under the ethics approval number: NWU-00025-15-A5 for experimental procedures on excised pig intestinal tissue (Addendum B). Porcine proximal jejunum tissue was collected from the local Potchefstroom abattoir immediately after slaughtering of pigs. Roughly 30-40 cm of excised jejunum tissue was rinsed out using cold KRB buffer, after which the tissue was stored and transported in ice cold KRB buffer.

Once in the laboratory, the dissected piece of jejunum tissue was pulled over a glass tube (Figure 3.1 A) and turned until the mesenteric border was visible (Figure 3.1 B). The tissue was constantly kept moist with KRB buffer (Figure 3.1 C), while the serosa was gently removed (Figure 3.1 D) by means of blunt dissection. Once the serosa was removed, an incision was made along the mesenteric border (Figure 3.1 E) and the tissue was removed from the glass tube and placed on wetted filter paper (Figure 3.1 F). The tissue was cut evenly (Figure 3.2 A & B) and mounted between the Sweetana Grass diffusion chamber half-cells. The apical side of the tissue was mounted facing down on the pins of the half-cells (Figure 3.2 C). If any Payer's patches were present, the tissue was removed and not used in the experiment. Once all of the half-cells were assembled (Figure 3.3 A & B), the cells were filled with transport medium and placed in the diffusion apparatus with the O₂/CO₂ supply connected (Figure 3.4).

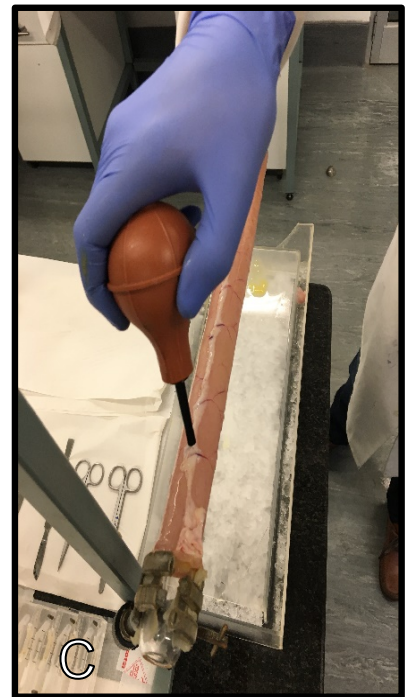
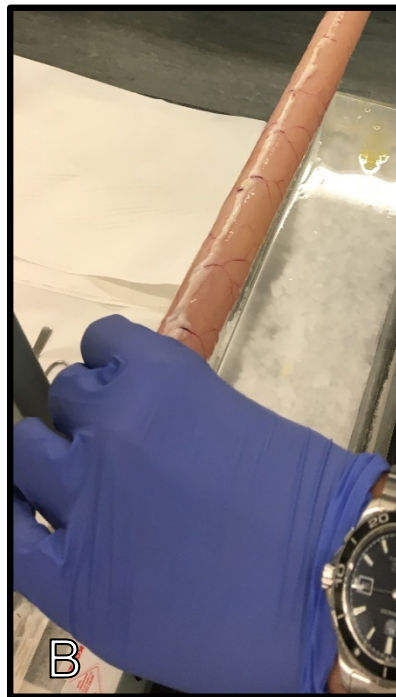


Figure 3.1: Photographs illustrating A) excised jejunum being pulled over glass tube, B) alignment of mesenteric border, C) wetting of tissue using KRB buffer, D) removal of serosa, E) cutting jejunum along the mesenteric border and F) jejunum tissue after removal from the glass tube flattened out onto filter paper

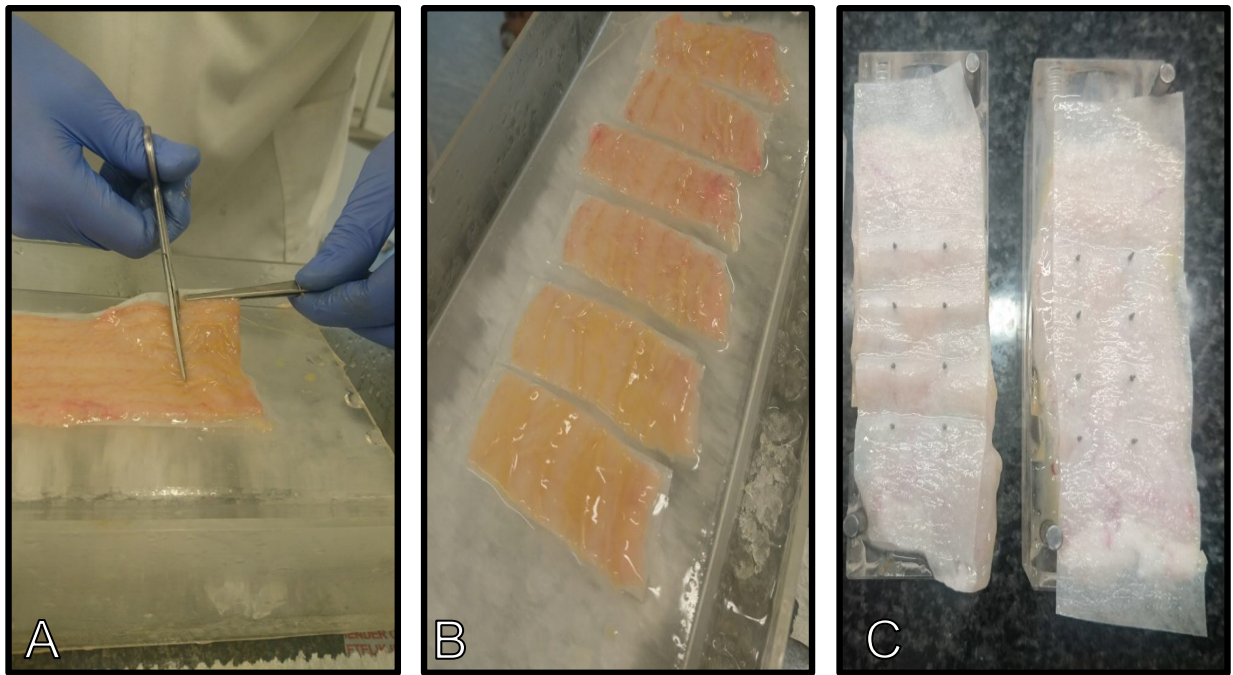


Figure 3.2: Photographs illustrating A) cutting of flattened jejunum tissue into even sized pieces, B) jejunum pieces ready to be mounted on Sweetana Grass diffusion chamber and C) mounted tissues on the half-cells with the spikes visible and filter paper on the basolateral side facing up

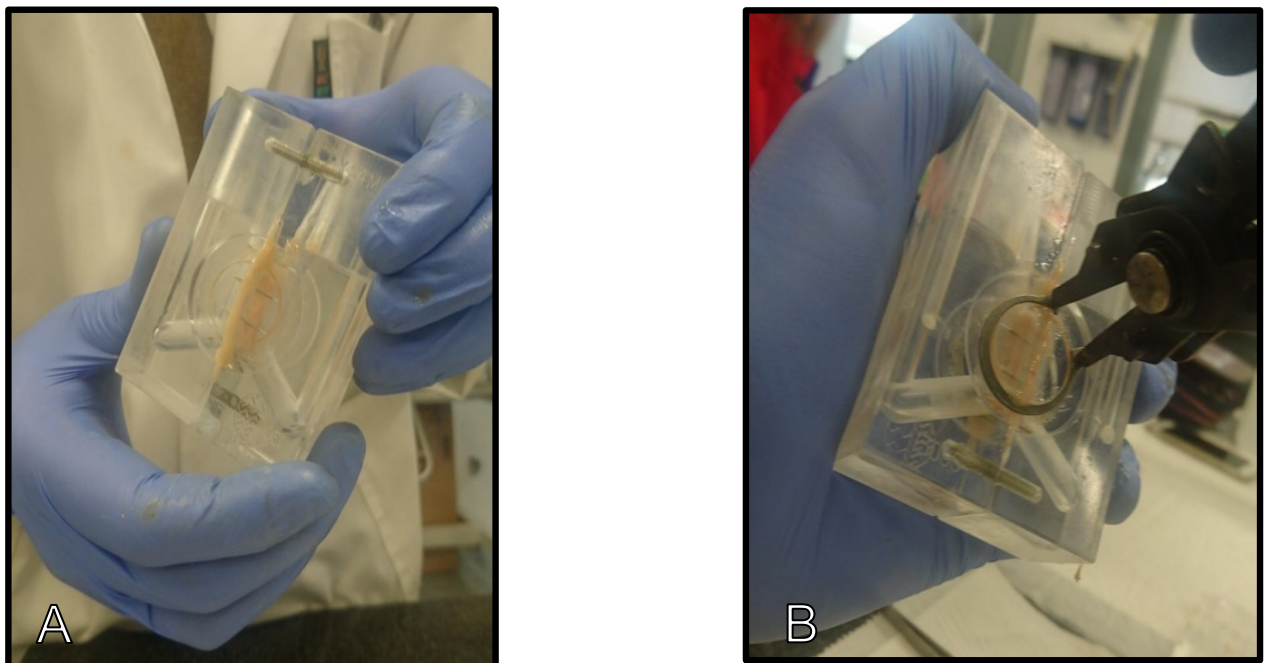


Figure 3.3: Photographs illustrating A) assembled half-cells, B) adding of sir-clips to hold half-cells together

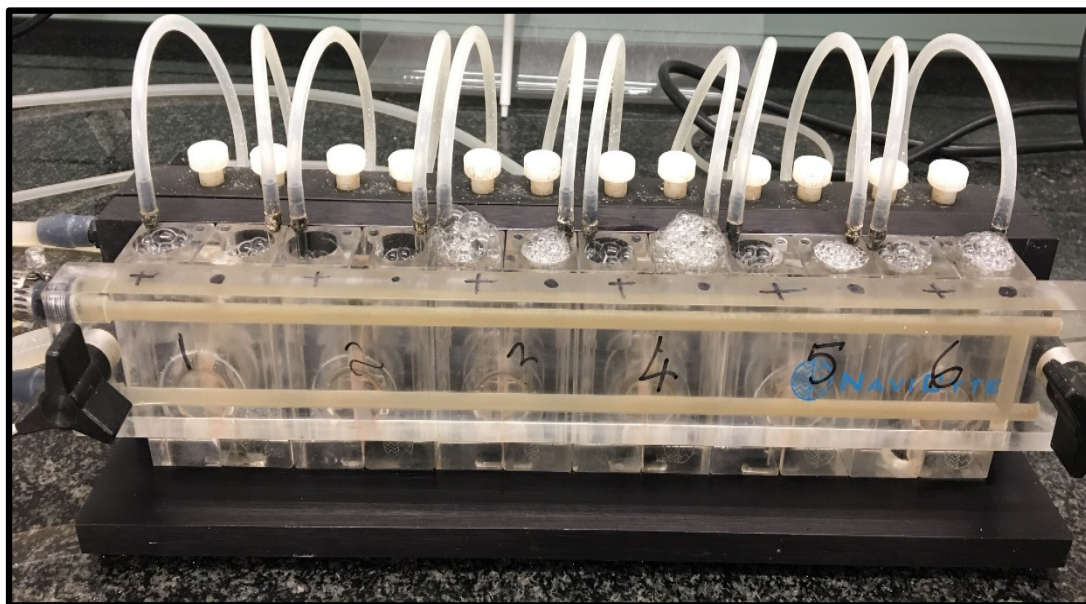


Figure 3.4: Photograph illustrating assembled half-cells placed in diffusion apparatus with KRB buffer in the chambers and connected O₂/CO₂ supply

3.7.3 Transport studies across the mounted intestinal tissues

Transport of FD-4 (formulated into micro-beads) across excised pig intestinal tissue was determined in the apical-to-basolateral direction. After the excised intestinal tissue was mounted, both the chambers (i.e. apical and basolateral) were filled with 7 ml of pre-heated KRB buffer whilst a mixture of 95% O₂ and 5% CO₂ was allowed to bubble through the buffer for 30 min to let the tissue adapt to the new environment (Grass and Sweetana, 1988).

Six samples (500 mg) from each of the micro-bead formulations were weighed off and placed in sealed containers, which were wetted with 42 ml of KRB for 15 min. The KRB buffer was aspirated (Integra vacusafe aspirator, Labotec, South Africa) from the apical side of all 6 chambers and replaced with experimental group suspensions (i.e. micro-beads (500 mg) from each formulation suspended in 7 ml KRB). Micro-beads containing FD-4 and Pharmacel[®] served as the control group for this study. Samples (200 µl) were withdrawn from the basolateral chamber every 20 min over a 2 h period and immediately replaced with 200 µl of pre-heated (37°C) KRB buffer after each withdrawal. The concentration of FD-4 in the transport samples was determined by means of a fluorometric method using a SpectraMax[®] Paradigm[®] plate reader.

The percentage FD-4 transported across the excised intestinal tissue was plotted as a function of time. Apparent permeability coefficient (P_{app}) values were calculated from these graphs using Equation 3.6 (Hellum & Nilsen, 2008:468).

$$P_{app} = \frac{dQ}{dt} \times \frac{1}{A \cdot C_o \cdot 60}$$
Equation 3.6

Where P_{app} represents the apparent permeability coefficient (cm/s), dQ/dt ($\mu\text{g.s}^{-1}$) represents the increase in the amount of drug in the receiver chamber, which is equivalent to the slope of the plot of drug transported as a function of time. A (cm^2) represents the effective surface area of the excised pig intestinal tissue between the apical and basolateral chambers and C_o is the initial FD-4 concentration in the apical chamber ($\mu\text{g.cm}^{-3}$).

3.7.4 Membrane integrity using Lucifer yellow

Lucifer yellow (LY), a fluorescent marker, was used to evaluate the integrity of the excised pig intestinal tissues mounted in the Sweetana-Grass diffusion chamber. LY solution was prepared by dissolving 2.5 mg of LY in 50 ml of KRB buffer to produce a 50 $\mu\text{g/ml}$ solution.

Samples (7 ml) containing 50 $\mu\text{g/ml}$ of LY were added to the apical side of all six chambers whilst 7 ml of preheated KRB buffer (37°C) was added to the basolateral side of all six chambers. Samples of 200 μl were withdrawn from the basolateral chambers every 20 min over a period of 2 h. All samples were analysed using a SpectraMax[®] Paradigm[®] plate reader set to an excitation wavelength of 485 nm and emission wavelength of 535 nm.

The data obtained was used to calculate the percentage transport as well as the P_{app} values for LY. In order to prove that membrane integrity had been upheld throughout the experiment, the percentage transport needed to be $\leq 3\%$, whilst the P_{app} values needed to be in the range of $8.2\text{--}9.1 \times 10^{-7}$ (Bhushani *et al.*, 2016; Sigma-Aldrich, 2013).

3.7.5 Statistical analysis

Data analyses on the transport results were performed with STATISTICA Ver 12. ANOVA's and statistically significant differences were accepted when $p < 0.05$.

CHAPTER 4

RESULTS AND DISCUSSION

4.1 INTRODUCTION

In this study, selected absorption enhancers together with a model macromolecular compound (i.e. fluorescein isothiocyanate (FITC)-dextran with a molecular weight of 4000 Da, FD-4) were incorporated into micro-beads ($\leq 500 \mu\text{m}$) that were prepared by means of extrusion spheronisation. The absorption enhancers that formed part of the micro-bead formulations included *Aloe vera* gel, *Aloe vera* whole leaf extract, chitosan, *N*-trimethyl chitosan chloride (TMC), sodium glycocholate. Most of these absorption enhancers have been tested for drug absorption enhancement in solutions, but their drug delivery performance needed to be tested in the form of dosage forms. In this study, it was decided to formulate solid oral dosage forms namely micro-beads. Although many techniques exist to prepare beads, extrusion spheronisation is a technique that produce uniformly sized beads that are spherical and is upscalable. The micro-bead formulations were evaluated in terms of particle size, morphology, FD-4 content and drug release profiles as well as FD-4 delivery across excised pig intestinal tissues.

Although the physical properties of the micro-beads were evaluated and could give some important information regarding this dosage form, such as uniformity of drug inclusion and release of the active ingredient, it was especially important to measure the dosage form's ability to deliver a macromolecular model compound across the intestinal epithelium. *Ex vivo* transport studies were conducted to measure the effectiveness of the micro-beads to deliver the model macromolecular compound (FD-4) across excised pig intestinal tissues, using a Sweetana-Grass diffusion apparatus. The percentage of FD-4 transported across the excised intestinal tissue was plotted as a function of time and the apparent permeability coefficient (P_{app}) values were calculated from these transport curves. The data obtained from this *ex vivo* transport study could indicate the effectiveness of the selected drug absorption enhancers as multi-functional excipients in a solid oral dosage form such as micro-beads.

METHOD VALIDATION RESULTS

4.2 FLUORESCENCE SPECTROMETRY METHOD VALIDATION

The analysis of Lucifer Yellow (LY) and FD-4 concentration in the assay and transport samples was done by means of fluorescence spectrometry using a Spectramax Paradigm® plate reader. Validity and reproducibility of this analysis method was confirmed by determining linearity, precision, limit of detection, limit of quantification and specificity.

4.2.1 Linearity

4.2.1.1 Linearity of FD-4

Figure 4.1 demonstrates the standard/regression curve obtained, which depicts the fluorescent values plotted as a function of FD-4 concentration. Typical fluorescence values as a function of FD-4 concentration are given in Table 4.1.

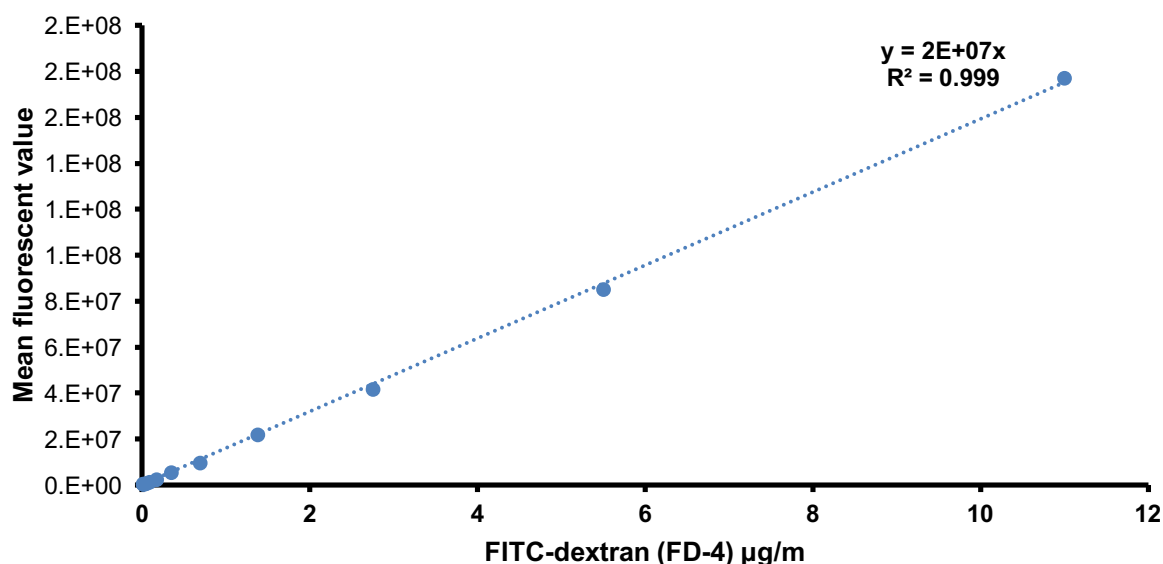


Figure 4.1: Linear regression curve of FD-4 with the straight line equation and correlation coefficient (R^2)

Table 4.1: Mean fluorescent values of FD-4 over a specified concentration range

µg/ml	Mean fluorescent value
11	177148598
5.5	85219334.3
2.75	41560342.3
1.375	21965652.3
0.688	9500312.33
0.344	5509191.33
0.172	2437919.33
0.086	1310178.33
0.043	527130.333
0.021	255802.333
0.011	425129.333
0.005	464727.333

From Figure 4.1 and Table 4.1, it is clear that the analytical method met the requirement for linearity as measured by means of the correlation coefficient (R^2) of the standard curve. The R^2 value of > 0.995 indicated that a linear relationship exists between the fluorescence values and concentration of FD-4 as measured with the Spectramax Paradigm[®] plate reader (Shabir, 2003; Singh, 2013).

4.2.1.2 Linearity of LY

Figure 4.2 demonstrates the standard/regression curve obtained, which depicts the fluorescent values plotted as a function of LY concentration. Typical fluorescence values as a function of LY concentration are given in Table 4.2.

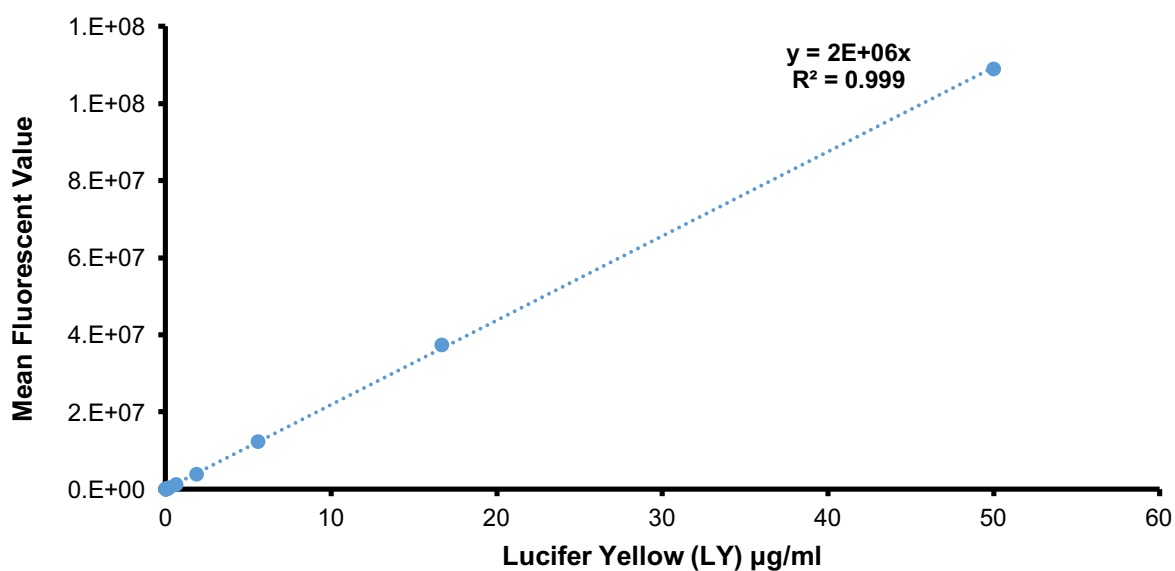


Figure 4.2: Linear regression curve of LY with the straight line equation and correlation coefficient (R^2)

Table 4.2: Mean fluorescent values of LY over a specified concentration range

µg/ml	Mean fluorescent value
50	109099528
16.667	37448948
5.556	12272638
1.852	3914932
0.617	1146500
0.206	301366
0.069	105170
0.023	51697
0.008	40986
0.003	30474
0.001	23466
0.0003	29489

From Figure 4.2 and Table 4.2, it is clear that the analytical method met the requirement for linearity as measured by means of the correlation coefficient (R^2) of the standard curve. The R^2 value of > 0.995 indicated that a linear relationship exists between the fluorescence values and concentration of LY as measured with the Spectramax Paradigm[®] plate reader (Shabir, 2003; Singh, 2013).

4.2.2 Precision

4.2.2.1.1 FD-4 intra-day precision

Table 4.3 displays the standard deviation and percentage relative standard deviation (%RSD) values that were calculated from the three FD-4 concentrations (i.e. 11 µg/ml, 5.5 µg/ml and 2.75 µg/ml) that were analysed by means of a fluorometric method at three different time points on the same day to determine the intra-day precision.

Table 4.3: Fluorescence values obtained during intra-day precision measurements of FD-4 as well as standard deviation and percentage relative standard deviation (%RSD) values

Concentration (µg/ml)	Time point	Mean fluorescence value	Standard deviation	% RSD
11	1	163468272	1894807.45	1.17
	2	162352608		
	3	159773984		
5.5	1	80846576	558504.60	0.69
	2	81571952		
	3	80473632		
2.75	1	40139776	587555.99	1.46
	2	39822312		
	3	40960880		

Table 4.3 demonstrates that the analytical method complied with the requirement for intra-day precision because all the %RSD values were $< 2\%$ (Shabir, 2003).

4.2.2.1.2 LY intra-day precision

Table 4.4 displays the standard deviation and percentage relative standard deviation (%RSD) values that were calculated from the three LY concentrations (i.e. 50 µg/ml, 25 µg/ml and 12.5 µg/ml) that were analysed by means of a fluorometric method at three different time points on the same day to determine the intra-day precision.

Table 4.4: Fluorescence values obtained during intra-day precision measurements of LY as well as standard deviation and percentage relative standard deviation (%RSD) values

Concentration (µg/ml)	Time point	Mean fluorescence value	Standard deviation	% RSD
50	1	108365091.56	878846.6	0.82
	2	107330120.89		
	3	107330120.89		
25	1	57434345.33	394090.7	0.69
	2	56469358.00		
	3	56973834.67		
12.5	1	27226753.60	311904.57	1.16
	2	27226753.60		
	3	26525780.80		

Table 4.4 demonstrates that the analytical method complied with the requirement for intra-day precision because all the %RSD values were < 2% (Shabir, 2003).

4.2.2.2.1 FD-4 inter-day precision

The fluorescence values of three different concentrations (i.e. 11 µg/ml, 5.5 µg/ml and 2.75 µg/ml) obtained for FD-4 as well as the standard deviation and %RSD values over a period of three consecutive days are given in Table 4.5.

Table 4.5: Fluorescence values obtained during inter-day precision measurements of FD-4 as well as standard deviation and percentage relative standard deviation (%RSD) values

Concentration (µg/ml)	Day	Mean fluorescent value	Standard deviation	%RSD
11	1	192701520	604151.31	0.31
	2	191697904		
	3	192782432		
5.5	1	94064128	1583206.72	1.65
	2	95901544		
	3	97216120		
2.75	1	47155456	748551.03	1.56
	2	47725184		
	3	48639296		

Table 4.5 indicates that the analytical method complied with the recommended accepted %RSD of < 5% for inter-day precision (ICH, 2005:4).

4.2.2.2.2 LY inter-day precision

The fluorescence values of three different concentrations (i.e. 50 µg/ml, 25 µg/ml and 12.5 µg/ml) obtained for LY as well as the standard deviation and %RSD values over a period of three consecutive days are given in Table 4.6.

Table 4.6: Fluorescence values obtained during inter-day precision measurements of LY as well as standard deviation and percentage relative standard deviation (%RSD) values

Concentration (µg/ml)	Day	Mean fluorescent value	Standard deviation	%RSD
11	1	109011683.20	954649.21	0.87
	2	110514439.33		
	3	111314638.22		
5.5	1	57906904.00	182339.87	0.31
	2	57713641.33		
	3	58158988.00		
2.75	1	27537871.56	95480.54	0.36
	2	27650164.67		
	3	27771689.43		

Table 4.6 indicates that the analytical method complied with the recommended accepted %RSD of < 5% for inter-day precision (ICH, 2005:4).

4.2.3 Limit of detection and limit of quantification

The limit of detection (LOD) and limit of quantification (LOQ) for FD-4 and LY was mathematically determined by using the standard deviation of the fluorescence values of the blanks (i.e. the background noise of the solvent only, the fluorescence which are shown in Table 4.7 & 4.8) and the slope of the standard/regression curve (as shown in Figure 4.1 & 4.2).

Table 4.7: Fluorescence values of the blanks (KRB buffer) for FD-4

Background noise	Average	Standard deviation
232306	226570.50	3798.50
220762		
229286		
223915		
224917		
228237		

The LOD was calculated to be 0.000779 µg/ml and the LOQ to be 0.00236 µg/ml for FD-4 measured by using the fluorometric analytical method. All the concentrations of FD-4 in the experimental samples were higher than these LOD and LOQ concentration values. This indicates the analytical method (i.e. fluorometry) was able to detect and quantify FD-4 accurately in the samples obtained in the assay and transport experiments.

Table 4.8: Fluorescence values of the blanks (KRB buffer) for LY

Background noise	Average	Standard deviation
23186	23733.67	735.38
23434		
24669		
23210		
24849		
23054		

The LOD was calculated to be 0.001031 µg/ml and the LOQ to be 0.003125 µg/ml for LY measured by using the fluorometric analytical method. All the concentrations of LY in the experimental samples were higher than these LOD and LOQ concentration values. This indicates

the analytical method (i.e. fluorometry) was able to detect and quantify LY accurately in the samples obtained in the transport experiments.

4.2.4 Specificity

To compensate for potential interferences by the excipients (i.e. Pharmacel[®] and absorption enhancers) used in the micro-bead formulations in the fluorometric analyses, standard/regression curves were constructed for FD-4 in the presence of each of these excipients. These standard curves were used for calculating FD-4 concentration in the presence of each excipient.

4.2.4.1 Calibration curve for FD-4 in the presence of *Aloe vera* gel

The calibration curve, straight line equation and correlation coefficient (R^2) value for FD-4 in the presence of *A. vera* gel and Pharmacel[®] are shown in Figure 4.3.

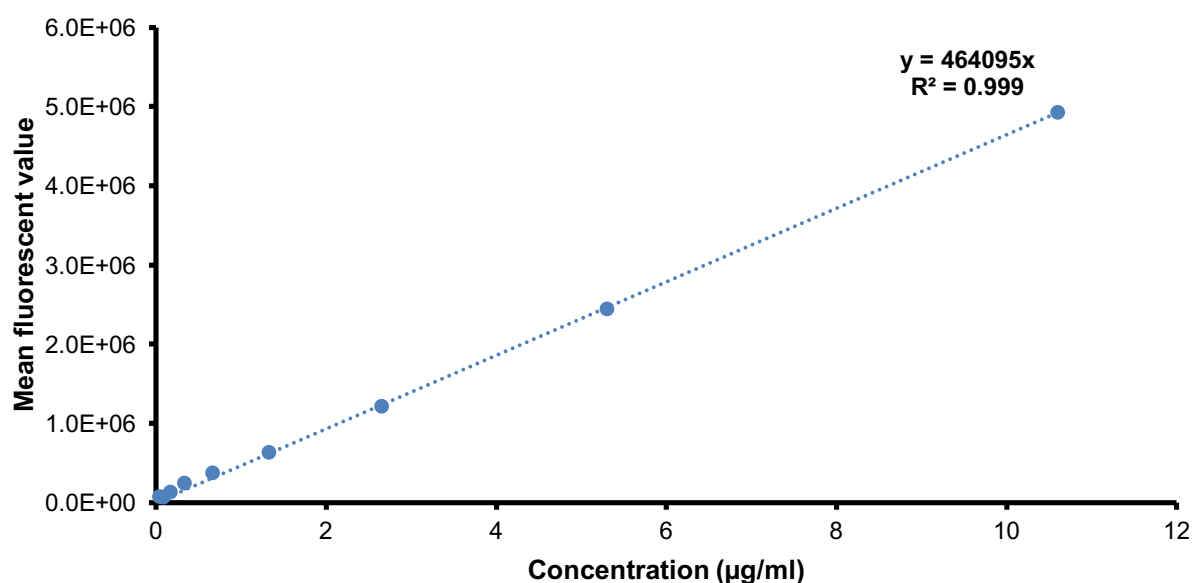


Figure 4.3: Graph illustrating calibration curve for FD-4 in the presence of *A. vera* gel and Pharmacel[®]

The calibration curve for FD-4 in the presence of *A. vera* gel and Pharmacel[®] presented with an R^2 value of 0.999, which complied with the requirement for linearity.

4.2.4.2 Calibration curve for FD-4 in the presence of *Aloe vera* whole leaf extract

The calibration curve, straight line equation and correlation coefficient (R^2) value for FD-4 in the presence of *A. vera* whole leaf extract and Pharmacel[®] are shown in Figure 4.4.

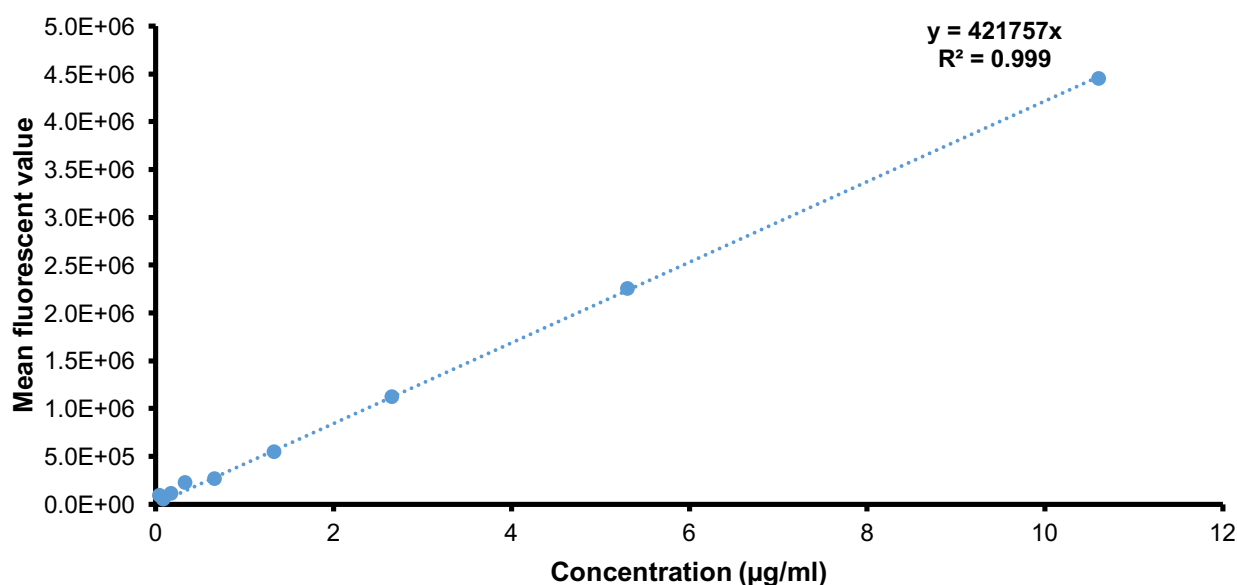


Figure 4.4: Graph illustrating calibration curve for FD-4 in the presence of *A. vera* whole leaf and Pharmacel®

The calibration curve for FD-4 in the presence of *A. vera* whole leaf extract and Pharmacel® presented with an R^2 value of 0.999, which complied with the requirement for linearity.

4.2.4.3 Calibration curve for FD-4 in the presence of chitosan

The calibration curve, straight line equation and correlation coefficient (R^2) value for FD-4 in the presence of chitosan and Pharmacel® are shown in Figure 4.5.

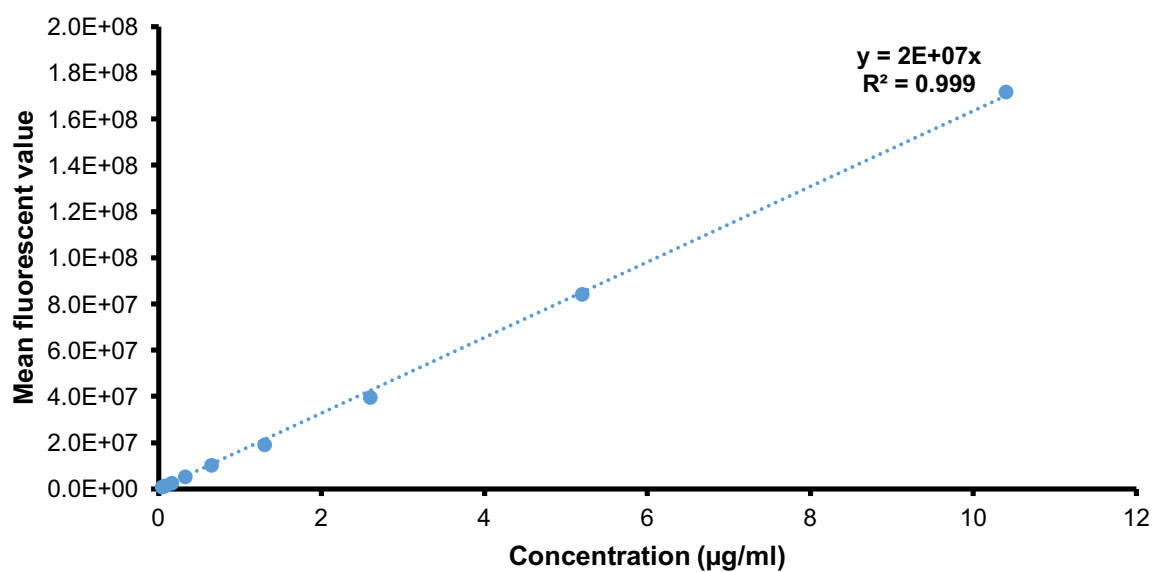


Figure 4.5: Graph illustrating calibration curve for FD-4 in the presence of chitosan and Pharmacel®

The calibration curve for FD-4 in the presence of chitosan and Pharmacel[®] presented with an R^2 value of 0.999, which complied with the requirement for linearity.

4.2.4.4 Calibration curve for FD-4 in the presence of *N*-trimethyl chitosan chloride (TMC)

The calibration curve, straight line equation and correlation coefficient (R^2) value for FD-4 in the presence of TMC and Pharmacel[®] are shown in Figure 4.6.

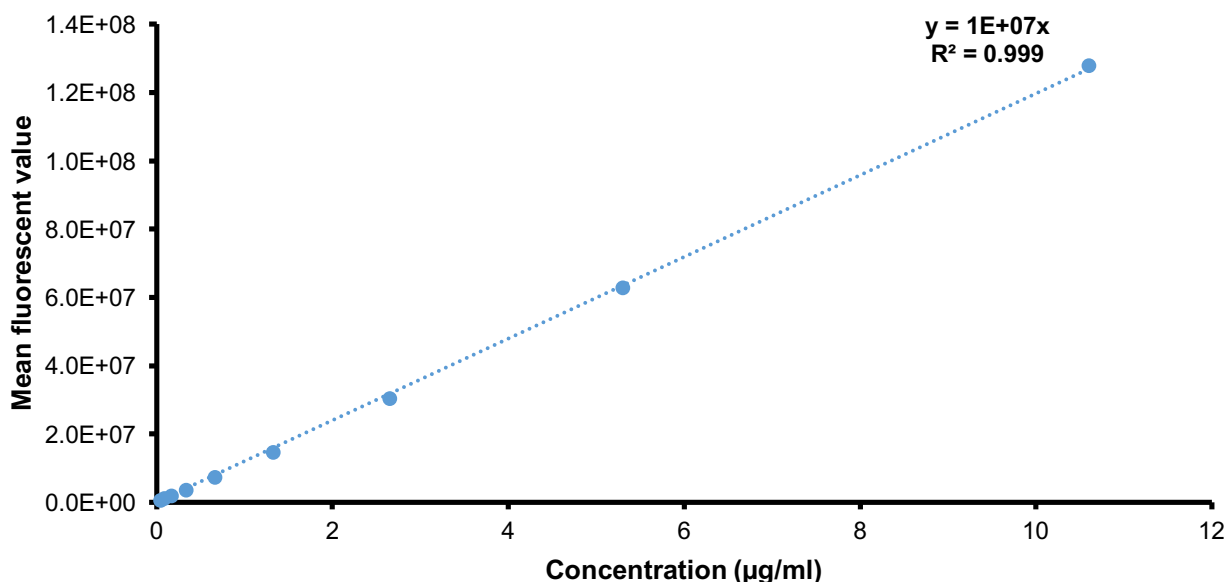


Figure 4.6: Graph illustrating calibration curve for FD-4 in the presence of TMC and Pharmacel[®]

The calibration curve for FD-4 in the presence of TMC and Pharmacel[®] presented with an R^2 value of 0.999, which complied with the requirement for linearity.

4.2.4.5 Calibration curve for FD-4 in the presence of sodium glycocholate hydrate

The calibration curve, straight line equation and correlation coefficient (R^2) value for FD-4 in the presence of sodium glycocholate hydrate and Pharmacel[®] are shown in Figure 4.7.

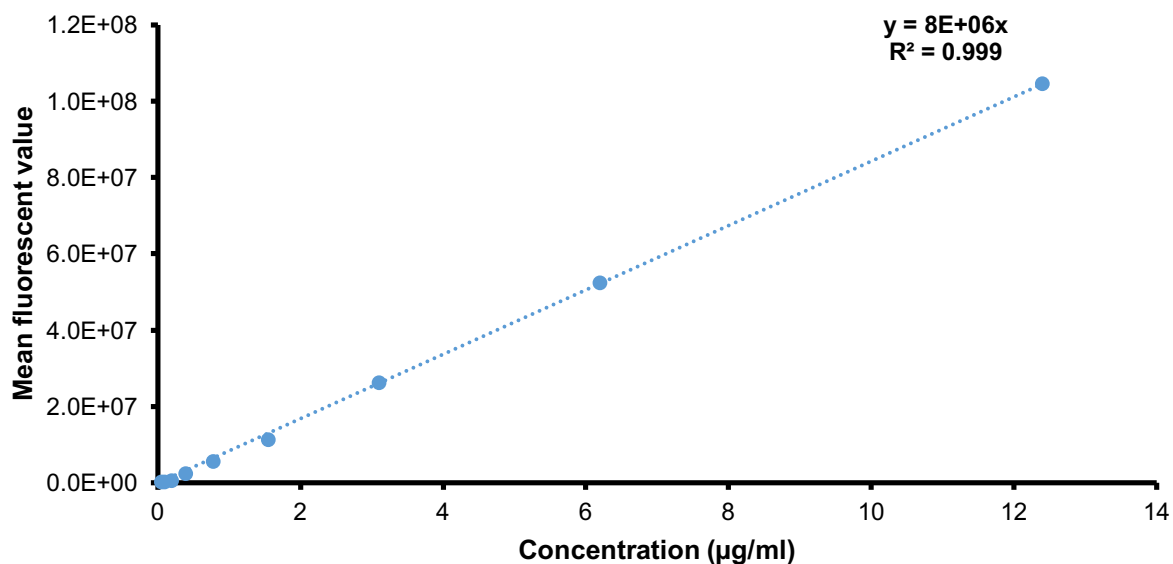


Figure 4.7: Graph illustrating calibration curve for FD-4 in the presence of sodium glycocholate hydrate and Pharmacerl®

The calibration curve for FD-4 in the presence of sodium glycocholate hydrate and Pharmacerl® presented with an R^2 value of 0.999, which complied with the requirement for linearity.

4.2.4.6 Calibration curve for FD-4 in the presence of Pharmacerl®

The calibration curve, straight line equation and correlation coefficient (R^2) value for FD-4 in the presence of Pharmacerl® are shown in Figure 4.8.

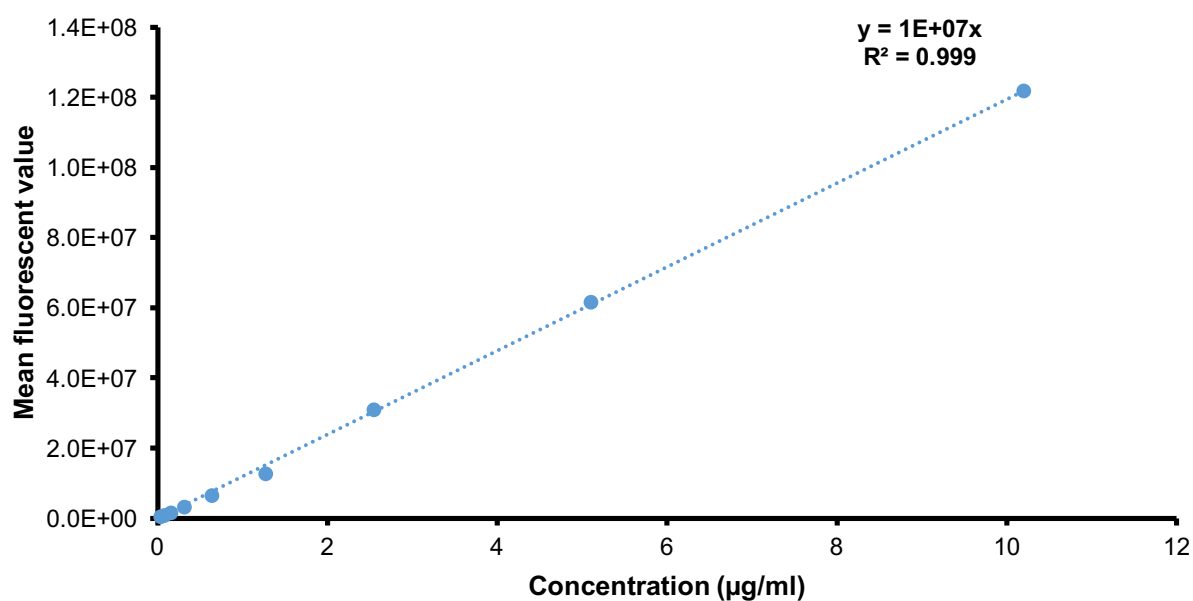


Figure 4.8: Graph illustrating calibration curve for FD-4 in the presence of Pharmacerl®

The calibration curve for FD-4 in the presence of Pharmacel[®] presented with an R^2 value of 0.999, which complied with the requirement for linearity.

4.2.5 Accuracy

Accuracy is defined as the closeness of the obtained result to that of the true value (Shabir, 2004). Recovery of solutions prepared at a specific concentration needs to be between 98% and 102% for the analytical method to be deemed accurate. Data obtained for accuracy of FD-4 are given in Table 4.9, whilst the data obtained for LY is giving in Table 4.10.

Table 4.9: Percentage recovery of FD-4 as an indication of accuracy of the fluorometric analytical method

Theoretical concentration (µg/ml)	Repeat	Measured concentration (µg/ml)	% Recovery	% Mean recovery
55	1	55.13	100.23	99.75
	2	54.99	99.98	
	3	54.48	99.05	
27.5	1	27.59	100.32	100.69
	2	28.05	101.99	
	3	27.44	99.76	
13.75	1	13.56	98.62	99.82
	2	13.73	99.86	
	3	13.89	100.99	

The mean recovery for all three concentrations of FD-4 fell within the specified range of $100 \pm 2\%$ and the analytical method thus complied with the requirements for accuracy (Shabir, 2004:214).

Table 4.10: Percentage recovery of LY as an indication of accuracy of the fluorometric analytical method

Theoretical concentration (µg/ml)	Repeat	Measured concentration (µg/ml)	% Recovery	% Mean recovery
50	1	49.47	98.94	99.95
	2	50.17	100.35	
	3	50.28	100.56	
25	1	25.07	100.29	100.27
	2	24.93	99.74	
	3	25.19	100.79	
12.5	1	12.52	100.13	99.17
	2	12.39	99.18	
	3	12.27	98.19	

The mean recovery for all three concentrations of LY fell within the specified range of $100 \pm 2\%$ and the analytical method thus complied with the requirements for accuracy (Shabir, 2004:214).

4.2.6 Validation results summary

The fluorometric analysis method for FD-4 and LY using the Spectramax Paradigm® plate reader complied with all the required validation criteria including linearity, precision, specificity, limit of detection, limit of quantification and accuracy.

4.3 CHEMICAL CHARACTERIZATION OF *N*-TRIMETHYL CHITOSAN CHLORIDE

Figure 4.9 shows the ^1H -NMR spectrum of *N*-trimethyl chitosan chloride (TMC).

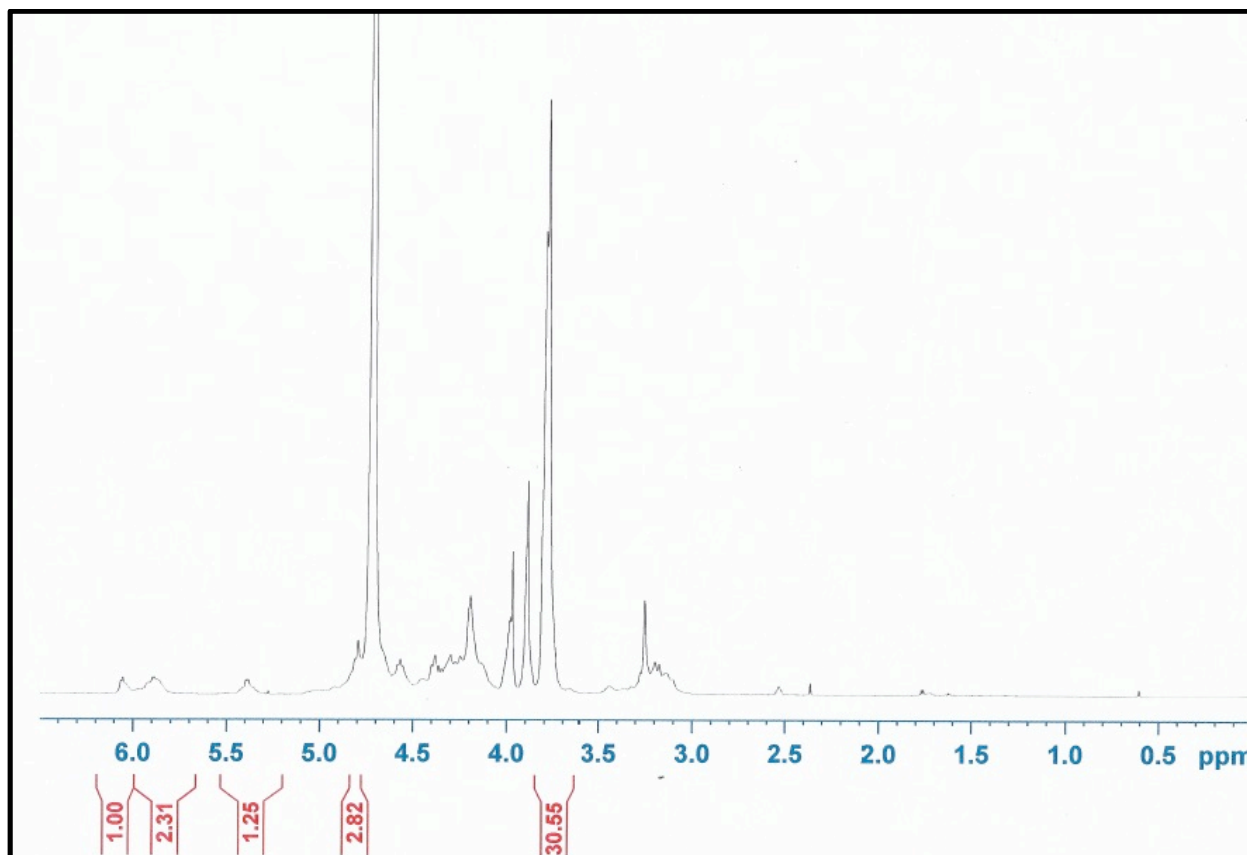


Figure 4.9: ^1H -NMR spectrum of *N*-trimethyl chitosan chloride (TMC)

$$\% \text{ } N,N,N - \text{Trimethylation} = \left[\frac{[\text{N}(\text{CH}_3)_3]}{[\text{H}-1]} \times \frac{1}{9} \times 100 \right]$$

$$= \left[\frac{[30.55]}{[7.38]} \times \frac{1}{9} \times 100 \right]$$

$$= 45.995 \% \approx 46 \%$$

From the calculations above it was determined that the degree of quaternisation of the TMC used in this study was 46%. Studies have found that an increase in the degree of quaternisation increases the absorption enhancing capabilities of TMC, with an optimal degree of quaternisation being reached at 48%. No significant increases in permeation enhancement capability was reported as the degree of quaternisation was increased above this value up to 59% (Hamman *et al.*, 2002). The TMC used in this study as absorption enhancer therefore had a degree of

quaternisation that was close to the optimal degree of quaternisation for drug absorption enhancement.

4.4 MICRO-BEAD EVALUATION

4.4.1 Assay

In order to determine the experimental quantity of FD-4 present in each micro-bead formulation, an assay was conducted on each of the six formulations. Results are given in Table 4.11, which includes the quantity of FD-4 contained in the micro-beads (expressed in µg/ml) in a 50 ml solution that was analyzed, the quantity of FD-4 (mg) per 1 g of micro-beads as well as the percentage of theoretical concentration.

Table 4.11: Quantity of FD-4 in each of the micro-bead formulations

Micro-bead formulation	Concentration FD-4 (µg/ml)	FD-4 per 1 g of micro-beads (mg)	% of theoretical concentration
<i>Aloe vera</i> gel (AVG)	38.09	3.77	125.68
<i>Aloe vera</i> whole leaf extract (AVWL)	43.95	4.23	133.76
Chitosan	27.18	2.61	90.00
<i>N</i> -trimethyl chitosan chloride (TMC)	29.91	2.99	99.35
Sodium glycocholate hydrate (SGH)	37.41	3.40	113.2
Control (FD-4 and Pharmacel [®] 101)	30.06	2.89	96.10

4.4.2 Particle size analysis

4.4.2.1 Micro-bead formulation consisting of Pharmacel[®] (Control)

The particle size and particle size distribution for micro-beads containing Pharmacel[®] and FD-4 can be seen in Figure 4.10. The particle size data obtained from the Mastersizer[®] show that the majority of Pharmacel[®] micro-beads ranged between 436.2 µm and 911.5 µm, with an average median distribution value (d(0.5)) of 623.8 µm. The average volume weighed size (D[4.3]) of the micro-beads was 654.8 µm. The span was found to be 0.76, which is representative of a relatively narrow particle size distribution. The relatively small particles observed on the left side of the histogram may be the result of powder particles or pieces of powder agglomerates that were released from the surface of the micro-beads during measurement procedure in the dispersion unit of the Malvern Mastersizer[®] apparatus.

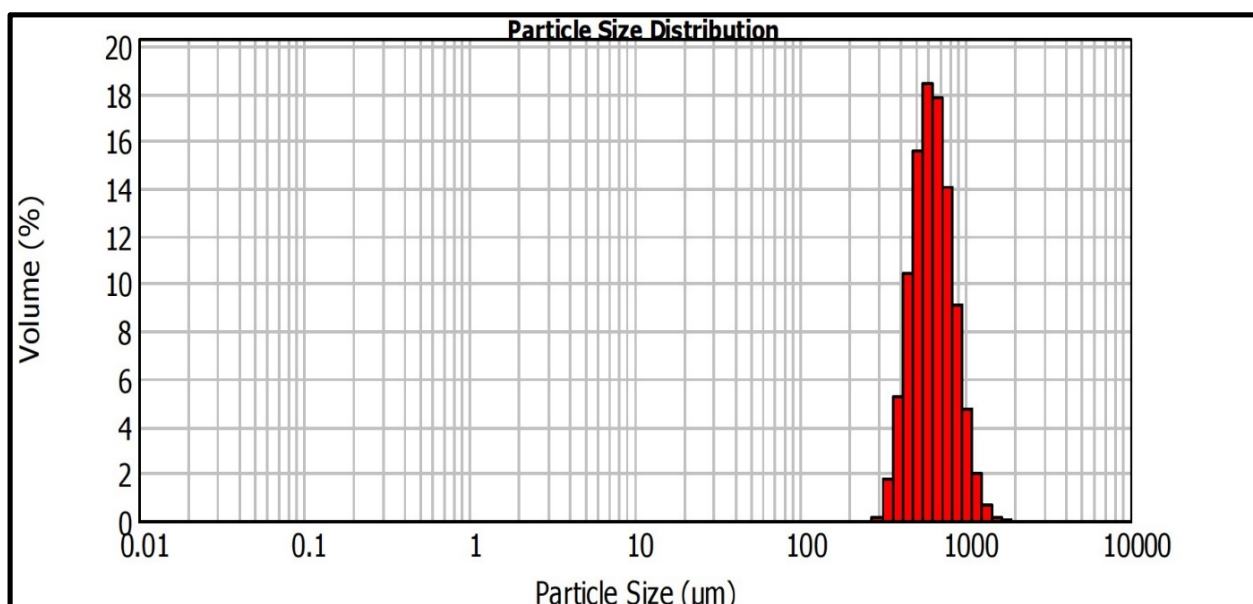


Figure 4.10: Pharmacel® and FD-4 micro-bead formulation particle size distribution plot

4.4.2.2 Micro-bead formulation containing *Aloe vera* gel

The results obtained from the particle size analysis on the Mastersizer® for micro-beads containing *A. vera* gel can be seen in Figure 4.11. The majority of *A. vera* gel containing micro-beads ranged between 405.0 µm and 717.2 µm, with an average median distribution value ($d(0.5)$) of 542.7 µm. The average volume weighed size of the micro-beads ($D[4.3]$) was 553.3 µm. The span was found to be 0.58, which is representative of a relatively narrow particle size distribution. The latter is expected of micro-beads prepared by means of extrusion spheronisation.

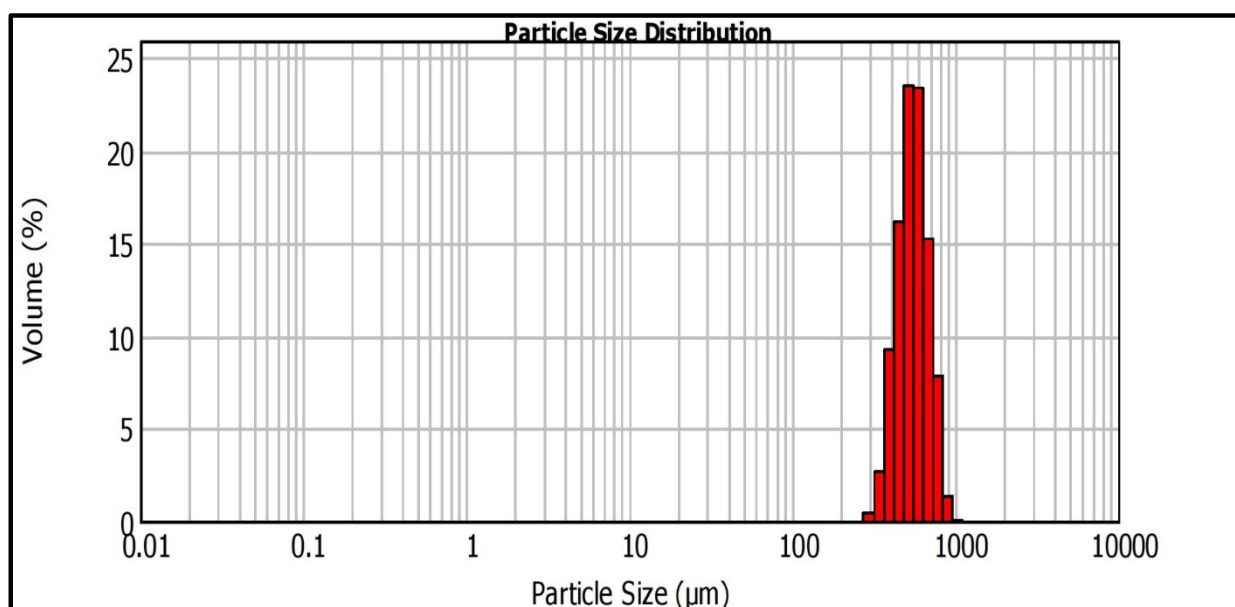


Figure 4.11: Particle size distribution plot of the *Aloe vera* gel containing micro-bead formulation

4.4.2.3 Micro-bead formulation containing *Aloe vera* whole leaf extract

The particle size analysis results for micro-beads containing *A. vera* whole leaf extract can be seen in Figure 4.12. The data obtained from the Mastersizer® show that the majority of *A. vera* whole leaf extract containing micro-beads ranged between 337.8 μm and 637.5 μm , with an average median distribution value ($d(0.5)$) of 467.9 μm . The average volume weighed size ($D[4.3]$) of the micro-beads was 479.5 μm . The span was found to be 0.64, which is representative of a relatively narrow particle size distribution, which is a physical property that is expected of micro-beads prepared by means of extrusion spheronisation.

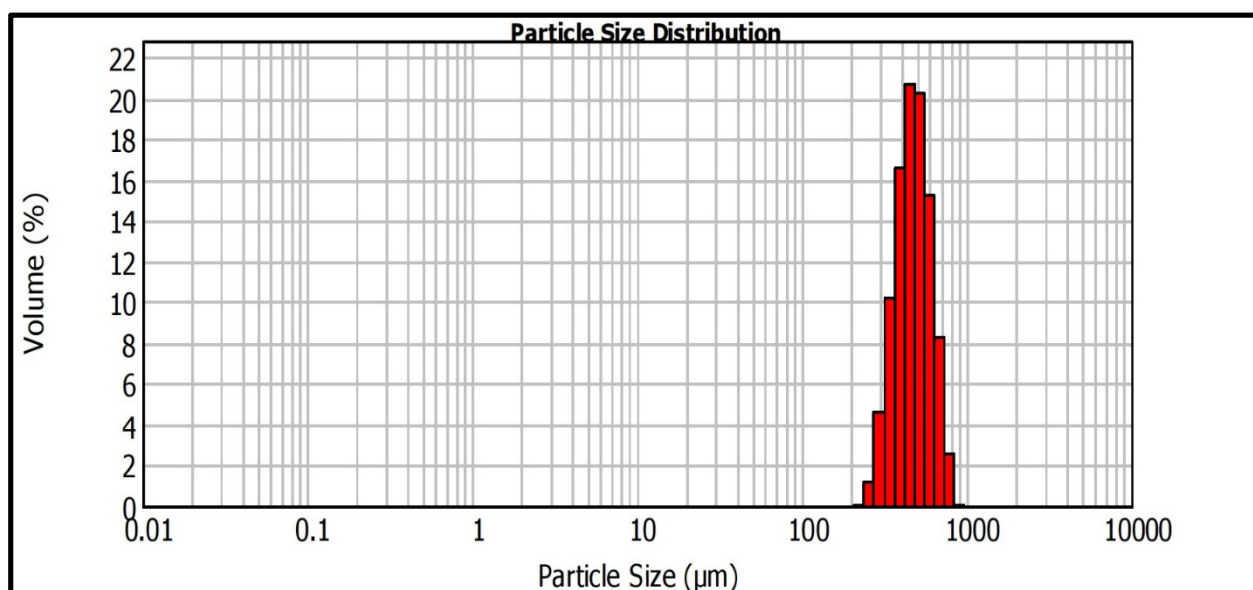


Figure 4.12: *Aloe vera* whole leaf extract micro-bead formulation particle size distribution plot

4.4.2.4 Micro-bead formulation containing chitosan

Results from the particle size analysis for micro-beads containing chitosan can be seen in Figure 4.13. The data obtained from the Mastersizer® show that the majority of chitosan micro-beads ranged between 393.4 μm and 737.2 μm , with an average median distribution value ($d(0.5)$) of 538.6 μm . The average volume weighed size ($D[4.3]$) of the micro-beads was 554.7 μm . The span was found to be 0.64, which is representative of a relatively narrow particle size distribution. The latter is expected of micro-beads prepared by means of extrusion spheronisation.

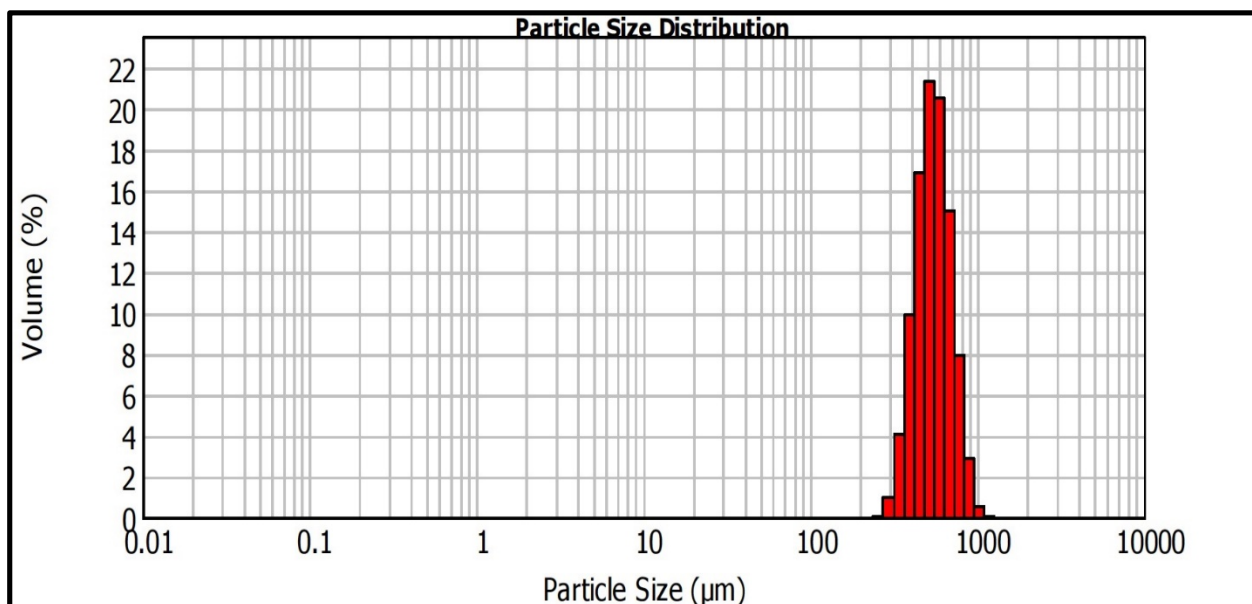


Figure 4.13: Chitosan micro-bead formulation particle size distribution plot

4.4.2.5 Micro-bead formulation containing *N*-trimethyl chitosan chloride (TMC)

The particle size analysis results for the micro-beads containing TMC can be seen in Figure 4.14. The data obtained from the Mastersizer® show that the majority of TMC micro-beads ranged between 428.6 μm and 785.1 μm, with an average median distribution value ($d(0.5)$) of 582.5 μm. The average volume weighed size ($D[4.3]$) of the micro-beads was 598.6 μm. The span was found to be 0.61, which is representative of a relatively narrow particle size distribution. As mentioned before, the latter is a known property of micro-beads prepared by means of extrusion spheronisation.

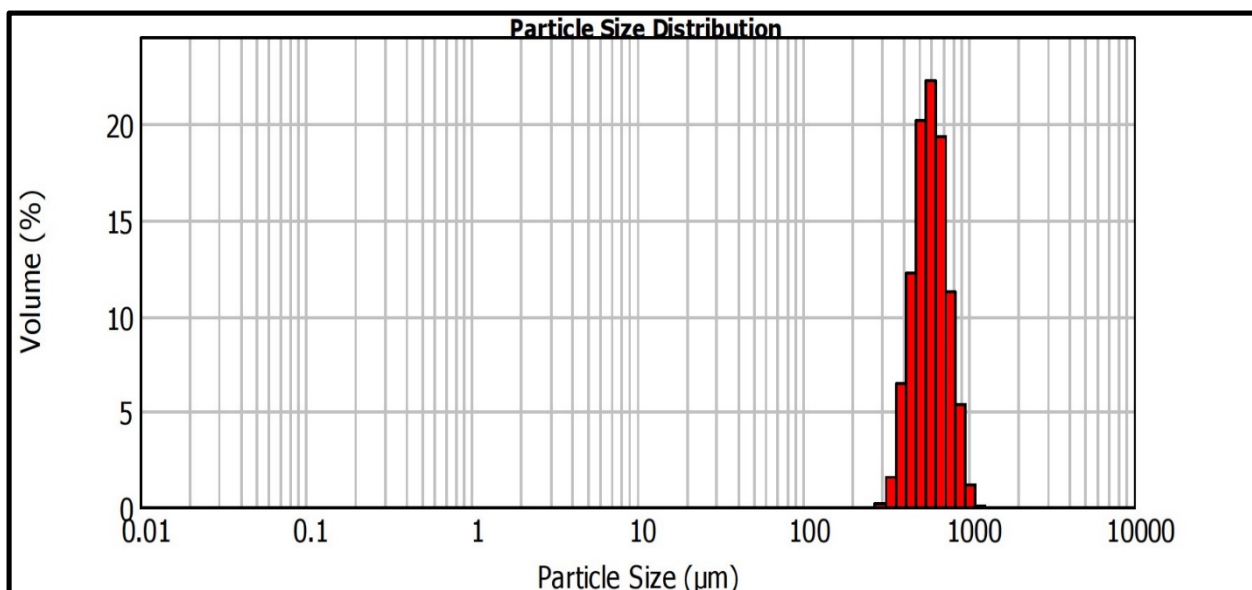


Figure 4.14: TMC micro-bead formulation particle size distribution plot

4.4.2.6 Micro-bead formulation containing sodium glycocholate hydrate

The results of the particle size analysis for micro-beads containing sodium glycocholate hydrate can be seen in Figure 4.15. The particle size data obtained from the Mastersizer[®] show that the majority of sodium glycocholate hydrate micro-beads ranged between 424.5 μm and 820.2 μm , with an average median distribution value ($d(0.5)$) of 588.3 μm . The average volume weighed size ($D[4.3]$) of the micro-beads was 609.0 μm . The span was found to be 0.67, which is an indication of a relatively narrow particle size distribution. The latter is expected of micro-beads prepared by means of extrusion spheronisation.

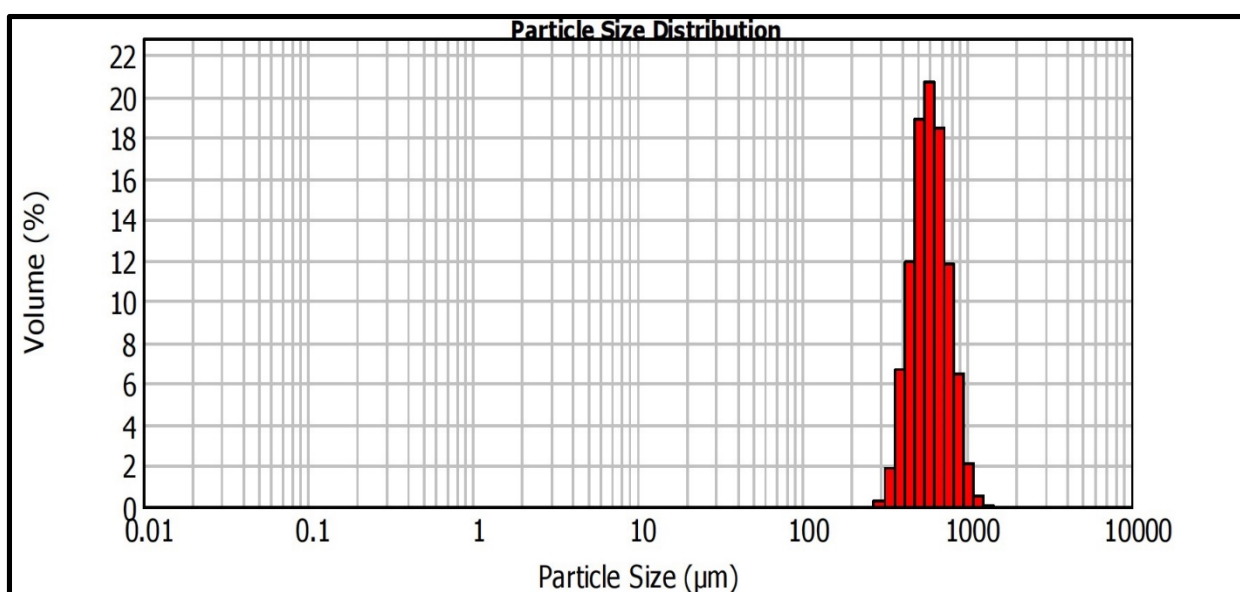


Figure 4.15: Sodium glycocholate hydrate micro-bead formulation particle size distribution plot

4.4.3 Micro-bead structure and morphology

Micrographs of the different micro-beads were captured using an FEI Quanta 200 environmental scanning electron microscope (ESEM) in order to investigate the surface morphology as well as internal structure of the micro-bead formulations.

4.4.3.1 Micro-bead formulation consisting of Pharmacel[®]

Figure 4.16 shows the external surface area of a micro-bead containing Pharmacel[®] and FD-4 that served as the control group. From the image, it can be seen that the micro-bead has an excellent spherical form and relatively smooth surface area. The spherical shape of the Pharmacel[®] micro-bead is expected from the bead preparation method used in this study (i.e. extrusion spheronisation). Figure 4.17 reveals the internal structure of a Pharmacel[®] and FD-4 containing micro-bead.

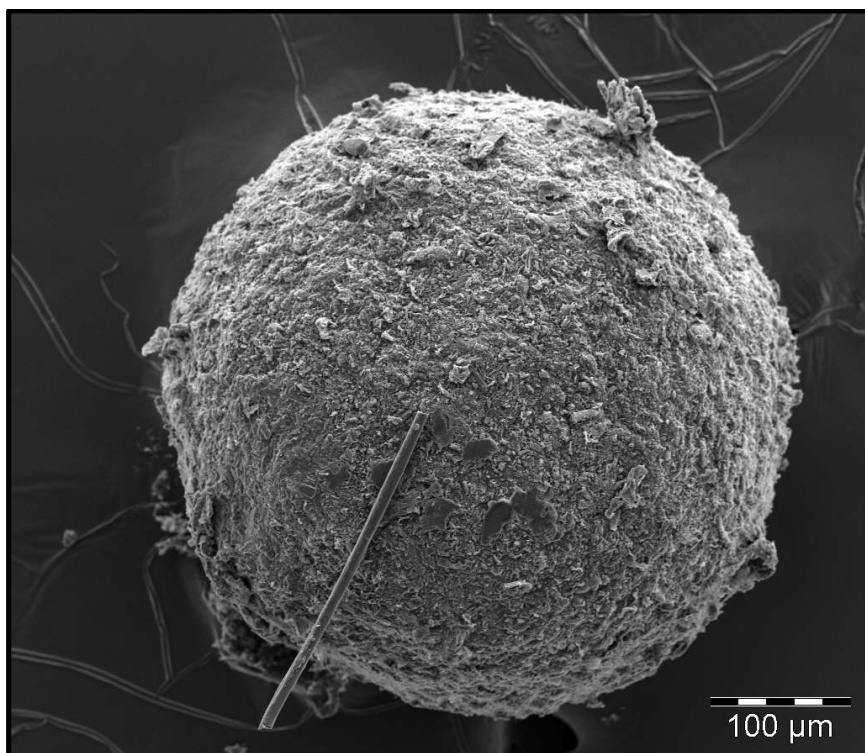


Figure 4.16: Micrograph illustrating the surface of a micro-bead containing Pharmacel[®] and FD-4 (control)

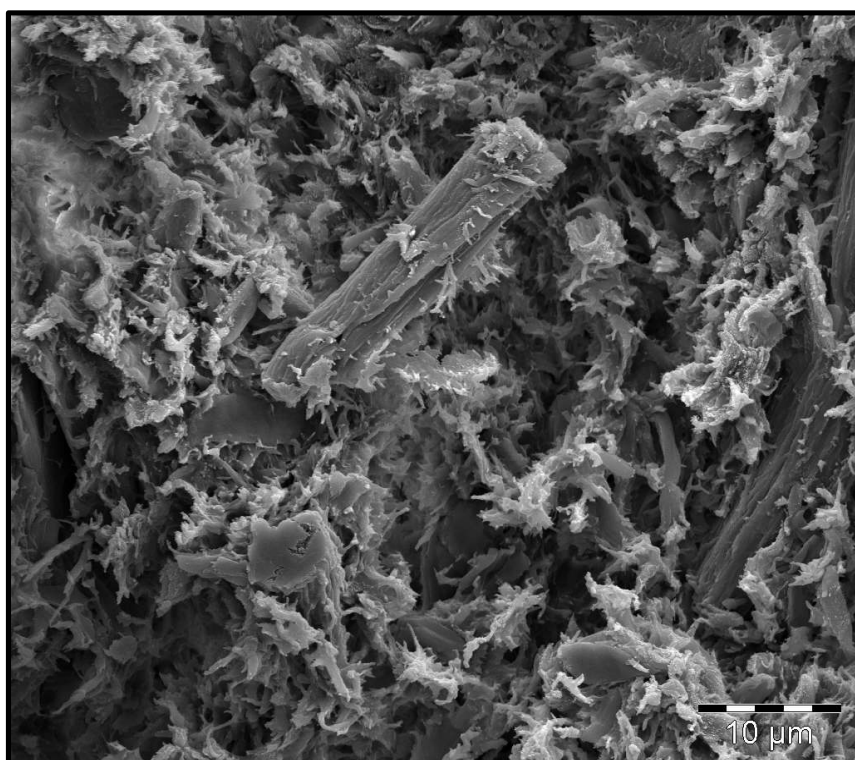


Figure 4.17: Micrograph illustrating the internal structure of a micro-bead containing Pharmacel[®] and FD-4 (control)

The internal structure exhibits a relatively densely packed core with the fibrous texture of the Pharmacel® powder particles clearly visible.

4.4.3.2 Micro-bead formulation containing *Aloe vera* gel

Figure 4.18 shows the external surface area of a micro-bead containing *A. vera* gel as drug absorption enhancer. From the image, it can be seen that the micro-bead has a relatively spherical form, which is expected from the bead preparation by means of extrusion spheronisation. The addition of the absorption enhancer (*A. vera* gel) is most probably responsible for the less spherical shape of the micro-bead in comparison to that of the control formulation (Pharmacel®). Furthermore, the surface of the micro-bead appears to be relatively rough with scale formation on some parts. Figure 4.19 reveals the internal structure of an *A. vera* gel containing micro-bead.

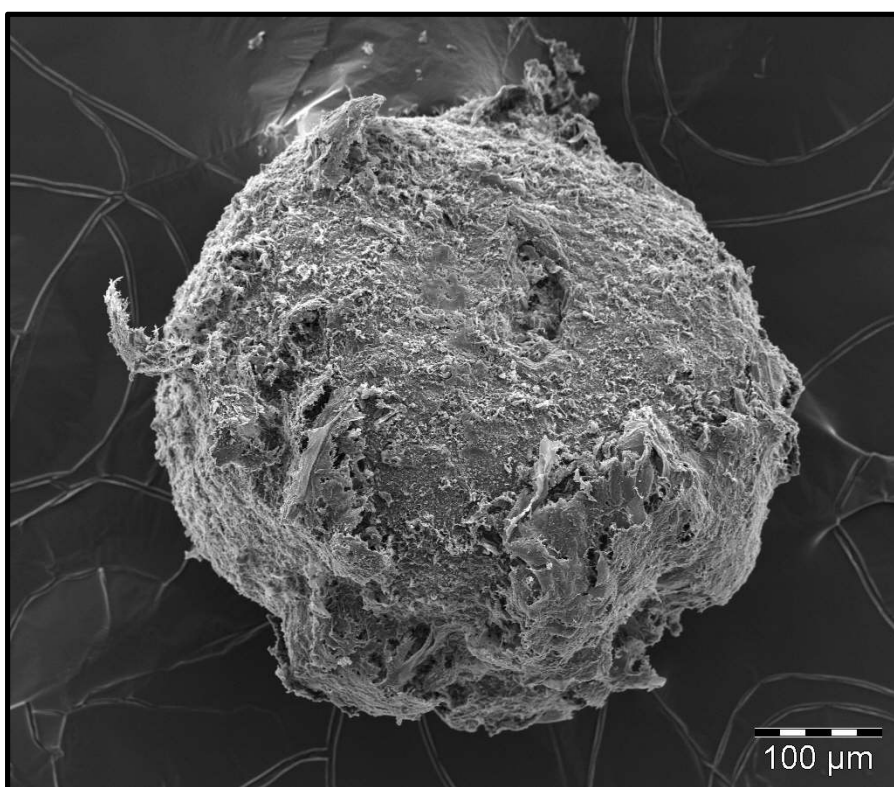


Figure 4.18: Micrograph illustrating the surface of a micro-bead containing *Aloe vera* gel

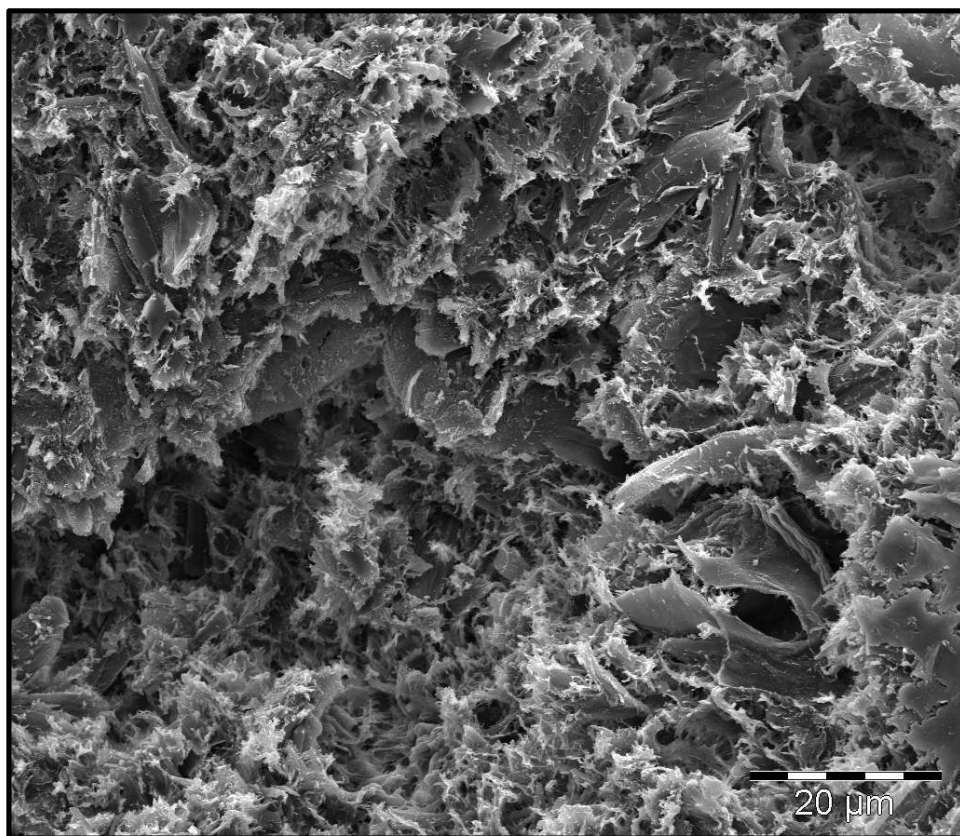


Figure 4.19: Micrograph illustrating the internal structure of a micro-bead containing *Aloe vera* gel

From Figure 4.19, the internal structure of the micro-bead containing *A. vera* gel appears relatively densely packed without visible pores or channels.

4.4.3.3 Micro-bead formulation containing *Aloe vera* whole leaf extract

Figure 4.20 shows the external surface area of a micro-bead containing *A. vera* whole leaf as absorption enhancing agent. From this image, it can be seen that the micro-bead has a relatively spherical form, albeit less spherical than that of the control formulation (Pharmacel®). The addition of the absorption enhancer (*A. vera* whole leaf extract), in comparison to the control group, was most probably responsible for the loss of sphericity due to the physical properties of this material. Furthermore, the surface of the micro-bead appears to be relatively rough with cracks clearly visible on some parts of the surface. These cracks could be the cause of less water (wetting agent) being used in the preparation of this micro-bead formulation in comparison to the control formulation. Some scale formation is also visible on the surface of the micro-bead, however, it is less pronounced as observed for the *A. vera* gel containing micro-beads.

Figure 4.21 reveals the internal structure of an *A. vera* whole leaf extract containing micro-bead.

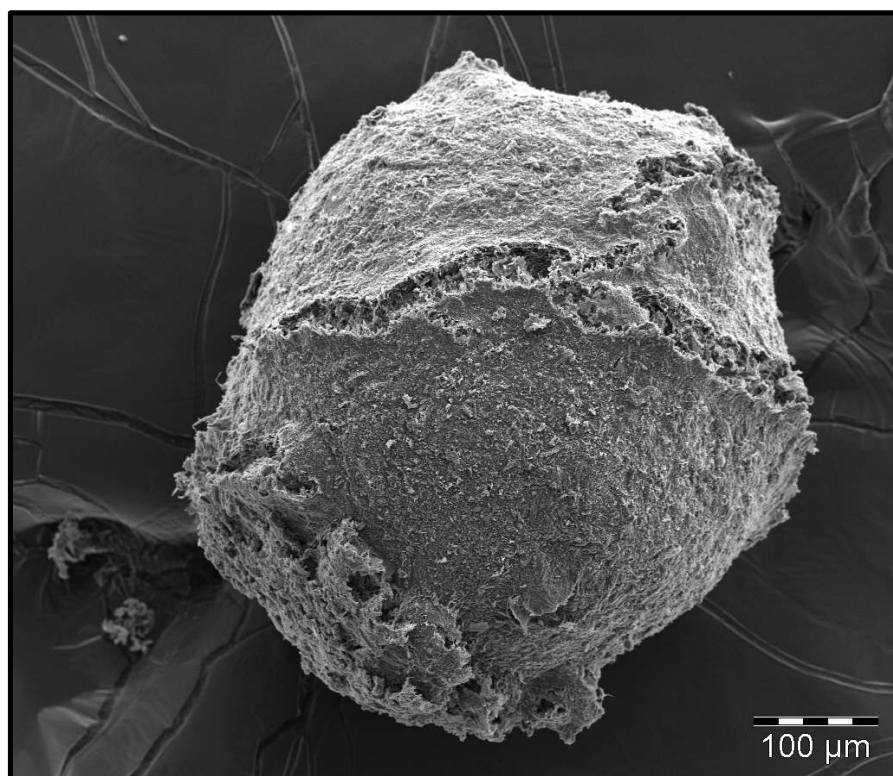


Figure 4.20: Micrograph illustrating the surface of a micro-bead containing *Aloe vera* whole leaf extract

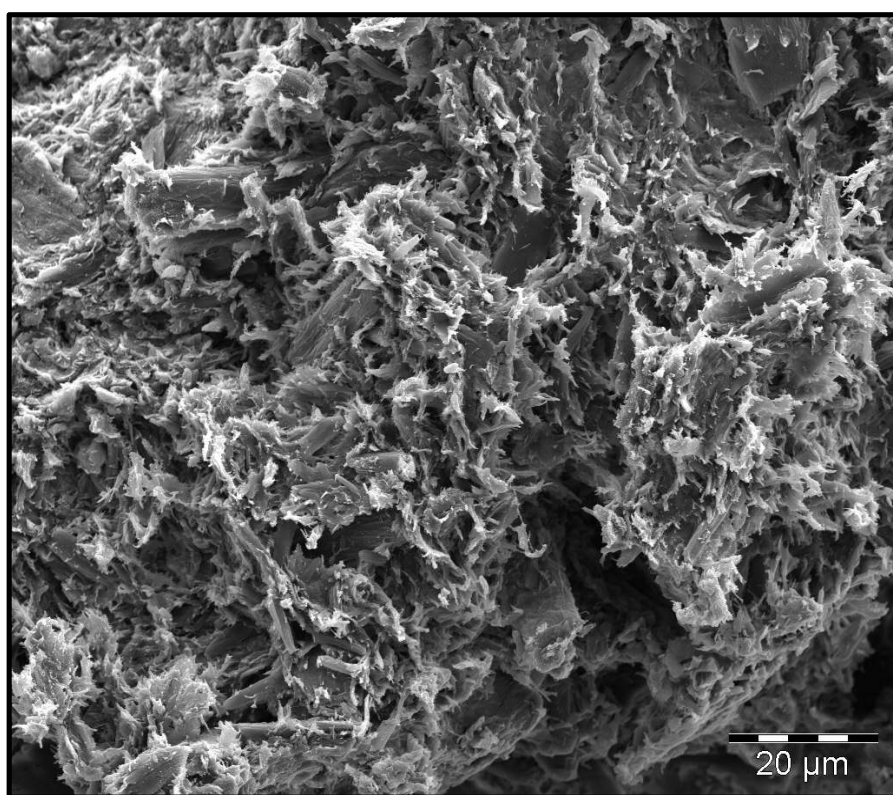


Figure 4.21 Micrograph illustrating the internal structure of a micro-bead containing *Aloe vera* whole leaf extract

4.4.3.4 Micro-bead formulation containing chitosan

Figure 4.22 shows the external surface area of micro-beads containing chitosan. From the image, it can be seen that the micro-beads have a relatively spherical form, which is similar to that of the control formulation and is a property of beads prepared by means of extrusion spheronisation. The addition of the absorption enhancer (chitosan) did not affect the sphericity of the micro-beads to the same extent as the *A. vera* leaf materials. This may be explained by different physical properties of chitosan (e.g. elasticity) compared to that of the *A. vera* leaf materials. Furthermore, the surface of the micro-bead appears to be relatively smooth with only one protrusion visible on the one micro-bead. Figure 4.23 reveals the internal structure of chitosan containing micro-beads.



Figure 4.22: Micrograph illustrating the surface of micro-beads containing chitosan

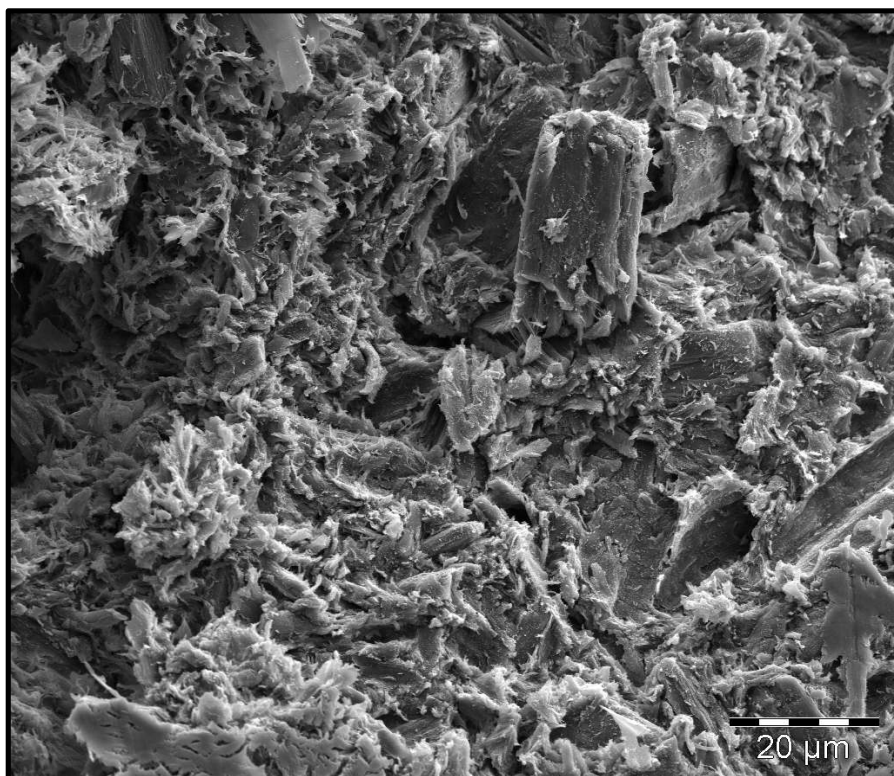


Figure 4.23: Micrograph illustrating the internal structure of a micro-bead containing chitosan

4.4.3.5 Micro-bead formulation containing *N*-trimethyl chitosan chloride (TMC)

Figure 4.24 shows the external surface area of a micro-bead containing TMC as absorption enhancing agent. From the image, it can be seen that the micro-bead has a relatively spherical form, but less spherical than that of the control formulation. The micro-bead structure is similar to that of the chitosan containing micro-beads, which can possibly be explained by the similarity in chemical properties/structures of chitosan and TMC. Furthermore, the surface of the micro-bead appears to be relatively smooth with only few relatively small cracks on some parts. Figure 4.25 reveals the internal structure of TMC containing micro-beads.

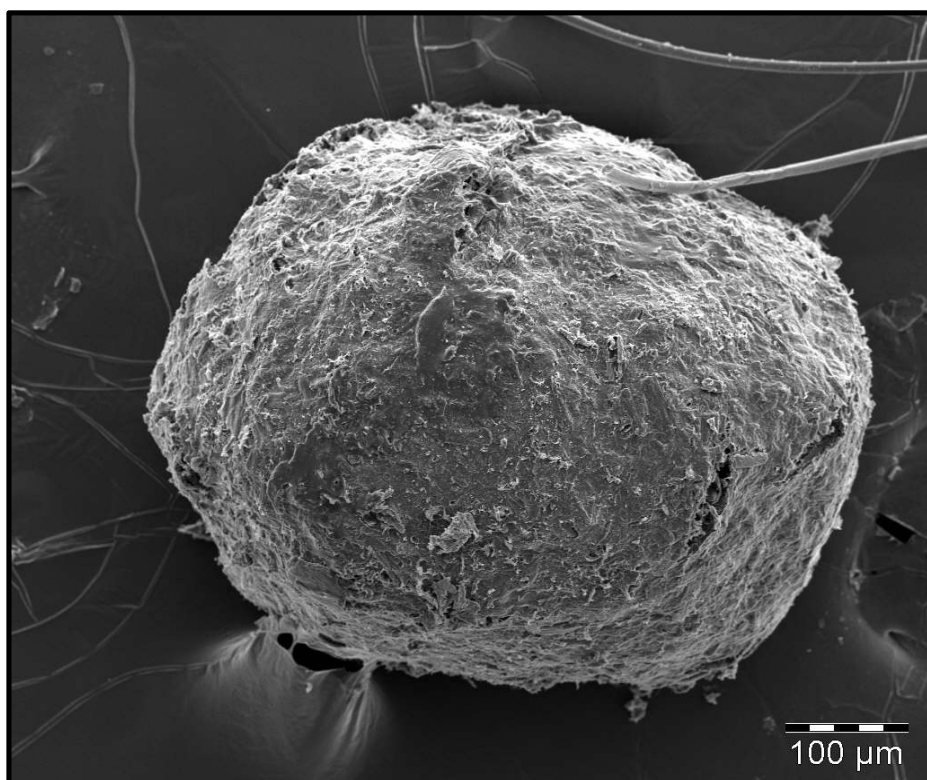


Figure 4.24: Micrograph illustrating the surface of a micro-bead containing *N*-trimethyl chitosan chloride (TMC)

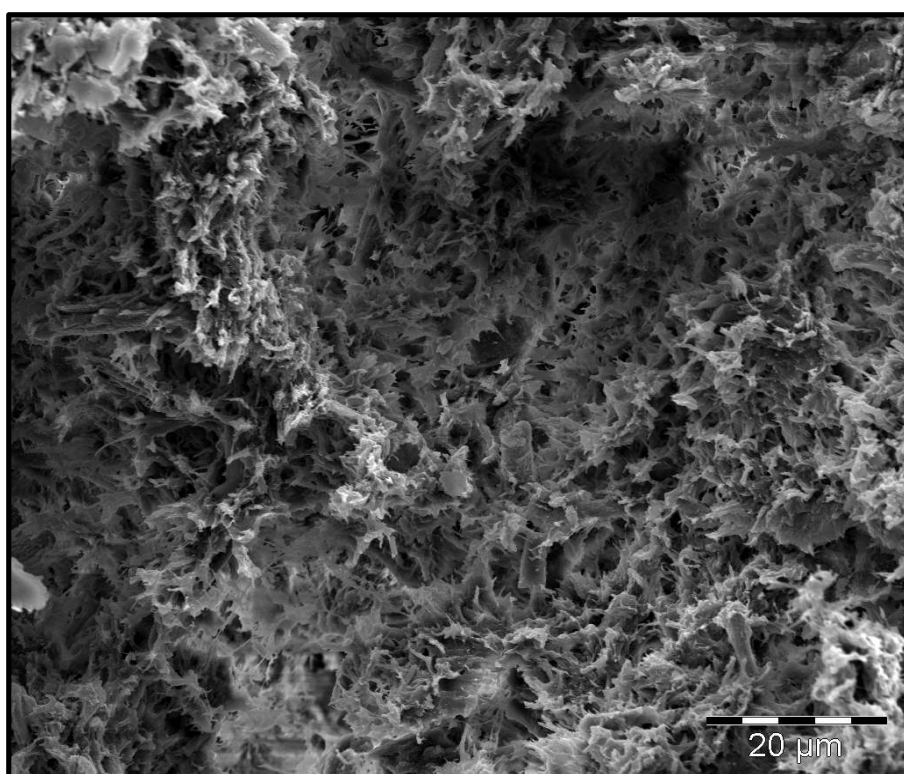


Figure 4.25: Micrograph illustrating the internal structure of a micro-bead containing *N*-trimethyl chitosan chloride (TMC)

4.4.3.6 Micro-bead formulation containing sodium glycocholate hydrate

Figure 4.26 shows the external surface area of a micro-bead containing the drug absorption enhancer, sodium glycocholate hydrate. From the image, it can be seen that the micro-bead has a relatively spherical form, albeit less spherical than that of the control micro-bead formulation. Furthermore, the surface of the micro-bead appears to be relatively rough, but only exhibited shallow crevices and dents. Figure 4.27 reveals the internal structure of sodium glycocholate hydrate containing micro-beads.

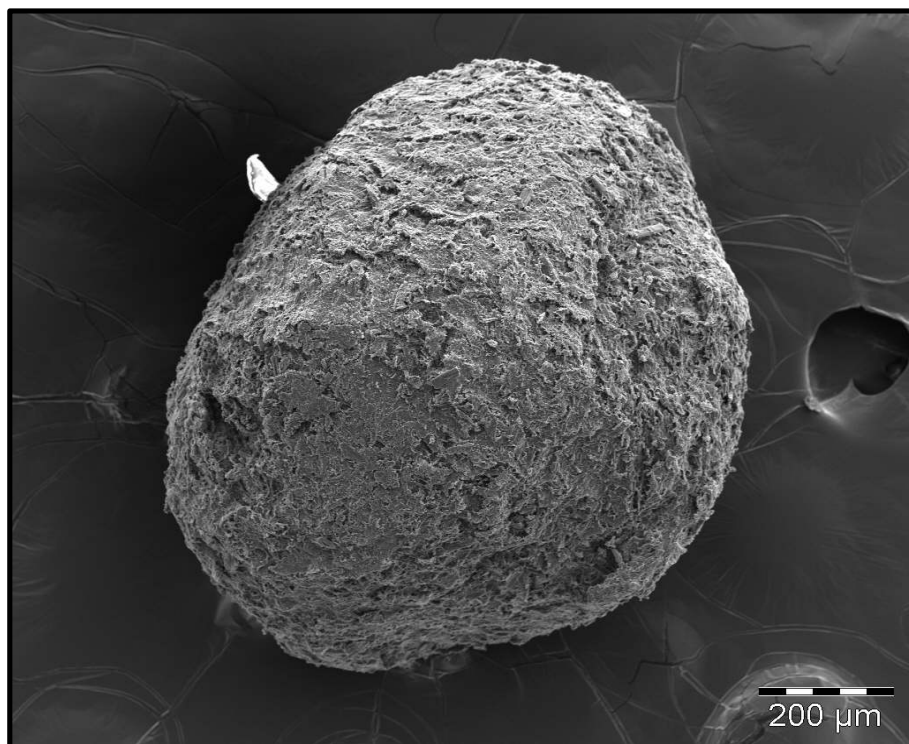


Figure 4.26 Micrograph illustrating the surface of a micro-bead containing sodium glycocholate hydrate

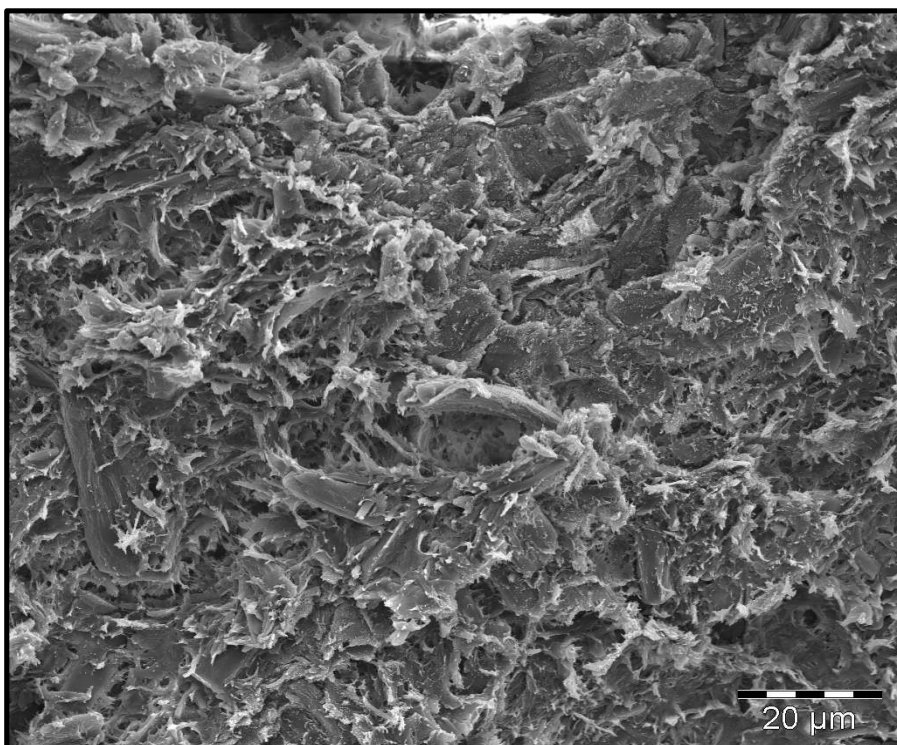


Figure 4.27: Micrograph illustrating the internal structure of a micro-bead containing sodium glycocholate hydrate

4.4.5 Dissolution

The percentage dissolution for all six micro-bead formulations were plotted as a function of time, which is shown in Figure 4.28.

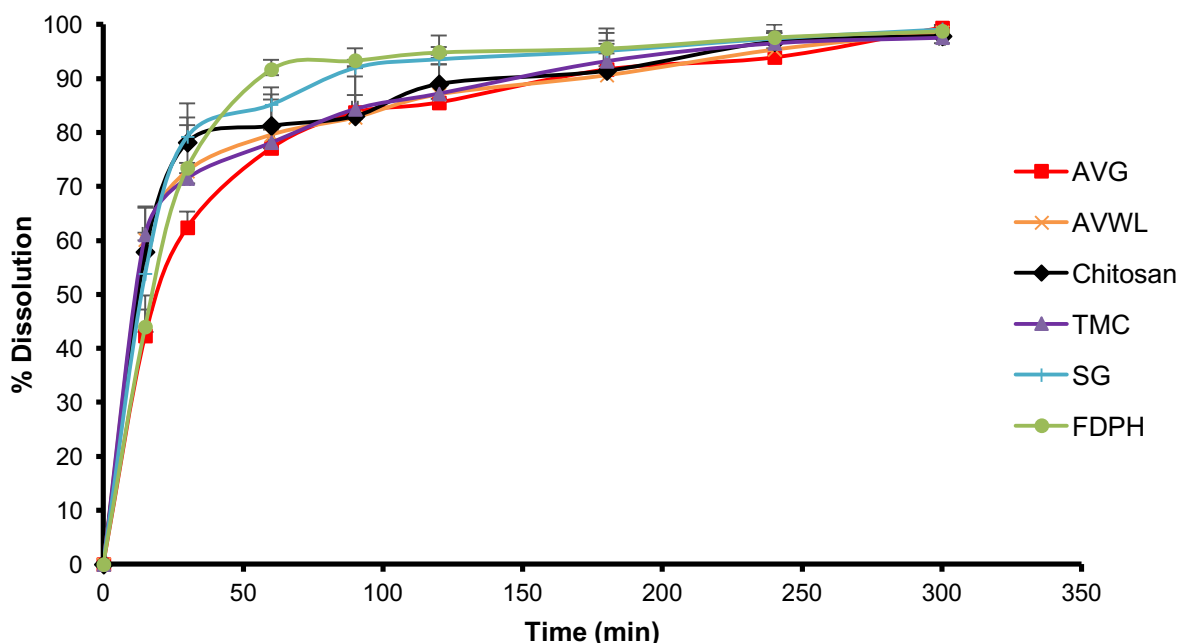


Figure 4.28: Percentage dissolution of FD-4 from micro-bead formulations containing *Aloe vera* gel (AVG), *Aloe vera* whole leaf extract (AVWL), chitosan, *N*-trimethyl chitosan chloride (TMC), sodium glycocholate hydrate (SG) and FD-4 and Pharmace[®] (FDPH)

From Figure 4.28, it can be seen that when *A. vera* gel (AVG) was incorporated into the micro-bead formulation, it reduced the initial dissolution rate of FD-4 when compared to that of the control formulation (FDPH). The micro-beads containing AVG showed only 42.38% FD-4 release after 15 min, while those containing TMC displayed the highest initial dissolution rate with 61.02% of the FD-4 already released after 15 min. This might be attributed to the high aqueous solubility of TMC (Jonker *et al.*, 2002) as well as the small surface cracks on these micro-beads that contributed to water uptake into the micro-beads. The difference in initial dissolution between AVG (42.38%) and AVWL (60.09%) containing micro-beads could be due to the more porous profile of AVWL as seen in Figure 4.20.

In general, all the micro-bead formulations demonstrated relatively fast dissolution of the FD-4, which resembles dissolution profiles of immediate release dosage forms. Although beads containing microcrystalline cellulose (Pharmace[®]) as filler material that are produced by means of extrusion spheronisation often provide sustained drug release properties (Ozarde *et al.*, 2012), the relatively fast dissolution from the beads prepared in this study can be attributed to their

relatively small size (i.e. micro-beads in the range of 500 – 700 μm ; pharmaceutical beads prepared from extrusion spheronisation usually fall within the 500 – 1500 μm range (Dukić-Ott *et al.*, 2009), with 500 μm being at the smaller spectrum.

4.5 EX VIVO TRANSPORT STUDIES

4.5.1 Transport of FD-4 across excised intestinal tissues after application of micro-beads consisting of Pharmacel[®] and FD-4 (control group)

Figure 4.29 shows the percentage FD-4 transported across excised pig intestinal tissues when micro-beads consisting of Pharmacel[®] and FD-4 were applied to the apical chamber of a Sweetana-Grass diffusion chamber over a period of 120 min. The micro-beads that consisted of Pharmacel[®] and FD-4 served as a control group, as this formulation did not contain any absorption enhancing agents.

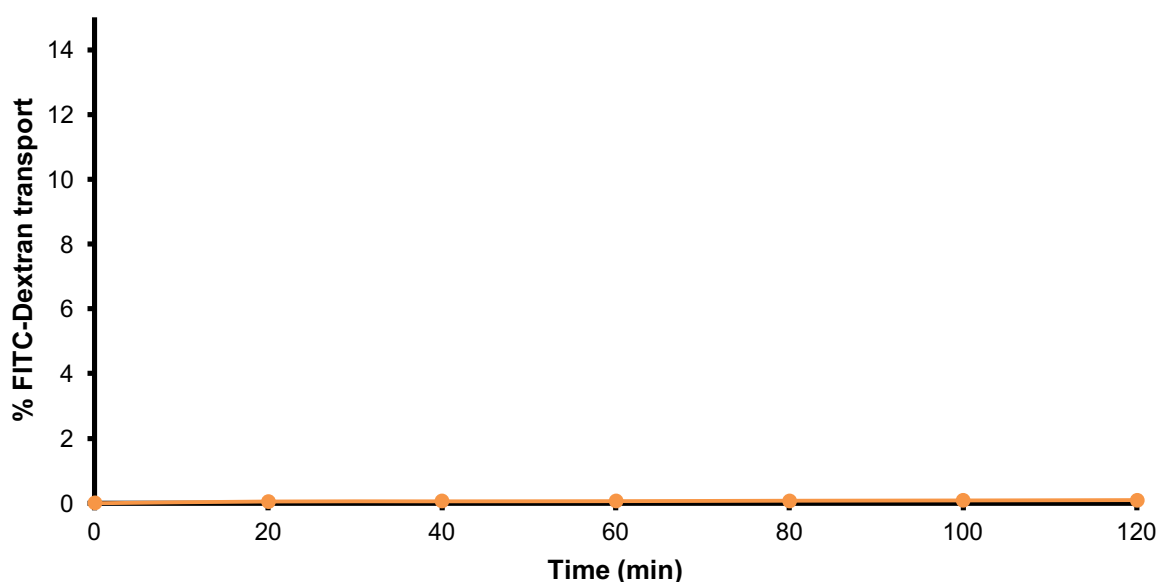


Figure 4.29: Graph illustrating the percentage FD-4 transported across excised pig intestinal tissue during exposure to micro-beads consisting of Pharmacel[®] and FD-4 (control group without any absorption enhancing agents)

Figure 4.29 shows that a relatively low quantity of FD-4 was transported from the apical to basolateral side (only 0.09% of the dose applied) of the excised pig intestinal tissue over a time period of 120 min. This is in agreement with previous results regarding the inability of macromolecular drugs to be transported across excised pig intestinal tissues (De Bruyn *et al.*, 2017). This is understandable if taken into consideration the physicochemical properties of large, hydrophilic compounds that prevents them from partitioning into the lipophilic bilayer structure of the biological membrane. It is also known that, in general, less than 1% of the administered dose of macromolecular drugs are able to reach the systemic circulation after oral administration (i.e.

bioavailability < 1%) without the aid of absorption enhancers (Renukuntla *et al.*, 2013). The main reasons for this low bioavailability are considered to be poor membrane permeation as well as enzymatic degradation (Wallis *et al.*, 2014).

4.5.2 Transport of FD-4 across excised intestinal tissues after application of micro-beads containing *Aloe vera* gel

Figure 4.30 shows the percentage FD-4 transported across excised pig intestinal tissues when micro-beads containing *A. vera* gel were applied to the apical chamber of a Sweetana-Grass diffusion chamber over a period of 120 min.

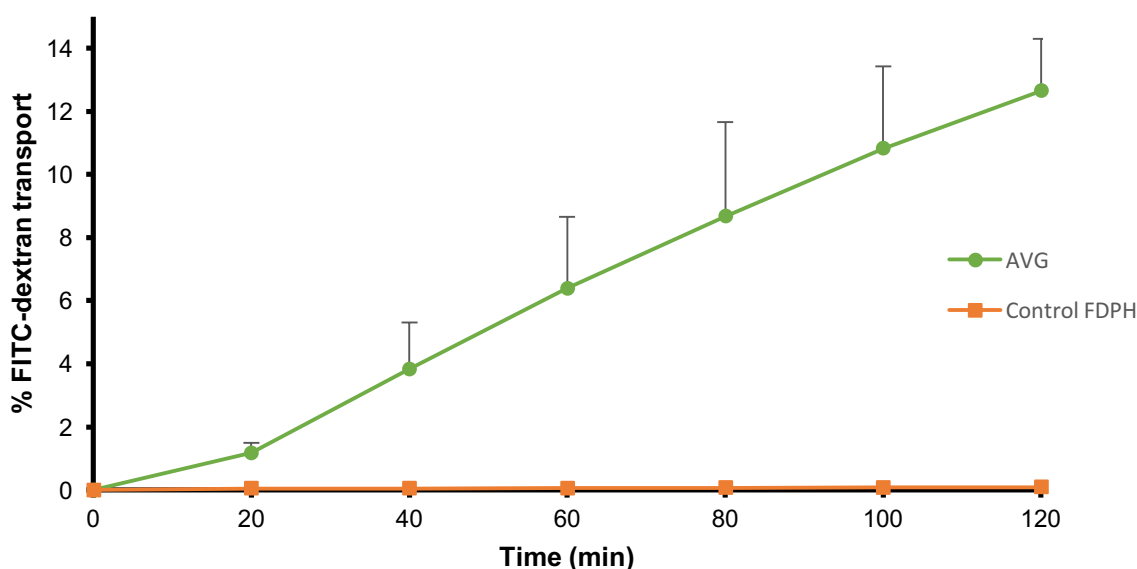


Figure 4.30: Graph illustrating the percentage FD-4 transported across excised pig intestinal tissue during exposure to micro-beads containing FD-4 and Pharmacel® (control), as well as micro-beads containing FD-4 and *Aloe vera* gel (AVG) as absorption enhancer

From Figure 4.30, it is clear that the exposure of pig intestine to micro-beads containing *A. vera* gel greatly enhanced the transport of FD-4 (13.8% cumulative transport) in comparison to the control group (0.09% cumulative transport, Figure 4.29). It has previously been shown that *A. vera* gel can enhance macromolecular drug transport across intestinal epithelia when applied in solution (Chen *et al.*, 2009; Lebitsa *et al.*, 2011; Beneke *et al.*, 2012). This is most probably due to enhanced paracellular absorption caused by the opening of tight junctions between adjacent epithelial cells by the *A. vera* gel (Chen *et al.*, 2009; Lemmer & Hamman, 2013).

The results from this study have confirmed that *A. vera* gel formulated into a micro-bead formulation instead of only being applied in solution, can deliver macromolecular drugs across the intestinal epithelium to a much higher level than when the drug is applied alone. This indicates

the usefulness of *A. vera* gel as a multi-functional excipient, especially in the formulation of solid oral dosage forms for oral delivery of macromolecular drugs (e.g. protein and peptide therapeutics). Although *A. vera* gel incorporated into macro-beads recently showed the ability to deliver insulin across excised pig intestinal tissues (5.8% cumulative transport of insulin) (De Bruyn *et al.*, 2017), it was shown in this study that micro-beads are more effective (13.8 % cumulative transport of FD-4). The increased effectiveness of the micro-beads in delivery might be attributed to the smaller size of these micro-beads with an increased surface area for drug release. However, the type of model drug may also be an influencing factor.

4.5.3 Transport of FD-4 across excised intestinal tissues after application of micro-beads containing *Aloe vera* whole leaf extract

Figure 4.31 shows the percentage FD-4 transported across excised pig intestinal tissue when micro-beads containing *A. vera* whole leaf extract were loaded in the apical chamber of a Sweetana-Grass diffusion chamber over a period of 120 min.

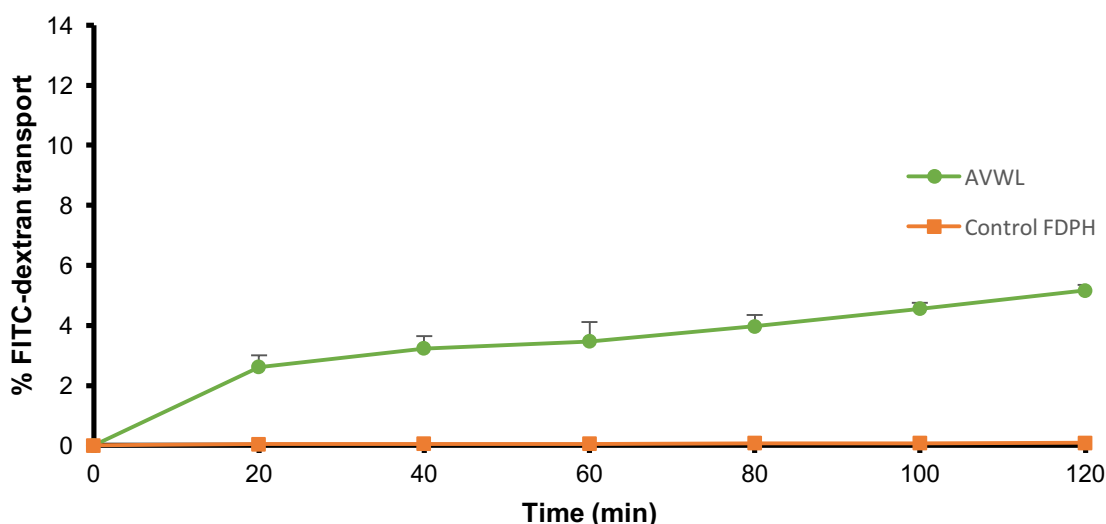


Figure 4.31: Graph illustrating the percentage FD-4 transport across excised pig intestinal tissue for micro-beads containing *Aloe vera* whole leaf extract compared to the control group (Control FDPH)

From Figure 4.31, it is clear that the exposure of pig intestine to micro-beads containing *A. vera* whole leaf extract enhanced the transport of FD-4 (5.2% cumulative transport) in comparison to the control group (0.09% cumulative transport, Figure 4.29). It has previously been shown that *A. vera* whole leaf extract can enhance drug transport across intestinal epithelia when applied in solution (Chen *et al.*, 2009; Lebitsa *et al.*, 2011; Beneke *et al.*, 2012). This is done in a similar way to that of *A. vera* gel, namely enhanced paracellular absorption caused by the opening of tight junctions (Chen *et al.*, 2009; Lemmer & Hamman, 2013). These findings are also in line with

a previous study that proved *A. vera* whole leaf extract formulated in a double phase multiple-unit dosage form (i.e. macro-beads) is in fact capable of delivering insulin across the intestinal epithelium (De Bruyn *et al.*, 2017).

This study therefore proved that *A. vera* whole leaf extract incorporated into a micro-bead formulation as a functional excipient, instead of only being applied in solution, can deliver macromolecular drugs across the intestinal epithelium to a much higher level than when the drug is applied alone.

4.5.4 Transport of FD-4 across excised intestinal tissues after application of micro-beads containing chitosan

Figure 4.32 shows the percentage FD-4 transported across excised pig intestinal tissue when micro-beads containing chitosan were loaded onto a Sweetana-Grass diffusion chamber for 120 min.

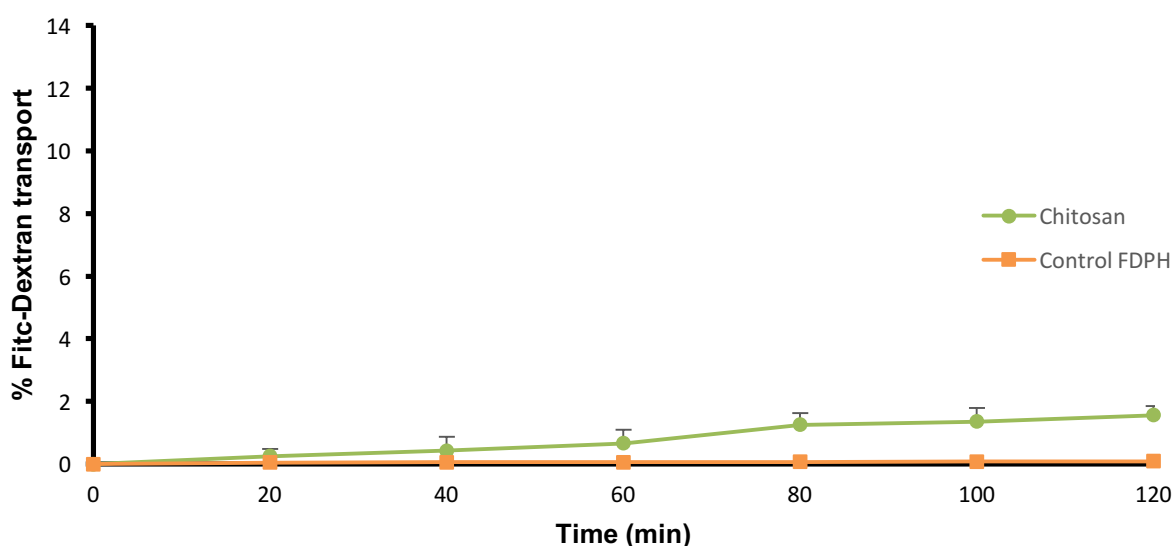


Figure 4.32: Graph illustrating the percentage FD-4 transport across excised pig intestinal tissue for micro-beads containing chitosan compared to the control group (Control FDPH)

Figure 4.32 indicates an increase in transport of FD-4 (1.6% cumulative transport) brought about by the micro-beads containing chitosan in comparison to that of the control group (0.09% cumulative transport, Figure 4.29). In total, the percentage transport of FD-4 from the chitosan containing micro-beads (1.6% cumulative transport) was lower than that of the TMC containing micro-beads (2.8% cumulative transport Figure 4.33). This might be attributed to the fact that chitosan mainly exerts its drug absorption enhancing effects in an acidic medium at a pH < 6.5 (Thanou *et al.*, 2000), while the transport studies were conducted using KRB buffer at a neutral pH (pH 7.4).

4.5.5 Transport of FD-4 across excised intestinal tissues after application of micro-beads containing *N*-trimethyl chitosan chloride (TMC)

Figure 4.33 shows the percentage FD-4 transported across excised pig intestinal tissue when micro-beads containing *N*-trimethyl chitosan chloride (TMC) were loaded onto a Sweetana-Grass diffusion chamber for 120 min.

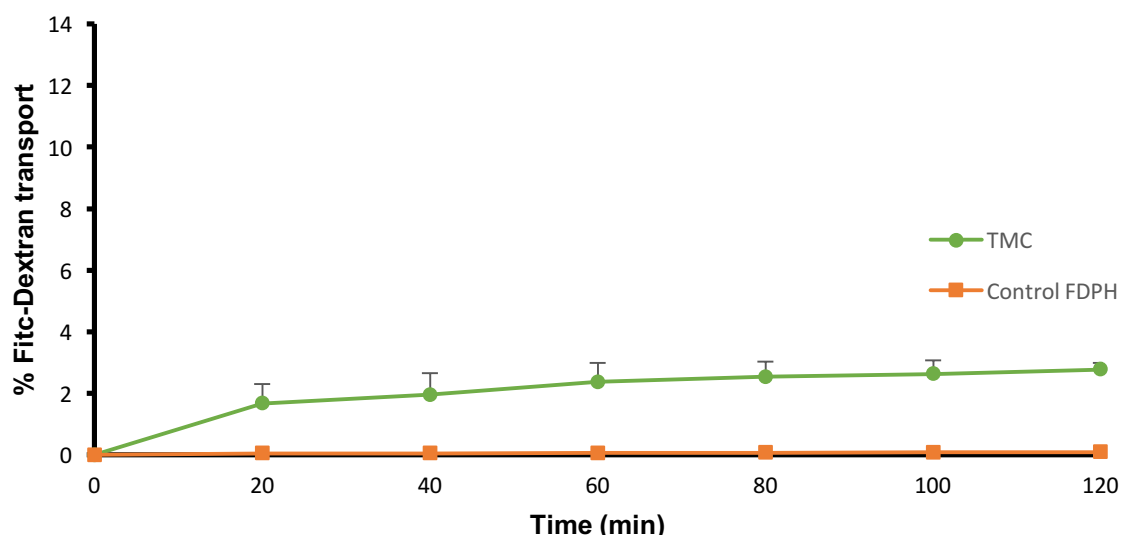


Figure 4.33: Graph illustrating the percentage FD-4 transport across excised pig intestinal tissue for micro-beads containing *N*-trimethyl chitosan chloride (TMC) compared to the control group (Control FDPH)

Figure 4.33 indicates an increase in transport of FD-4 (2.8% cumulative transport) from the TMC containing micro-beads in comparison to that of the control group (0.09% cumulative transport, Figure 4.29). TMC is a partially quaternised derivative of chitosan with improved solubility in neutral and basic environments. Since these *ex vivo* transport studies took place at a neutral pH, the increased solubility might have aided in the increase in FD-4 transport that was higher compared to that of chitosan containing micro-beads. Furthermore, confocal laser scanning microscopy has revealed that TMC (like chitosan) is capable of reversibly opening tight junctions to allow the passage of macromolecular drugs through the intestinal epithelium (Thanou *et al.*, 2000).

This study showed that both chitosan and TMC are capable of enhancing the permeation of a macromolecular compound across excised intestinal tissues when formulated into micro-beads. However, the *A. vera* gel and whole leaf materials formulated into micro-beads were able to enhance the permeation of FD-4 to a larger extent than that of the TMC and chitosan.

4.5.6 Transport of FD-4 across excised intestinal tissues after application of micro-beads containing sodium glycocholate hydrate

Figure 4.34 shows the percentage FD-4 transported across excised pig intestinal tissue when micro-beads containing sodium glycocholate hydrate were loaded onto a Sweetana-Grass diffusion chamber for 120 min.

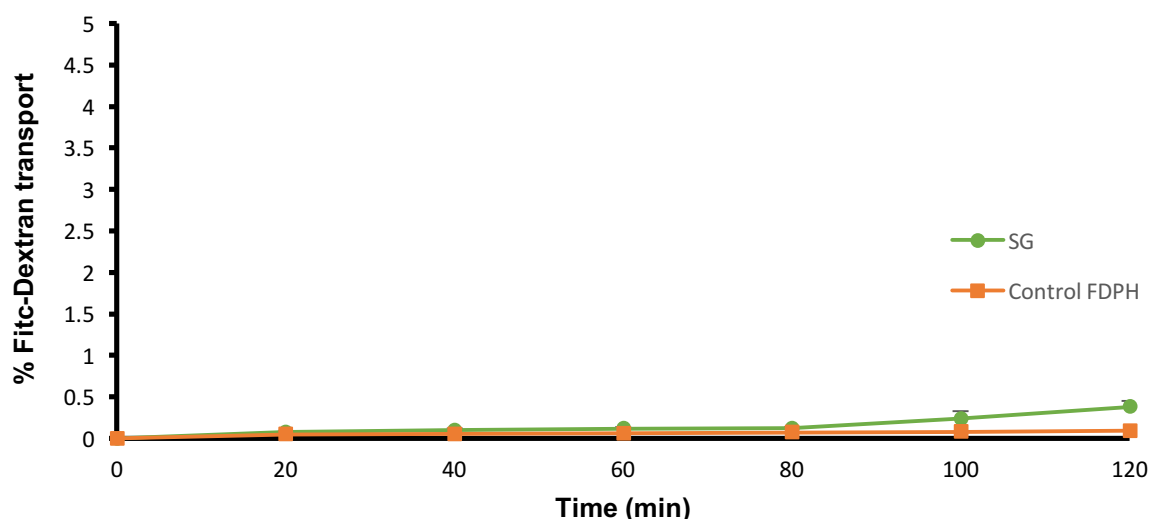


Figure 4.34: Graph illustrating the percentage FD-4 transport across excised pig intestinal tissue for micro-beads containing sodium glycocholate hydrate (SG) compared to the control group (Control FDPH)

Figure 4.34 shows that sodium glycocholate hydrate in micro-beads could increase the transport of FD-4 (0.3% cumulative transport) slightly in comparison to the control group (0.09% transport, Figure 4.29). Previous studies have shown that sodium glycocholate hydrate might have an effect on the integrity of tight junctions, which may allow macromolecular drugs to pass through the intestines (Lindhardt & Bechgaard, 2003). In comparison to the other four micro-bead formulations containing absorption enhancers, sodium glycocholate hydrate has exhibited the lowest increase in FD-4 transport. This increase is in accordance with another study where sodium glycocholate hydrate had displayed the lowest ability of increasing the transport of macromolecular drugs across excised pig intestinal tissues (De Bruyn *et al.*, 2017).

4.5.7 Transport of Lucifer yellow

The transport of the exclusion marker molecule, Lucifer yellow (LY), across excised pig intestinal tissues is given in Figure 4.35. It was found that the average transport of LY after 120 min was 0.58%. This is well below the recommended transport value of 3% (Sigma-Aldrich, 2013), which indicates intact membrane integrity was maintained over the period of the transport studies of

120 min. The P_{app} values obtained from the transport data are shown in Figure 4.36 (average P_{app} value of 4×10^{-7} cm/s), which is well below the maximum accepted range of $8.2\text{--}9.1 \times 10^{-7}$ cm/s (Bhushani *et al.*, 2016).

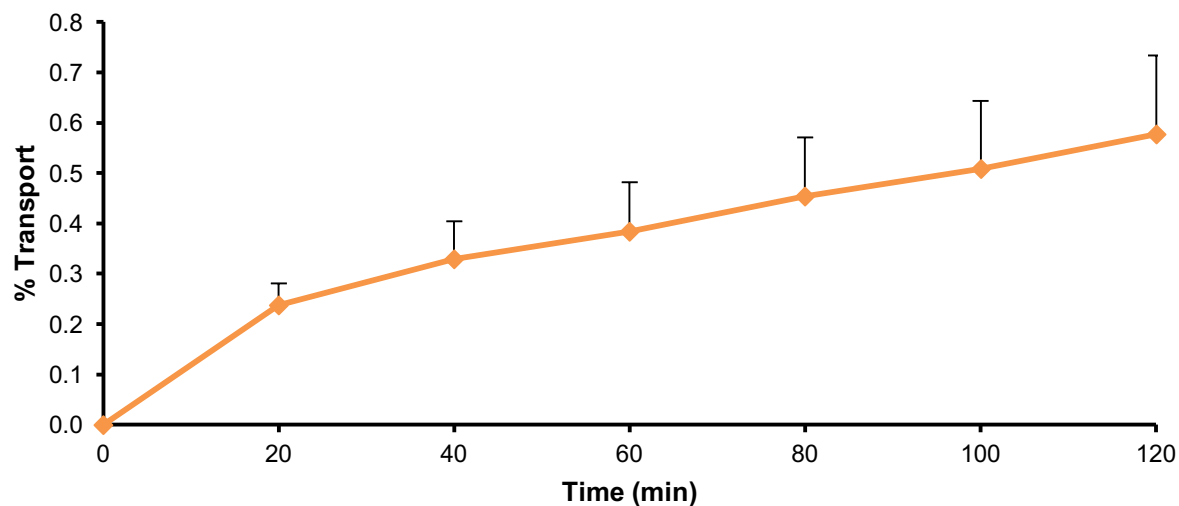


Figure 4.35: Graph illustrating the average percentage Lucifer yellow transport

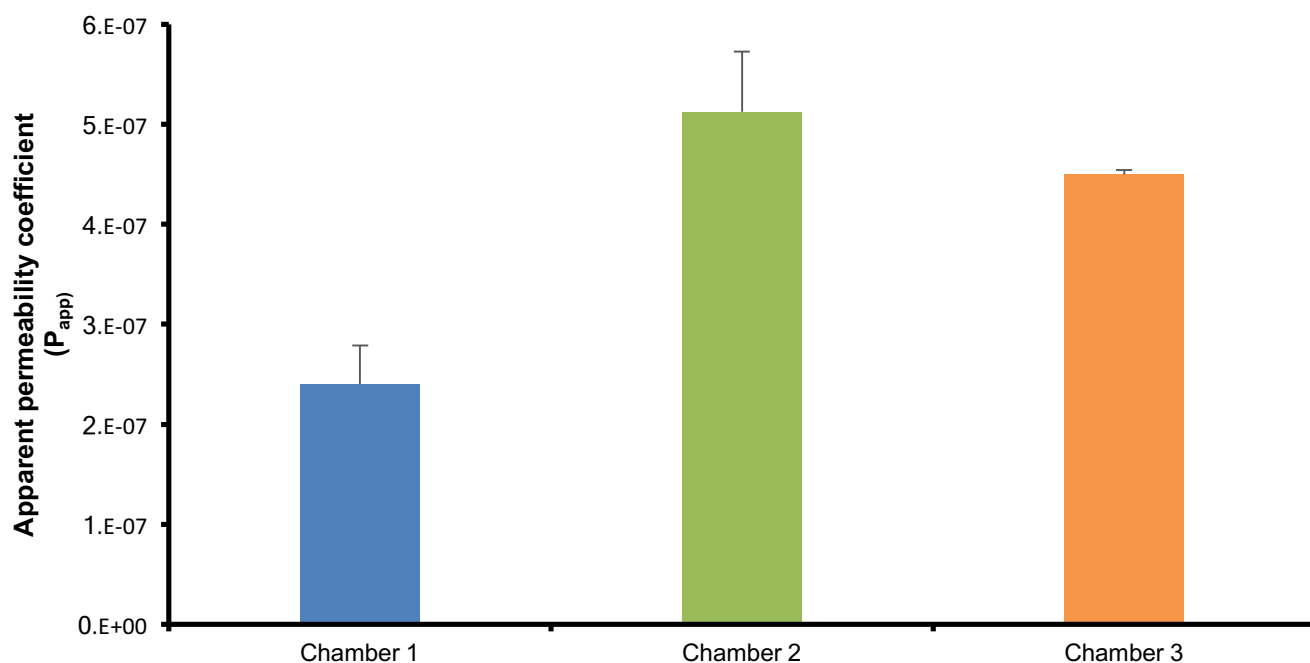


Figure 4.36: Graph illustrating the apparent permeability coefficient (P_{app}) of Lucifer yellow solution applied to intestine after transport study

4.5.8 Comparison of the FD-4 delivery across excised pig intestinal tissues from all the micro-bead formulations

The apparent permeability coefficient (P_{app}) values for FD-4 across excised pig intestinal tissues for each micro-bead formulation was calculated from the percentage transport curves. Figure 4.37 shows the P_{app} values for all six micro-bead formulations evaluated in this study.

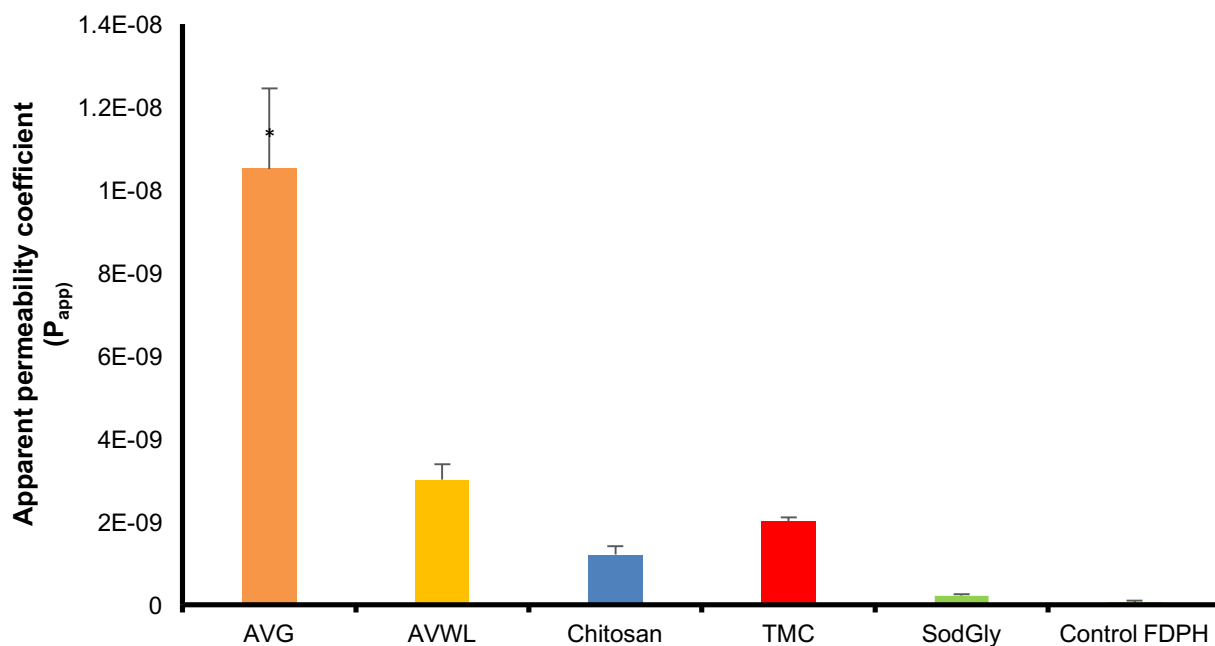


Figure 4.37: Graph illustrating the apparent permeability coefficient (P_{app}) for FD-4 after application of micro-beads containing *Aloe vera* gel (AVG), *Aloe vera* whole leaf extract (AVWL), chitosan, *N*-trimethyl chitosan chloride (TMC), sodium glycocholate (SodGly) and the control group (FDPH). * Denotes a statistically significant difference from the control group based on an ANOVA analysis

From Figure 4.37, it is clear that micro-beads containing *Aloe vera* gel ($P_{app} = 1.05 \times 10^{-8}$ cm/s) had the greatest effect on FD-4 transport as reflected in the P_{app} value. According to the ANOVA statistical analysis, this was statistically significantly different to the control group ($P_{app} = 6.47 \times 10^{-9}$ cm/s). The transport of FD-4 as modulated by the *A. vera* leaf materials in the micro-beads is in accordance with previous studies conducted using a double-phase multiple-unit dosage form (macro-beads) in order to transport a macromolecular drug (insulin) across the intestinal epithelium (De Bruyn *et al.*, 2017). Although *A. vera* whole leaf extract had also increased the transport of FD-4, it was not to the same extent as that of *A. vera* gel and it was not statically significantly different from the control group.

It is interesting to note that *A. vera* gel had a much higher effect on the transport of FD-4 than other well-known absorption enhancers such as chitosan and TMC, which have been shown to be effective also by means of *in vivo* studies (Thanou *et al.*, 2000; Pan *et al.*, 2002). The results from this study therefore indicate the potential of *A. vera* gel and whole leaf materials to be effective drug absorption enhancers, specifically when formulated into solid oral dosage forms.

4.6 CONCLUSION

The analytical method used in this study to measure the concentration of FD-4 in the transport samples complied with all the validation specifications of linearity, limit of detection, limit of quantification, precision, specificity and accuracy. The dissolution test showed that all the micro-bead formulations followed immediate drug release profiles. All of the micro-bead formulations showed an increase in FD-4 transport across the intestinal epithelium, with only *Aloe vera* gel showing a statistically significant increase in the transport of FD-4 across excised pig intestinal tissues. Membrane integrity was upheld throughout all transport experiments as evident from the exclusion marker (Lucifer yellow) transport studies. Transport enhancement of macromolecular drugs across the intestinal epithelium has previously been shown to be possible by application of solutions of the selected drug absorption enhancers (i.e. *A. vera* gel, *A. vera* whole leaf extract, chitosan, TMC and sodium glycocholate) as well as using double-phase multiple-unit delivery systems (i.e. macro-beads). The results from this study confirmed the transport enhancement effects of the selected drug absorption enhancers when formulated into micro-bead formulations on a macromolecular model compound (FD-4). The micro-beads containing *A. vera* gel could deliver FD-4 statistically significantly higher than the control group across excised pig intestinal tissues. This study has made a significant contribution towards finding an effective solid oral dosage form for delivery of macromolecular drugs that normally have very low bioavailability and unfavourable pharmacokinetic profiles after oral administration. However, in order to prove the oral macromolecular delivery efficacy in terms of bioavailability and to determine if these absorption enhancement effects would be sufficient to provide clinically effective blood plasma levels, *in vivo* testing in human subjects is needed.

CHAPTER 5

FINAL CONCLUSIONS AND FUTURE RECOMMENDATIONS

5.1 Final conclusions

The main aim of this study was to develop an oral dosage form capable of effectively delivering macromolecular drugs across the gastrointestinal epithelium. All of the selected absorption enhancers (i.e. *Aloe vera* gel, *Aloe vera* whole leaf extract, chitosan, *N*-trimethyl chitosan chloride (TMC), sodium glycocholate hydrate and a control group containing only FD-4 and Pharmacel®) were incorporated in micro-bead formulations with sizes in the range of $\pm 500 \mu\text{m}$. The micro-beads were evaluated in terms of size, size distribution, drug release profile and finally assayed in order to determine the actual concentration of FD-4 in each batch.

Electron microscope images of the micro-beads provided detailed information on micro-bead surface morphology, form and internal structure. All the micro-bead formulations showed relatively spherical shapes, which is expected of beads prepared by the extrusion spheronisation technique. Dissolution studies revealed that all the micro-bead formulations followed similar immediate release profiles. The micro-beads containing *A. vera* gel exhibited slightly slower initial release, while those containing TMC had the highest initial dissolution rate. *A. vera* whole leaf extract also displayed a higher initial release of FD-4 compared to that of the *A. vera* gel formulation. From the microscopic images it was revealed that the micro-beads containing *A. vera* whole leaf extract had clearly visible cracks, which were absent in the micro-beads containing *A. vera* gel. This might have been the cause of the higher initial FD-4 release from the micro-beads containing *A. vera* whole leaf extract.

From the *ex vivo* transport studies it was clear that all five the micro-bead formulations increased the transport of FD-4 across excised intestinal tissues compared to the control group (FD-4 alone). The Lucifer yellow transport proved that membrane integrity had been maintained throughout the experiments, indicating effective transport with no deteriorating effect on the intestinal tissue. The micro-beads containing *A. vera* gel showed the highest increase in FD-4 transport of all the micro-bead formulations. The micro-bead formulation containing *A. vera* gel was the only formulation capable of delivering FD-4 statistically significantly higher than the control group across the excised pig intestinal tissues.

Previous studies focused on enhancing transport of macromolecular drugs through application of solutions or double phase solid oral dosage forms that contain absorption enhancers. This study has proven that enhanced intestinal transport of macromolecular drugs can be achieved from a micro-bead formulation containing absorption enhancers. The efficacy of absorption enhancers

can be ranked as follow: *A. vera* gel > *A. vera* whole leaf extract > TMC > chitosan > sodium glycocholate hydrate. This study has made a significant contribution towards finding an effective solid oral dosage form for delivery of macromolecular drugs that normally have very low bioavailability and unfavourable pharmacokinetic profiles after oral administration.

5.2 Future recommendations

During this study, the micro-bead dosage form displayed promising results with regards to macromolecular drug delivery. This study proved that enhanced intestinal absorption of macromolecular drugs is possible, however, further testing is required as follows:

- Due to variations in different macromolecular drugs, formulation of different peptide drugs (e.g. insulin) into micro-beads along with absorption enhancers should be tested.
- *Aloe* plants must be sourced from the same area to make sure that acetylated mannan concentration remains the same and chemical components are similar.
- A wider range of testing could be done on different transport models, including human intestinal epithelial cell culture monolayers (Caco-2) as well as tissue from different species of animals.
- *In vivo* testing would help to prove the oral macromolecular delivery efficacy in terms of bioavailability and if the absorption enhancing effects would be sufficient to provide clinically effective blood plasma levels.
- Modifications can be made to the micro-bead formulations in order to try and achieve sustained release profiles.
- Toxicity studies could be conducted to test the effect of prolonged exposure of the absorption enhancer to the intestines.
- A micro-bead formulation consisting of a combination of absorption enhancers can be investigated.

REFERENCES

- Agarwal V., Reddy I.K. & Khan M.A. 2000. Oral delivery of proteins: effect of chicken and duck ovomucoid on the stability of insulin in the presence of α -chymotrypsin and trypsin. *Pharmacy and pharmacology communications*, 6:223-227.
- Aguirre T., Teijeiro-Osorio D., Rosa M., Coulter I., Alonso M. & Brayden D. 2016. Current status of selected oral peptide technologies in advanced preclinical development and in clinical trials. *Advanced drug delivery reviews*, 106:223-241.
- Anderle, P. 2009. Kinetics and pathways of intestinal absorption and enzymatic cleavage of therapeutic proteins upon peroral delivery. Zürich: Swiss Federal Institute of Technology. (Dissertation-PhD).
- Artursson, P. & Palm, K. 2012. Caco-2 monolayers in experimental and theoretical predictions of drug transport. *Advanced drug delivery reviews*, 64:280-289.
- Ashford, M. 2002. The gastrointestinal tract: physiology and drug absorption. (*In* Aulton, M.E., ed. *Pharmaceutics: the science of dosage form design*. Edinburgh: Churchill Livingstone. P.217-233).
- Ashford, M. 2007. The gastrointestinal physiology and drug absorption. (*In* Aulton, M.E., ed. *Aulton's pharmaceutics. The design and manufacture of medicines*. New York: Churchill Livingstone, p.270-285).
- Aungst, B. 2000. Intestinal Permeation Enhancers. *Journal of pharmaceutical sciences*, 89:429-442.
- Beneke, C., Viljoen, A., & Hamman, J.H. 2012. *In vitro* absorption enhancement effects of *Aloe vera* and *Aloe ferox*. *Scientia pharmaceutica*, 80:475-486.
- Bernkop-Schnürch A., Krauland A., Leitner V. & Palmberger T. 2004. Thiomers: potential excipients for non-invasive peptide delivery systems. *European journal of pharmaceutics and biopharmaceutics*, 58:253-263.
- Bhushani, J., Karthik, P. & Anandharamakrishnan, C. 2016. Nanoemulsion based delivery system for improved bioaccessibility and Caco-2 cell monolayer permeability of green tea catechins. *Food hydrocolloids*, 56:372-382.
- BP (British Pharmacopoeia). 2013. London: TSO. <https://www.pharmacopoeia-com.nwulib.nwu.ac.za/bp-2017/appendices/appendix-01/appendix-01-d/phosphate-buffer-ph-6->

8--mixed.html?text=phosphate%20buffer%206.8&published-date=2016-08-23# Date of access: 19 Feb 2017

Brayden D.J. & Maher S. 2010. Oral absorption enhancement: taking the next steps in therapeutic delivery. *Therapeutic delivery*, 1:5-9.

Brown, L. 2005. Commercial challenges of protein drug delivery. *Expert opinion on drug delivery*, 2:29-42.

Chen, W., Lu, Z., Viljoen, A. & Hamman, J.H. 2009. Intestinal drug transport enhancement by *Aloe vera*. *Planta medica*, 76:587-595.

Choonara, B.F., Choonara, Y.E., Kumar, P., Bijukumar, D., Du Toit, L.C. & Pillay, V. 2014. A Review of advanced oral drug delivery technologies facilitating the protection and absorption of protein and peptide molecules. *Biotechnology advances*, 32:1269-1282.

De Bruyn, S., Willers, C., Steyn, D., Steenekamp, J. & Hamman, J.H. 2017. Development and evaluation of a double-phase multiple-unit dosage form for enhanced insulin intestinal delivery. *Drug delivery letters*, 7:1-9

Di Paquale, G. & Chiorini, J.A. 2006. AVV transcytosis through barrier epithelia and endothelium. *Molecular therapy*, 13:506-515.

Dobson, P.D. & Kell, D.B. 2008. Carrier mediated cellular uptake of pharmaceutical drugs: an exception or the rule? *Nature reviews drug discovery*, 7:205-220.

Dorkoosh, F., Verhoef, J., Borchard, G., Rafiee-Tehrani, M. & Junginger, H. 2001. Development and characterisation of a novel peroral peptide drug delivery system. *Journal of controlled release*, 71: 307-318.

Gandhi, R., Lal Kaul, C. & Panchagnula, R. 1999. Extrusion and spheronization in the development of oral controlled-release dosage forms. *Pharmaceutical science and technology today*, 2:160-170.

Gangwar, S., Pauletti, G., Wang, B., Siahaan, T., Stella V. & Borchardt, R. 1997. Prodrug strategies to enhance the intestinal absorption of peptides. *Drug discovery today*, 2:148-155.

Goldberg, M. & Gomez-Orellana, I. 2003. Challenges for oral delivery of macromolecules. *Nature reviews drug discovery*, 2:289-295.

Grass, G.M. & Sweetana, S.A. 1988. *In vitro* measurement of gastrointestinal tissue permeability using a new diffusion cell. *Journal of pharmaceutical research*, 5:372-376.

Grass, S.M. 2012. Mechanisms of carrier-mediated transport. (In Sperelakis, N., ed. Cell physiology: source book. 4th ed. San Diego: CA Academic. p.153-165).

Hamman, J.H., Stander, M., & Kotzé, A. 2002. Effect of the degree of quaternisation of *N*-trimethyl chitosan chloride on absorption enhancement: *in vivo* evaluation in rat nasal epithelia. *International journal of pharmaceutics*, 232:235-242

Hamman, J.H & Kotzé, A.F. 2001. Effect of the Type of Base and Number of Reaction Steps on the degree of quaternization and molecular weight of *N*-trimethyl chitosan chloride. *Drug Development and industrial pharmacy*, 27(5):373-380.

Hamman, J.H., Enslin, G.M. & Kotzé, A.F. 2005. Oral delivery of peptide drugs: Barriers and developments. *Biodrugs*, 19(3):165-177.

Hejazi, R. & Amiji, M. 2003. Chitosan-based gastrointestinal delivery systems. *Journal of controlled release*, 89(2):151-165.

Hellum, B.H. & Nilsen, O.G. 2008. *In vitro* inhibition of CYP3A4 metabolism and P-glycoprotein mediated transport by trade herbal products. *Basic and clinical pharmacology and toxicology*, 102:462-475.

Hinds, K., & Kim, S. 2002. Effects of PEG conjugation on insulin properties. *Advanced drug delivery review*, 54:505-530.

Hochman, J. & Artursson, P. 1994. Mechanisms of absorption enhancement and tight junction regulation. *Journal of controlled release*, 29: 253-267.

ICH. Expert working Group. 2005. Validation of analytical procedures: text and methodology Q2(R1).

http://www.ich.org/fileadmin/Public_Web_Site/ICH_Products/Guidelines/Quality/Q2_R1/Step4/Q2_R1__Guideline.pdf Date of access: 10 Sep. 2016.

Jonker, C., Hamman, J.H. & Kotzé, A.F. 2002. Intestinal paracellular permeation enhancement with quaternised chitosan: *in situ* and *in vitro* evaluation. *International journal of pharmaceutics*, 238:205-213.

Kerns, E.H. & Di, L. 2008. Permeability. (In Drug-like properties: concepts, structure design and methods from ADME to toxicity optimization. Amsterdam: Academic Press. p.86-99).

Kesarwani, K & Gupta, R. 2013. Bioavailability enhancers of herbal origin: an overview. *Asian pacific journal of tropical biomedicine*, 3: 253-266.

- Khafagy, E., Morishita, M., Onuki, Y. & Takayama, K. 2007. Current challenges in non-invasive insulin delivery systems: a comparative review. *Advanced drug delivery reviews*, 59:1521-1546.
- Kotzé, A., Lueßen, H., De Leeuw, B., De Boer, A., Verhoef, J. & Junginger, H.E. 1998. Comparison of the effect of different chitosan salts and *N*-trimethyl chitosan chloride on the permeability of intestinal epithelial cells (Caco-2). *Journal of controlled release*, 51:35-46.
- Lapierre, L.A. 2000. The molecular structure of the tight junction. *Advanced drug delivery reviews*, 41:255-264.
- Lee, H.J. & Amidon, G.L. 2002. The effect of enzyme inhibitor and absorption site following [D-al², D-leu⁵] enkephalin oral administration in rats. *Biopharmaceutics drug disposition journal*, 23:131-141.
- Lee, V.H.L., Traver, R.D. & Taub, M.E. 1991. Enzymatic barriers to peptide and protein drugdelivery. (In Lee, V.H.L., ed. Peptide and protein drug delivery. NY: Marcel Dekker Inc. p 303-358).
- Lee, Y.C. 2004. Method validation for HPLC analysis of related substances in pharmaceutical drug products. (In Chan, C.C, Lee, Y.C., Lam, H. & Zhang, X.M., eds. Analytical method validation and instrument performance verification. NJ: Wiley. p. 27-51).
- Lehr, C. 2000. Lectin-mediated drug delivery: the second generation of bioadhesives. *Journal of controlled release*, 65:19-29.
- Lemmer, H.J. & Hamman, J.H. 2013. Paracellular drug absorption enhancement through tight junction modulation. *Expert opinion in drug delivery*, 10:103-114.
- Lennernäs, H. 1998. Human intestinal permeability. *Journal of pharmaceutical sciences*, 87:403-410.
- Lindhardt, K. & Bechgaard, E. 2003. Sodium glycocholate transport across Caco-2 cell monolayers, and the enhancement of mannitol transport relative to transepithelial electrical resistance. *International journal of pharmaceutics*, 252:181-186.
- Liu, Z., Wang, S. & Hu, M. 2009. Oral absorption basics: pathways, physico-chemical and biological factors affecting. (In Developing solid oral dosage forms: pharmaceutical theory and practice, Massachusetts: Academic Press. p. 265-287).
- Lowman, A., Morishita, M., Kajita, M., Nagai, T. & Peppas, N. 1999. Oral delivery of insulin using pH-responsive complexation gels. *Journal of pharmaceutical sciences*, 88:933-937.

- Maher, S. & Brayden, D.J. 2012. Overcoming poor permeability: translating permeation enhancers for oral peptide delivery. *Drug discovery today: Technology*, 9:113-119.
- Mayersohn, M. 2002. Principles of drug absorption. (In Banker, G.S. & Rhodes C.T. eds. Modern pharmaceuticals. 4th ed. NY: Marcel Dekker. p. 23-66).
- Moeller, E. & Jorgensen, L. 2008. Alternative routes of administration for systemic delivery of protein pharmaceuticals. *Drug discovery today: Technologies*, 5:89-94.
- Moroz, E., Matoori, S. & Leroux, J.C. 2016. Oral delivery of macromolecular drugs: Where we are after almost 100 years of attempts. *Advanced drug delivery reviews*, 101:108-122.
- Muranishi, S. 1990. Absorption enhancers. *Critical reviews in therapeutic drug carrier systems*. 7:1-33.
- Ni, Y. & Tizard, I. 2004. Analytical methodology: the gel-analysis of aloe pulp and its derivatives. (In: Reynolds, T., ed. Aloes the genus *Aloe*. FL: CRC. p. 111-126).
- Pauletti, G.M., Gangwar, S. & Knipp, G.T. 1996. Structural requirements for intestinal absorption of peptide drugs. *Journal of Controlled Release*, 41: 3-17.
- Pfister, D. & Morbidelli, M. 2014. Process for protein PEGylation. *Journal of controlled release*, 180:134-149.
- Ponchel, G., Montisci, M., Dembri, A., Durrer C. & Duchêne, D. 1997. Mucoadhesion of colloidal particulate systems in the gastro-intestinal tract. *European Journal of pharmaceuticals and biopharmaceutics*, 44:25–31.
- Renukuntla, J., Vadlapudi, A., Patel, A., Boddu, S. & Mitra, A. 2013. Approaches for enhancing oral bioavailability of peptides and proteins. *International journal of pharmaceuticals*, 447:75-93.
- Rosenthal, R., Heydt, M.S., Amasheh, M., Stein, C., Fromm, M. & Amasheh, S. 2012. Analysis of absorption enhancers in epithelial cell models. *Annals of the New York Academy of Science*, 1258:86-92.
- Rubio-Aliaga, I. & Daniel, H. 2002. Mammalian peptide transporters as targets for drug delivery. *Trends in pharmacological sciences*, 23: 434-440.
- Rúnarsson, O.V., Holappa, J., Nevalainen, T., Hjálmsdóttir, M., Järvinen, T., Loftsson, T., Einarsson, J.M., Jónsdóttir, S., Valdimarsdóttir, M. & Másson, M. 2007. Antibacterial activity of methylated chitosan and chitooligomer derivatives: synthesis and structure activity relationships. *European polymer journal*, 43:2660-2671.

Sato, H., Sugiyama, Y., Tsuji, A. & Horikoshi, I. 1996. Importance of receptor-mediated endocytosis in peptide delivery and targeting: kinetic aspects. *Advanced drug delivery reviews*, 19:445-467.

Shabir, G. A. 2004. A practical approach to validation of HPLC methods under current good manufacturing practices. *Journal of validation technology*, 10:29-37

Shabir, G.A. 2003. Validation of high-performance liquid chromatography methods for pharmaceutical analysis understanding the differences and similarities between validation requirements of the US Food and Drug Administration, the US Pharmacopeia and the International Conference on Harmonization. *Journal of chromatography A*, 987:57-66.

Shargel, L., Wu-Pong, S. & Yu, A.B.C. 2005. Physiologic factors related to drug absorption. (In Shargel, L., Wu-Pong, S. & Yu, A.B.C. eds. *Applied biopharmaceutics and pharmacokinetics*. 5th ed. NY: McGraw-Hill, p. 371-408).

Shen, W.C. 2003. Oral peptide and protein delivery: unfulfilled promises? *Drug discovery today*, 8: 607-608.

Sigma-Aldrich. 2013. Lucifer yellow: product information.

<https://www.sigmaaldrich.com/content/dam/sigma-aldrich/docs/Sigma/Bulletin/1/mtox1000p24bul.pdf>

Date of access: 7 Dec 2016

Silverstein, S.C., Steinman, R.M. & Cohn, Z.A. 1977. Endocytosis. *Annual Review of Biochemistry*, 46:669-772.

Singh, R. 2013. HPLC method development and validation – an overview. *Indian journal of pharmaceutical education and research*, 4:26-33.

Sinko, P.J., Hu, M. & Amidon, G.L. 1987. Carrier mediated transport of amino acids, small peptides and their analogs. *Journal of controlled release*, 6:115-121.

Thanou, M., Verhoef, J., Marbach, P. & Junginger, H. 2000. Intestinal absorption of octreotide: N-trimethyl chitosan chloride (TMC) ameliorates the permeability and absorption properties of the somatostatin analogue *in vitro* and *in vivo*. *Journal of pharmaceutical sciences*, 89:951-957.

Torchilin, V.P. & Lukyanov, A.N. 2003. Peptide and protein drug delivery to and into tumors: challenges and solutions. *Drug discovery today*, 8:259-266.

Versantvoort, C.H.M., Rempelberg, C.J.M. & Sips, A.J.A.M. 2000. Methodologies to study human intestinal absorption. A review. *Research for man and environment*, RIVM report 630030 001.

<http://rivm.openrepository.com/rivm/bitstream/10029/9613/1/630030001.pdf> Date of access: 15 Oct 2016

Vinson, J.A., Al Kharrat, H. & Andreoli, L. 2005. Effect of *Aloe vera* preparations on the human bioavailability of vitamins C and E. *Phytomedicine*, 12:760-765.

Wallis, L., Kleynhans, E., Du Toit, T., Gouws, C., Steyn, D., Steenekamp, J., Viljoen, J., & Hamman, J.H. 2014. Novel non-invasive protein and peptide drug delivery approaches. *Protein and peptide letters*, 21:1087-1101.



Ward, P.D., Tippin, T.K. & Thakker, D.R. 2000. Enhancing paracellular permeability by modulating epithelial tight junctions. *Pharmaceutical science & technology today*, 3:346-358.

Yamamoto, A., Taniguchi, T., Rikyu, K., Tsuji, T., Fujita, T., Murakami, M. & Muranishi, S. 1994. Effects of various protease inhibitors on the intestinal absorption and degradation of insulin in rats. *Pharmaceutical research*, 11:1496-1500.

ADDENDUM A

STANDARD OPERATING PROCEDURE: BIOLOGICAL WASTE MANAGEMENT

Filename: Pharmacen_SOP001_v02_Biological waste management

  <div>NORTH-WEST UNIVERSITY YUNIBESITHI YA BOKONE-BOPHIRIMA NOORDWES-UNIVERSITEIT POTCHEFSTROOMKAMPUS</div>		
STANDARD OPERATING PROCEDURE		
Document type: Standard Operating Procedure (SOP)	Section: Research laboratories in Buildings G2; G16 and G20	
TITLE: BIOLOGICAL WASTE MANAGEMENT	Date issued: 30 June 2016	
	Review Date: 30 June 2018	
	Compiled by: Sias Hamman, Chrisna Gouws, Happiness Netsimbupfe	
SOP No: Pharmacén_SOP001_v02_Biological waste management	Version No: 01	Page 1 of 12

1. Definitions

The following definitions are applicable to this SOP:

Waste (according to the Waste Amendment Act, 2014 (Act No 26 of 2014)): "Any substance, material or object, that is unwanted, rejected, abandoned, discarded or disposed of, by the holder of the substance, material or object, whether or not such substance, material or object can be re-used, recycled or recovered and includes all wastes as defined in Schedule 3 to this Act".

Hazardous waste (Act No 26 of 2014): "Any waste that contains organic or inorganic elements of compounds that may, owing to the inherent physical, chemical or toxicological characteristics of that waste, have a detrimental impact on health and the environment".

Biological waste: Waste containing mostly natural organic materials such as cell cultures, animal/human tissues or blood, animal excrements, microbiological cultures etc.

2. Purpose

To manage biological waste in the research laboratory of Building G2, G16 and G20 on the Potchefstroom campus of the North-West University to ensure the safety and health of the researchers (both staff and students) as well as to ensure that the environment is not contaminated by waste materials of a potential hazardous nature. This ensures compliance with the policy regarding the use of unsealed radioactive nuclides, which is subject to regulatory control in terms of the Hazardous Substance Act, 1973 (Act 15 of 1973).

3. Objective

To ensure safe handling, storage and removal of liquid and/or solid biological waste materials as well as needles and sharp waste generated in the research laboratories of Buildings G2, G16 and G20.

4. Scope

This SOP is applicable to the all research laboratories in buildings G2, G11 and G20 generating potentially hazardous liquid and/or solid biological and sharp waste materials.

5. Responsibilities

All staff and students working inside the research laboratories of buildings G2, G16 and G20 are responsible to follow the procedures outlined in this SOP. The safety officers are responsible for completion of documentation such as disposal request form, treatment request form, communication with the contracted waste removal company (currently Averda), as well as reporting any incidents to the Occupational Health and Safety Committee.

6. Apparatus and equipment

Apparatus/equipment	Location (Room No.)	Check points	Criteria for approval/rejection
Autoclave	LAMB (G14)	Preheat until jacket pressure and temperature reach minimum level to start an autoclave cycle	Autoclave must be serviced once a year, and Sterikon+ bio-indicator for check on autoclaving quality must be done quarterly
Hazardous waste containers	All research laboratories	Appropriately labelled	Correct label and container for waste type

7. List of other SOPs relevant to this SOP

None.

8. Safety measures

The following general safety measures should always be followed:

- All staff and students working in the research laboratories of buildings G2, G16 and G20 should familiarise themselves with the potential hazardousness and other safety aspects such as incompatibilities between chemicals or potential presence of pathogens in biological material before handling them.
- All staff and students must be appropriately trained in handling hazardous waste materials.
- Adherence to dress code: always wear a laboratory coat, gloves and, if the need arise, eye protective goggles or a face mask during handling of biological materials.
- All biological materials should be regarded as potentially hazardous and therefore be handled with care.
- Emergency post for eye washing should be available in all laboratories.
- Disinfect all needles, blades, loops and slides by autoclaving before discarding.
- Keep large enough bins for broken glass in the laboratory (store room).

9. Procedures

9.1 Waste containers

- 9.1.1 Only use waste containers supplied by the removal company that is compatible with the type of waste material.
- 9.1.2 Different types of waste containers shall be available for different types of waste as prescribed by the waste company which may include: biological waste – sharps/needles (plastic bucket with lid), biological waste – solids (box with red liner), biological waste – liquid (plastic drum with screw lid), medical waste – solids, liquids and sludge (plastic drum with screw lid) (Refer to Addendum A).
- 9.1.3 Containers shall be labeled correctly with all appropriate information: Site information include campus name, building number, room number and date, Waste information include full names and class of biological material as prescribed by the waste removal company before removal.
- 9.1.4 Containers must remain closed at all times (except when waste is added) and be sealed appropriately.

9.1.5 Containers must be kept clean and dry.

9.1.6 Containers for liquids must never be filled to the top to allow space for expansion (only fill to about 90% of container volume). Incompatible liquids are not allowed to be mixed in any waste container.

9.2 Contaminated sharps and needles

9.2.1 Place the sharps and needles in the designated waste bins provided by the waste removal company (yellow buckets).

9.2.2 No waste other than the sharps and needles shall be placed in these containers.

9.2.3 When the need arises for removal of the waste (e.g. container is full), the safety officer should be informed to complete a disposal request form and to notify the contracted waste removal company (currently Averda).

9.3 Biological materials and contaminated disposable items

9.3.1 Biological materials (e.g. tissue and blood) and contaminated disposable items (other than sharps and needles) are placed in the disposable red plastic bag that is placed inside the appropriate waste container and stored in the refrigerator in Room G14, Building G20.

9.3.2 When the need arises for removal of the waste (e.g. container is full), the safety officer should be informed to complete a disposal request form and to notify the medical waste company (currently Oricol) according to the procedure described in Addendum A.

9.4 Contaminated broken glassware

9.4.1 Place the broken glassware (after it has been decontaminated by autoclaving) in the designated bins for broken glass.

9.4.2 No other waste should be placed in this container.

10. Records and data sheets

There should be material safety data sheets (MSDS) available on all chemicals used in the specified laboratories. Record the type and volume of waste disposed on record books placed next to the waste container.

All records (including copies of disposal request forms and treatment request forms) must be kept for 5 years at the North-West University by the safety officer.

11. Scheme of SOP development

Action	Designated person	Signature	Date
Compile	H. Netsimbupfe		2015/09/03
Compile	C. Gouws		2016/06/30
Proof read	J.H. Hamman		2016/06/30
Discussed	Scientific committee		2016/07/29



Chemical, pharmaceutical and medical waste procedure

Aim

To control and manage the booking, collecting, handling and disposal of all chemical, pharmaceutical and medical waste originating from clients. To prevent incompatible chemicals being stored and transported together.

Scope

This procedure applies to all Oricol and client personnel requesting the assistance of Oricol staff in the disposal of chemical, pharmaceutical and medical waste.

Responsibility

- Oricol contract manager and/or sales representative
- Oricol drivers and assistants
- Client
- Booking clerk
- Hazardous waste clerk
- Logistics management

Method

Client responsibility

Chemical waste

- When the need to dispose of chemical waste arises, a TRF (treatment request form) must be completed and sent to the Oricol contract manager or sales representative. An example of a TRF can be seen in Appendix A and should be in Word format where possible.
- Campus name, Building number, building name and room number and date must be completed in full in order to ensure that the waste is collected from the right site.
- Chemical names must be written out in full on the TRF and the storage containers and no abbreviations or chemical formulas may be used (i.e. "Ether" instead of "Et₂O" and "Dimethylphosphinoethane" instead of "DMPE").
- A separate TRF must be completed for the following chemicals and/or their compounds as the incinerator is not permitted to accept and incinerate them. These will be collected and disposed of separately at the hazardous waste landfill:
 - Arsenic (As)
 - Astatine (At)
 - Cadmium (Cd)
 - Chromium (Cr)
 - Cesium (Cs)
 - Cyanide(CN')
 - Francium (Fr)
 - Iodine (I)
 - Krypton (Kr)
 - Lead (Pb)
 - Mercury (Hg)
 - Nickel (Ni)
 - Phosphorous (P)
 - Rubidium (Rb)
 - Selenium (Se)

Last printed	Date	Document Writer	Authorised By	Doc Rev No	Page No.
12/06/2014 3:31 PM	03/01/2012	Paul Eloff	Peter Allen	6	1 of 7

Once printed this document is an uncontrolled version and should be checked against the electronic version for validity.

Document: Procedure



Chemical, pharmaceutical and medical waste procedure

- The UN number and class of the chemicals must also be completed. The chemicals must then be grouped together in the following classes. Should the container be a mixture of chemicals, the highest concentration constituent applies:

- Class 3 (Flammable Liquids); 4.1 (Flammable Solids); 4.2 (Spontaneously Combustible material); 4.3 (Dangerous when Wet material); 8.2 (Alkalis) and 9. (Miscellaneous materials not classified). A GREEN sticker must be placed on the box or container.

Examples: Acetone, Magnesium, white phosphorous, sodium hydroxide, calcium

- Class 6.1 (Toxic Substances). A RED sticker must be placed on the box or container

Examples: Potassium cyanide, mercuric chloride

- Class 5.1 (Oxidizing Agents) and 8.1. (Acids). A ORANGE sticker must be placed on the box or container

Examples: Calcium hypochlorite, ammonium nitrate, hydrogen peroxide

- Class 5.2 (Organic Peroxides) must be grouped separately and a BLUE sticker must be placed on the box or container. These chemicals will be transported with Class 5.1 (Oxidizing Agents) and 8.1. (Acids).

Examples: benzoyl peroxides, cumene hydroperoxide, hydrochloric acid.

(Note: no collection will take place if chemicals aren't identified by means of a colour coded sticker & class)

- Each grouped class will be collected on different days/loads to ensure legal compliance.
- All chemical containers must be properly sealed. The bottle or jar must have a cap that fits tightly. If the chemical is a liquid, there must be at least 3 cm of room at the top of the container. The outside of the container must be clean and dry.
(Note: Chemicals shall not be removed if they are in leaking or otherwise inappropriate containers)
- The chemical, pharmaceutical and medical waste that needs to be disposed of, must be kept until your TRF or DRF has been returned by Oricol indicating service date and reference number.
- When the need to dispose of medical or pharmaceutical waste, a DRF (disposal request form) must be completed and sent to the Oricol contract manager or sales representative. An example of a DRF can be seen in Appendix B and should be in Word format where possible.
- On the day of collection, all chemical, pharmaceutical and medical waste needs to be at a centralised area at the collection point. A customer copy of the TRF/DRF must be placed with the waste. This TRF/DRF will have a unique number. A TRF/DRF that has not got a unique number on that matches Oricol's TRF/DRF will not be collected
- This is important as the collection staff will use this TRF/DRF to match up the TRF/DRF that was received to ensure the correct waste is removed.

Last printed	Date	Document Writer	Authorised By	Doc Rev No	Page No.
12/06/2014 3:31 PM	03/01/2012	Paul Eloff	Peter Allen	6	2 of 7

Once printed this document is an uncontrolled version and should be checked against the electronic version for validity.
Document: Procedure



Chemical, pharmaceutical and medical waste procedure

- Medical waste containers must be properly sealed. Bio-hazardous tape must be used in the case of medical waste boxes.
- The maximum weights for containers are shown below. Under no circumstances must the weight of the containers exceed the maximum weight.

Container	Maximum allowed weight in kg
5L Sharps and Lids (Needles Ect)	2.5
10L Sharps and Lids (Needles Ect)	3.5
20L Sharps and Lids (Needles Ect)	8
5L Anatomical Waste	2.5
10L Anatomical Waste	5
20L Anatomical Waste	12
20L Pharmaceutical waste	12
50L Box & Liner	9
142L Box & Liner	15

Bookings (For Oricol ES use only)

- The sales representative or Oricol contract manager will forward the TRF/DRF received from the client to the Hazardous Waste Clerk to generate a unique number.
- In the case of TRF's, a quote will be requested from the disposal site by the hazardous waste clerk.
- Once the disposal site sent the quote, the Hazardous waste clerk will reply with an acceptance form to the disposal site.
- The Hazardous waste clerk will make a booking with the Booking clerk. More than one booking shall be made if the TRF contains more than one group of classes. The Booking Clerk will complete the booking ref number and service date on the TRF/DRF and send it to the Hazardous waste Clerk.
- The Hazardous waste clerk will print out the TRF/DRF with the reference number and service date and prepare the stock.
- The Hazardous waste clerk will request delivery notes on daily basis from the logistics department which he will then use to match up with the TRF's/DRF's. Special care must be taken to ensure the waste type is correct and reflects the classes for collection.
- The Bookings waste clerk will then communicate the service date and reference number to the sales representative or Oricol contract manager which in turn needs to communicate this information with the client.

Collection and Handling (For Oricol ES use only)

- The collection staff will take the crates and a trolley with to ease loading and offloading of the waste
- When arriving at the site, the collection staff will confirm the TRF/DRF corresponds to the client's DRF/TRF. They will only check that the TRF/DRF is the same and not check each chemical item for item. It is still the client's responsibility to supply them with the correct waste.
- The collections staff will confirm containers are labelled sealed and have no residue.
- Oricol staff will not remove any waste that does not conform.

Last printed	Date	Document Writer	Authorised By	Doc Rev No	Page No.
12/06/2014 3:31 PM	03/01/2012	Paul Eloff	Peter Allen	6	3 of 7

Once printed this document is an uncontrolled version and should be checked against the electronic version for validity.
Document: Procedure



Chemical, pharmaceutical and medical waste procedure

- In the case of chemical waste, collection staff will collect chemicals as per the delivery note instruction of which colour to collect
- The client will then sign the delivery note to confirm collection. Should there be no one to sign for the collection; the waste will not be removed.
- The crate must then be sealed and the trolley used to transport the waste to the vehicle. When arriving at the vehicle, the boxes will be offloaded and placed inside the vehicle for chemical waste.
- In the case of medical waste, the trolley must be used to transport the containers or boxes to the vehicle.
- The waste will then be transported and disposed of at the appropriate disposal site.

Last printed	Date	Document Writer	Authorised By	Doc Rev No	Page No.
12/06/2014 3:31 PM	03/01/2012	Paul Eloff	Peter Allen	6	4 of 7

Once printed this document is an uncontrolled version and should be checked against the electronic version for validity.
Document: Procedure



Chemical, pharmaceutical and medical waste procedure

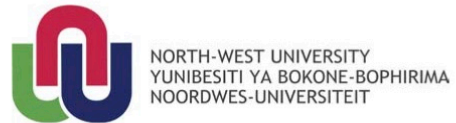
Revision Notes		
Date	Rev: No	Notes
26 January 2012	02	Added dangerous good load compatibility chart
24 September 2012	03	Added medical waste to procedure
9 October 2012	04	Added Account number and Site
31 January 2013	05	Update TRF document in landscape mode
23 May 2013	06	Update of collecting an packing of chemicals
22 October 2013	07	Update of classifying and packing
11 June 2014	08	Update checking of TRF/DRF

Last printed	Date	Document Writer	Authorised By	Doc Rev No	Page No.
12/06/2014 3:31 PM	03/01/2012	Paul Eloff	Peter Allen	6	7 of 7

Once printed this document is an uncontrolled version and should be checked against the electronic version for validity.
Document: Procedure

ADDENDUM B

ETHICS APPROVAL



Private Bag X6001, Potchefstroom
South Africa 2520

Tel: (018) 299-4900
Faks: (018) 299-4910
Web: <http://www.nwu.ac.za>

Ethics Committee

Tel +27 18 299 4849
Email Ethics@nwu.ac.za

ETHICS APPROVAL OF PROJECT

The North-West University Research Ethics Regulatory Committee (NWU-RERC) hereby approves your project as indicated below. This implies that the NWU-RERC grants its permission that provided the special conditions specified below are met and pending any other authorisation that may be necessary, the project may be initiated, using the ethics number below.

Project title: Excised pig buccal and intestinal tissues as in vitro models for pharmacokinetic studies																																						
Project Leader: Prof Sias Hamman																																						
Ethics number:		<table border="1"><tr><td>N</td><td>W</td><td>U</td><td>-</td><td>0</td><td>0</td><td>0</td><td>2</td><td>5</td><td>-</td><td>1</td><td>5</td><td>-</td><td>A</td><td>5</td></tr><tr><td colspan="3">Institution</td><td colspan="5">Project Number</td><td colspan="3">Year</td><td colspan="3">Status</td></tr></table>								N	W	U	-	0	0	0	2	5	-	1	5	-	A	5	Institution			Project Number					Year			Status		
N	W	U	-	0	0	0	2	5	-	1	5	-	A	5																								
Institution			Project Number					Year			Status																											
Status: S = Submission; R = Re-Submission; P = Provisional Authorisation; A = Authorisation																																						
Approval date: 2015-04-16					Expiry date: 2020-04-15																																	

Special conditions of the approval (if any): None

General conditions:

While this ethics approval is subject to all declarations, undertakings and agreements incorporated and signed in the application form, please note the following:

- The project leader (principle investigator) must report in the prescribed format to the NWU-RERC:
 - annually (or as otherwise requested) on the progress of the project,
 - without any delay in case of any adverse event (or any matter that interrupts sound ethical principles) during the course of the project.
- The approval applies strictly to the protocol as stipulated in the application form. Would any changes to the protocol be deemed necessary during the course of the project, the project leader must apply for approval of these changes at the NWU-RERC. Would there be deviation from the project protocol without the necessary approval of such changes, the ethics approval is immediately and automatically forfeited.
- The date of approval indicates the first date that the project may be started. Would the project have to continue after the expiry date, a new application must be made to the NWU-RERC and new approval received before or on the expiry date.
- In the interest of ethical responsibility the NWU-RERC retains the right to:
 - request access to any information or data at any time during the course or after completion of the project;
 - withdraw or postpone approval if:
 - any unethical principles or practices of the project are revealed or suspected,
 - it becomes apparent that any relevant information was withheld from the NWU-RERC or that information has been false or misrepresented,
 - the required annual report and reporting of adverse events was not done timely and accurately,
 - new institutional rules, national legislation or international conventions deem it necessary.

The Ethics Committee would like to remain at your service as scientist and researcher, and wishes you well with your project. Please do not hesitate to contact the Ethics Committee for any further enquiries or requests for assistance.

Yours sincerely

Linda du Plessis

Digitally signed by Linda du Plessis
DN: cn=Linda du Plessis, o=NWU,
Vaal Triangle Campus, ou=Vice-
Rector: Academic,
email=linda.duplessis@nwu.ac.za,
c=US
Date: 2015.04.20 20:35:13 +02'00'

Prof Linda du Plessis

Chair NWU Research Ethics Regulatory Committee (RERC)

ADDENDUM C

Aloe vera leaf materials ^1H -NMR spectra

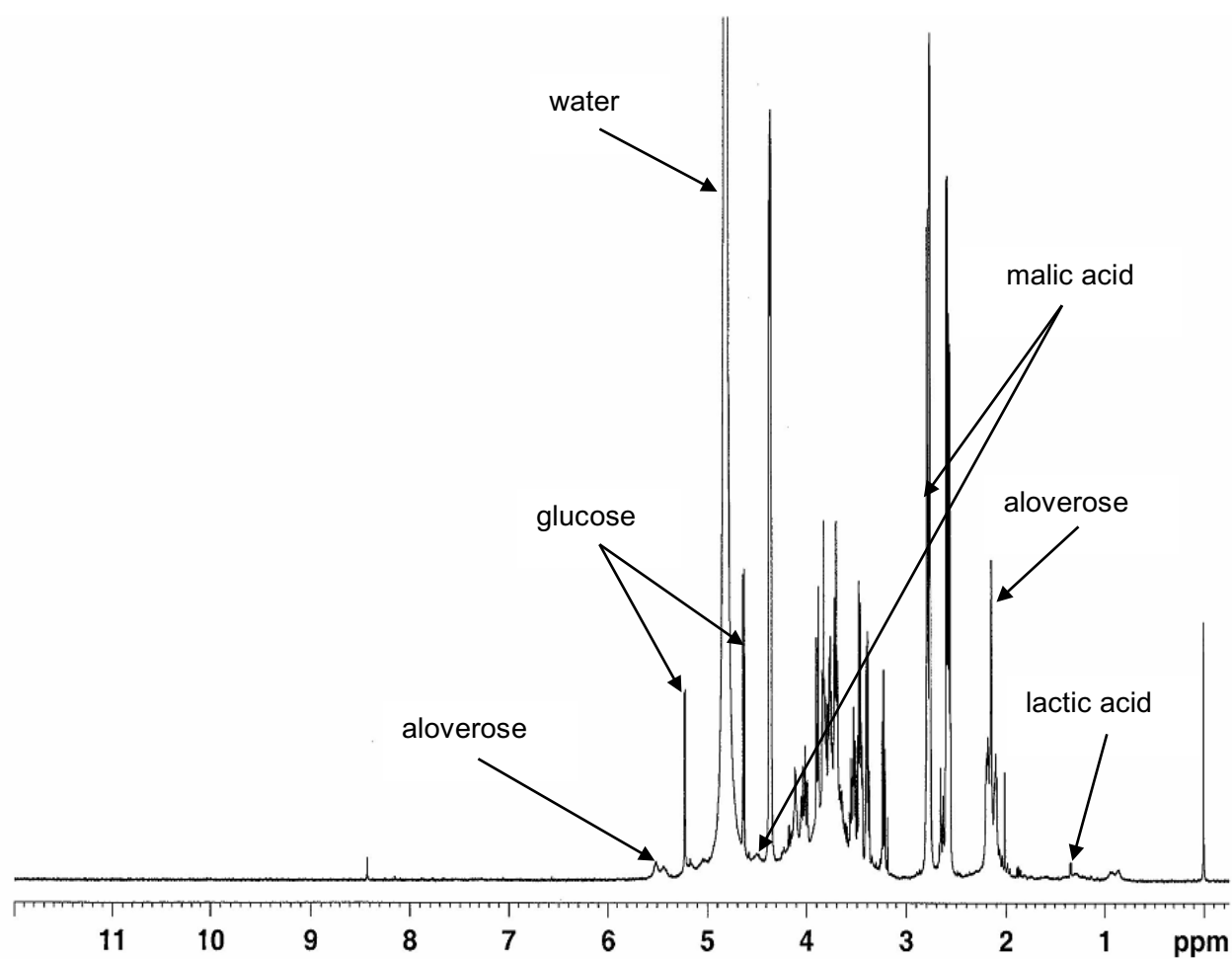


Figure C.1: ^1H -NMR spectrum of *Aloe vera* gel (Daltonmax)

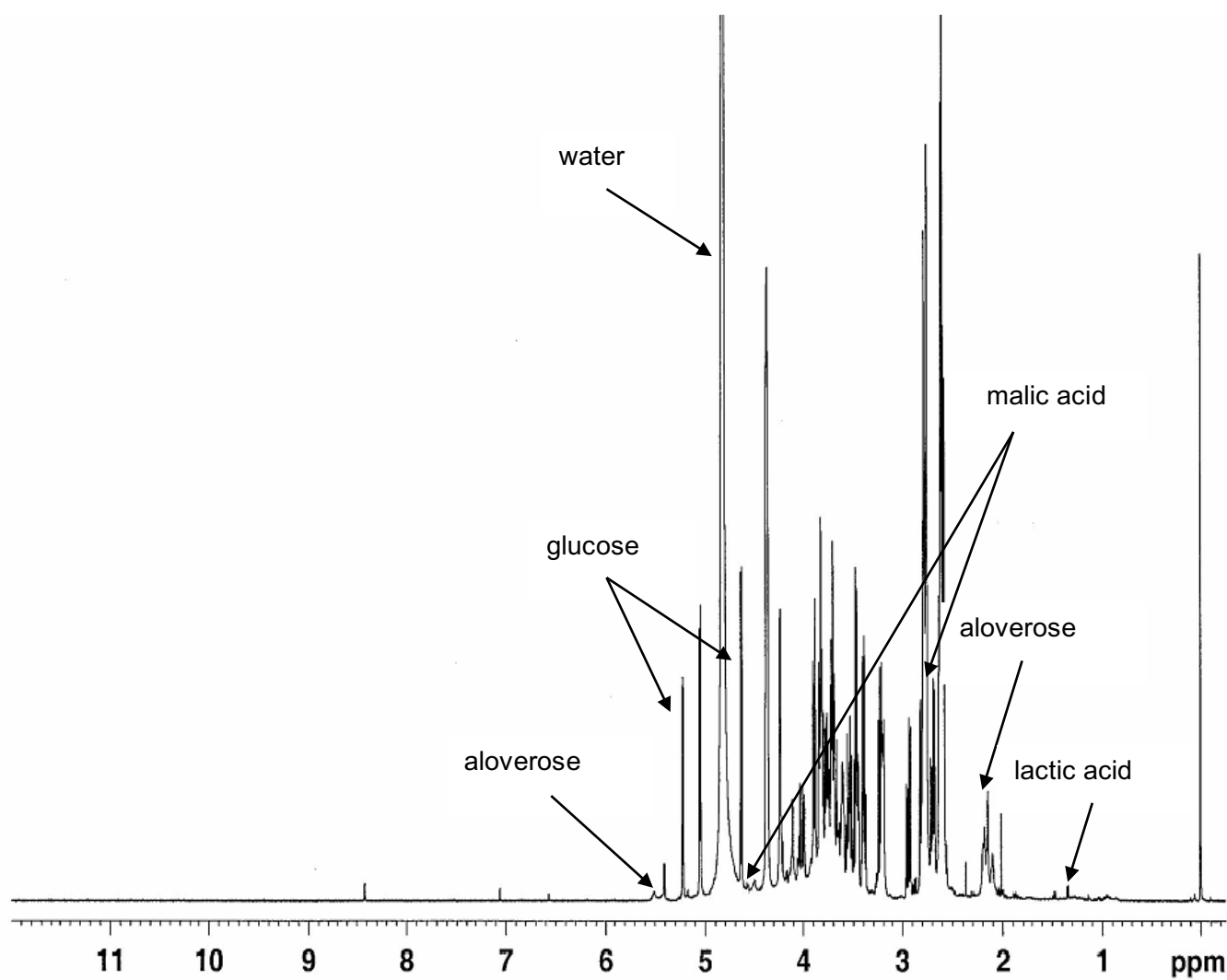


Figure C.2: ^1H -NMR spectrum of *Aloe vera* whole leaf (Daltonmax)

ADDENDUM D

Extrusion-spheronisation process



Figure D.1: Front view of wetted mass being extruded



Figure D.2: Side view of wetted mass being extruded

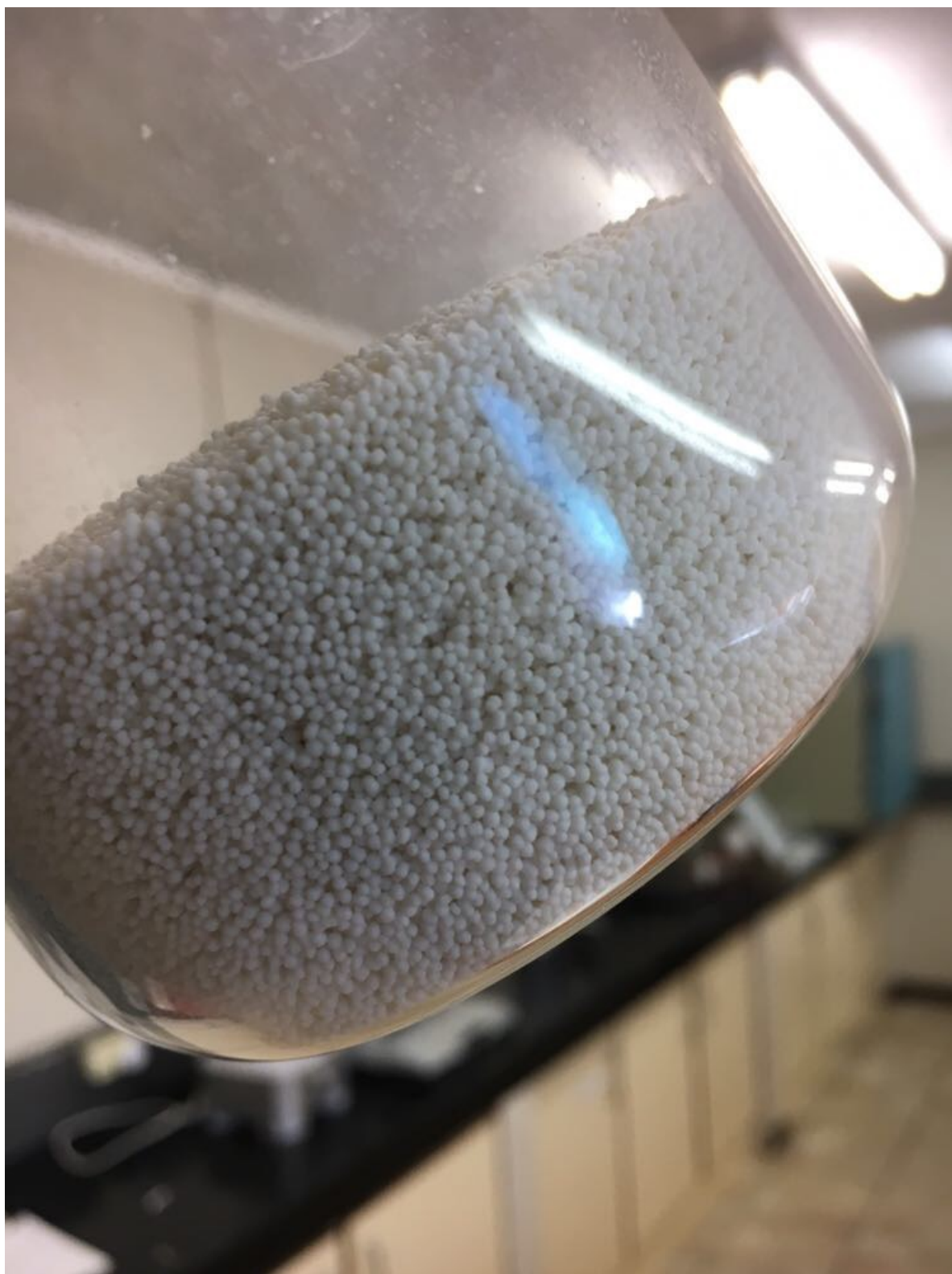


Figure D.3: Spheronised micro-beads

Addendum E

Experimental data

Ex vivo transport data

Table E.1: Apical to basolateral transport of micro-beads containing FD-4 and Pharmacerl®

FDPH	% Transport				
Time	1	2	3	Average	STDEV
0	0	0	0	0	0
20	0.017604017	0.035718215	0.095708225	0.049676819	0.040880299
40	0.023356348	0.037730621	0.102489893	0.054525621	0.042155468
60	0.027521051	0.041778929	0.109890511	0.059730164	0.044021212
80	0.030343665	0.065887357	0.118529938	0.071586986	0.044368559
100	0.030833105	0.07966727	0.127070639	0.079190338	0.04812054
120	0.042371831	0.090690873	0.135837936	0.089633547	0.046742022

Table E.2: Apical to basolateral transport of micro-beads containing FD-4 and *Aloe vera* gel as an absorption enhancer

AVG	% Transport				
Time	1	2	3	Average	STDEV
0	0	0	0	0	0
20	1.530290798	0.934246664	1.0747622	1.179766554	0.311587208
40	5.193052822	4.039390456	2.270550171	3.83433115	1.472002862
60	7.995172907	7.366468244	3.806147682	6.389262944	2.259022074
80	10.5022578	10.28315677	5.239409215	8.674941262	2.977274198
100	12.82207838	11.75660658	7.874151612	10.81761219	2.604184648
120	13.83768068	13.33326149	10.77510082	12.648681	1.642052582

Table E.3: Apical to basolateral transport of micro-beads containing FD-4 and *Aloe vera* whole leaf extract as an absorption enhancer

AVWL	% Transport				
Time	1	2	3	Average	STDEV
0	0	0	0	0	0
20	2.397450996	2.391210447	3.058868717	2.615843387	0.383683878
40	3.681300613	2.876295097	3.136647464	3.231414391	0.410784674
60	4.070836546	2.787663304	3.533022084	3.463840645	0.644377953
80	4.309644846	4.035091213	3.549761619	3.964832559	0.384782846
100	4.55374618	4.346327978	4.755071979	4.551715379	0.204379568
120	5.16299302	4.97115416	5.343770492	5.159305891	0.186335528

Table E.4: Apical to basolateral transport of micro-beads containing FD-4 and chitosan as an absorption enhancer

Chitosan	% Transport				
Time	1	2	3	Average	STDEV
0	0	0	0	0	0
20	0.473997381	0.265954822	0.002107212	0.247353138	0.236494397
40	0.89366913	0.351140731	0.036657286	0.427155716	0.433533198
60	1.137652088	0.533367477	0.314421278	0.661813615	0.426381343
80	1.676854654	1.131253209	0.959556709	1.255888191	0.374539042
100	1.859312601	1.148853909	1.052409213	1.353525241	0.440671119
120	1.890156105	1.376409756	1.40400442	1.55685676	0.288975269

Table E.5: Apical to basolateral transport of micro-beads containing FD-4 and TMC as an absorption enhancer

TMC	% Transport				
Time	1	2	3	Average	STDEV
0	0	0	0	0	0
20	1.730924935	1.029946543	2.268965728	1.676612402	0.621292623
40	2.238422132	1.156991729	2.477803675	1.957739178	0.703720995
60	2.515262182	1.70102777	2.898286863	2.371525605	0.611434777
80	2.73759536	1.977142497	2.902843961	2.53919394	0.493713624
100	2.860531437	2.104489077	2.914282399	2.626434304	0.452816085
120	2.832135276	2.550248361	2.950004719	2.777462785	0.205409584

Table E.6: Apical to basolateral transport of micro-beads containing FD-4 and TMC as an absorption enhancer

SG	% Transport				
Time	1	2	3	Average	STDEV
0	0	0	0	0	0
20	0.068879709	0.08191703	0.077467539	0.076088092	0.006627224
40	0.08361625	0.124925898	0.083390409	0.097310852	0.023915598
60	0.104731012	0.13892731	0.108981263	0.117546528	0.018637852
80	0.105712898	0.130586051	0.127559488	0.121286146	0.013571461
100	0.335249778	0.20998083	0.165607375	0.236945995	0.087977135
120	0.466478289	0.347272008	0.330622881	0.381457726	0.074099059

Dissolution studies

Table E.7: Dissolution of micro-bead formulation containing FD-4 and and Pharmacel®

FD Pharma	% Dissolution				
Time	1	2	3	Average	STDE
0	0	0	0	0	0
15	39.10928881	42.64971501	50.31506939	44.02469107	5.728027497
30	80.16269657	75.42816909	64.69558538	73.42881701	7.925019792
60	91.33101441	90.11205426	93.57646846	91.67317904	1.757369889
90	93.16921236	91.09589675	95.71061956	93.32524289	2.311314734
120	95.60854332	91.51006908	97.48753418	94.86871553	3.05663722
180	95.94208732	91.7644221	99.07774374	95.59475105	3.669012159
240	98.90678275	95.00434058	99.05945754	97.65686029	2.2984175
300	99.49080136	97.62504294	99.2970667	98.80430367	1.025853388

Table E.8: Dissolution of micro-bead formulation containing FD-4 and and *Aloe vera* gel

AVG	% Dissolution				
Time	1	2	3	Average	STDE
0	0	0	0	0	0
15	38.61463648	40.73570567	47.77512054	42.37515423	4.795253983
30	64.68859244	58.94810021	63.48816891	62.37495386	3.027829022
60	89.49627052	74.42847207	67.35712858	77.09395706	11.3076969
90	92.84286994	77.10738852	81.14870989	83.69965612	8.172015591
120	93.51450783	80.24724177	82.94747801	85.56974254	7.0115826
180	94.97941711	94.53066485	85.53774634	91.68260943	5.326335653
240	95.12183324	97.77472828	88.86090875	93.91915676	4.5769933
300	98.73701192	99.65290774	99.97320804	99.4543759	0.641565573

Table E.9: Dissolution of micro-bead formulation containing FD-4 and and *Aloe vera* whole leaf extract

AVWL	% Dissolution				
Time	1	2	3	Average	STDE
0	0	0	0	0	0
15	59.45901558	57.88794011	62.9126164	60.08652403	2.570441225
30	68.75138408	76.3221457	73.42431781	72.83261586	3.819907233
60	70.62816541	83.42718954	84.57750967	79.54428821	7.742980264
90	73.97202423	86.70285139	87.56846078	82.7477788	7.612340055
120	82.55072835	89.86446507	88.67816948	87.03112097	3.925208635
180	88.71469535	93.29778585	89.69587125	90.56945082	2.413200279
240	95.34393545	95.35517415	95.26228353	95.32046437	0.050698476
300	96.46280869	99.73799135	99.56142478	98.58740827	1.842073965

Table E.10: Dissolution of micro-bead formulation containing FD-4 and and chitosan

Chitosan	% Dissolution				
Time	1	2	3	Average	STDE
0	0	0	0	0	0
15	58.89706558	53.80062421	60.77037316	57.82268765	3.606946914
30	75.90911507	75.1802304	83.46359421	78.18431322	4.586493649
60	77.36755385	79.61664009	86.69101155	81.2250685	4.865387687
90	79.84545037	81.91354539	87.3321506	83.03038212	3.866285463
120	84.91209392	92.11982025	89.93081944	88.98757787	3.695281884
180	86.77117997	93.98828498	93.57153112	91.44366536	4.051852747
240	95.29882852	96.63319176	98.60288296	96.84496774	1.662176505
300	97.29646989	96.74136844	99.6898498	97.90922938	1.566841161

Table E.11: Dissolution of micro-bead formulation containing FD-4 and and TMC

TMC	% Dissolution				
Time	1	2	3	Average	STDE
0	0	0	0	0	0
15	65.85451389	61.76928057	55.44677446	61.02352297	5.243794029
30	72.08952139	74.01497287	68.45767623	71.5207235	2.821973563
60	80.31088895	78.51039683	75.54633585	78.12254054	2.405839966
90	89.1989973	86.33259973	77.54275531	84.35811745	6.07379038
120	92.00762089	90.75890064	78.93159117	87.23270423	7.216036594
180	94.50112321	97.68495697	87.54657035	93.24421684	5.184745029
240	94.5731016	98.2822059	96.81662555	96.55731102	1.868099759
300	95.24241541	99.8396271	97.70515753	97.59573334	2.300558421

Table E.12: Dissolution of micro-bead formulation containing FD-4 and and sodium glycocholate hydrate

SodGly	% Dissolution				
Time	1	2	3	Average	STDE
0	0	0	0	0	0
15	53.58823405	66.23372114	41.7197039	53.8472197	12.25906055
30	75.12289778	86.33306401	76.27748511	79.2444823	6.165976077
60	83.16156526	86.97307086	85.41991287	85.18484966	1.916594577
90	91.03633884	91.258833	93.72014961	92.00510715	1.489430729
120	93.0315049	91.68849385	96.0964213	93.60547335	2.259322009
180	94.81935045	94.10975594	96.60834006	95.17914882	1.287564288
240	96.37691431	96.95638091	99.0320985	97.45513124	1.396089068
300	99.32862832	98.58360877	99.54956169	99.15393293	0.506117694

Validation: Specificity

Table E.13: Fluorescence values for micro-beads containing FD-4 and Pharmacel[®]

FD Pharma	
Concentration	Fluorescence - Background noise
10.2	121838859
5.1	61578127
2.55	30806935
1.275	12672004
0.637	6404681
0.319	3089493
0.159	1411943
0.08	734007
0.04	347625

Table E.14: Fluorescence values for micro-beads containing FD-4 and *Aloe vera* gel

AVG	
Concentration	Fluorescence - Background noise
10.6	4922061
5.3	2441864
2.65	1213312
1.325	633377
0.662	371712
0.331	243735
0.166	129364
0.083	65120
0.041	76446

Table E.15: Fluorescence values for micro-beads containing FD-4 and *Aloe vera* whole leaf extract

AVWL	
Concentration	Fluorescence - Background noise
10.6	4455128
5.3	2256754
2.65	1127476
1.325	552622
0.662	266996
0.331	226916
0.166	114078
0.083	53718
0.041	92852

Table E.16: Fluorescence values for micro-beads containing FD-4 and chitosan

Chitosan	
Concentration	Fluorescence - Background noise
10.4	171505527
5.2	84118399
2.6	39397599
1.3	18784049
0.65	10008481
0.325	4930716
0.163	2407813
0.081	1219696
0.041	541854

Table E.17: Fluorescence values for micro-beads containing FD-4 and TMC

TMC	
Concentration	Fluorescence - Background noise
10.6	127827295
5.3	62757871
2.65	30242129
1.325	14527412
0.662	7157982
0.331	3488194
0.166	1766654
0.083	968198
0.041	512084

Table E.18: Fluorescence values for micro-beads containing FD-4 and sodium glycocholate hydrate

SG	
Concentration	Fluorescence - Background noise
12.4	104656418.7
6.2	52427674.67
3.1	26231400.67
1.55	11374102.67
0.775	5695002.667
0.388	2401560.667
0.194	561792.6667
0.097	260607.3333
0.048	184759.3333